UNITED STATES DEPARTMENT OF THE INTERIOR

GEOLOGICAL SURVEY

THE COALINGA EARTHQUAKE SEQUENCE COMMENCING MAY 2, 1983

(Preliminary Report on Field Investigations
and
Data Collected as of May 12, 1983)

Compiled by

Roger D. Borcherdt

Open-File Report 83-511

CONTENTS

INTRODUCTION

Roger D. Borcherdt

U.S. Geological Survey
345 Middlefield Road
Menlo Park, CA 94025

A moderate earthquake (M_L 6.5) occurred on May 2, 1983 (23h 42m 37.85 GMT) near Coalinga, California (36 13.99N; 120 17.59W). The earthquake, approximately 10 km northeast of Coalinga and 30 km northeast of the San Andreas fault, caused at least 33 million dollars in damage, primarily to older structures in the communities of Coalinga and Avenal. A variety of seismological, geological, and geotechnical investigations were undertaken by the U.S. Geological Survey immediately following the main event. This report provides a preliminary summary of field investigations and resulting data sets collected through May 12, 1983. This report, compiled on June 1, 1983, is intended to facilitate and assist in coordinating further studies. Preliminary event locations are provided but expected to vary by as much as 2 km with improved crustal models (Reasenberg, oral commun.).

Field investigations, commencing on the evening of May 2, 1983, include:

1) on-line computer analysis of event location and characteristics of aftershock sequence using an automatic P-wave arrival detection system applied to data from Central California Seismic Telemetry Network (Eaton; Reasenberg, and others),

2) acquisition of wide dynamic range on-scale recordings in the epicentral region of the aftershock zone using 18 portable digital recording systems (GEOS, DR-100; Borcherdt and others) and 8 analog strong-motion instruments (SMA-1; Maley and others),

3) augmentation of seismic telemetry network with 12 portable high gain recording systems and four additional seismic telemetry stations (Eaton; Reasenberg and others),

4) field investigations of surface ruptures to determine if tectonic surface faulting accompanied the main event (Clark and others),

5) geotechnical investigations concerned with secondary ground failures including landslides and liquefaction (Keefer, and others),

6) acquisitiion and processing of strong-motion records obtained on U.S. National Strong Motion Network (Maley and others),

7) releveling surveys to infer regional tectonic surface deformation (Stein and others), and

8) crustal structure determinations using 100 portable cassette recorders (Walters and others, oral commun.).

Brief descriptions of these investigations and resulting data sets are provided together with a preliminary summary of the tectonic setting of the Coalinga area (Brown). The field investigations were conducted in coordination with those initiated by the Earthquake Engineering Research Institute and the California Division of Mines and Geology.

TECTONIC SETTING

Robert D. Brown

U.S. Geological Survey
345 Middlefield Road
Menlo Park, CA 94025

The Coalinga earthquake and its aftershocks occurred about 30 km northeast of the San Andreas fault, in a structural setting that reflects more than 20 m.y. of cumulative deformation near the margin of the continental plate. The dominant and most obvious evidence of this deformation is the San Andreas fault, which trends N40°W in the Coast Ranges of central California. The San Andreas is a right lateral strike-slip fault and accommodates a part of the 6 cm/yr of relative movement between the North American and Pacific plates. The balance of this movement is expressed in other ways, among which are folding and faulting along pre-existing structures that are remote from the San Andreas. Faulting in the anticlinal core of one such structure appears the most likely explanation for the Coalinga earthquake.

The Coalinga earthquake of May 2, 1983, its aftershocks, and a smaller earthquake sequence on October 25, 1982, 20 km to the northwest, define a diffuse zone of seismic activity, about 40 km long, 15 km wide, and extending to depths of more than 10 km (Eaton, this report; Reasenberg and others, this report). The general trend of the zone, N30-35°W, may contain shorter segments with different trends, but in plan view the pattern of seismicity closely follows the trend of the Coalinga anticline. Near Coalinga this southeasterly plunging anticline is well defined by surface geologic mapping (Dibblee, 1971, 1979; Jennings, 1977) and by subsurface data (Kaplow, 1945). North and northwest of Coalinga it is locally complicated by smaller folds, but it can be traced as a major structure nearly to the San Andreas fault. Its exposed length from the San Joaquin Valley to the San Andreas fault is about 65 km. The northern part of the anticline trends about N70°W, but north of Coalinga, near the epicenter of the May 2 main shock, the trend becomes more northerly, about S40°W.

Surface geologic maps (Dibblee, 1971, sheets 5 and 8) of the anticline in the epicentral region of May 2, 1983 earthquake exhibit simple fold relations, unbroken by any major faults. Structure-contour maps of the Coalinga oil field (Kaplow, 1945) also show simple structures, evidently uncut by any major faults to depths of 1500 to 2000 m below sea level. These relations, the 10 km depth of the main shock, and the non-tectonic origin of all of the fractures observed in the epicentral area after the earthquake (Clark and others, this report) do not entirely preclude shallow faulting, but they do encourage consideration of a deep source for the earthquakes. As described below, anticlinal cores in this part of the Coast Ranges may provide a setting for these and other similar earthquakes.

The Coalinga anticline (fig. 1) is one of several southeast-plunging folds with similar rock sequences and geometry along the northeast side of the San Andreas fault (Dibblee, 1971, 1979; Jennings, 1977). Anticlines in this region are 15 to 25 km from crest to crest. Except near the San Andreas fault, the anticlines exhibit simple fold relations in the strata of Cretaceous and Tertiary age that are exposed on their limbs and noses. The

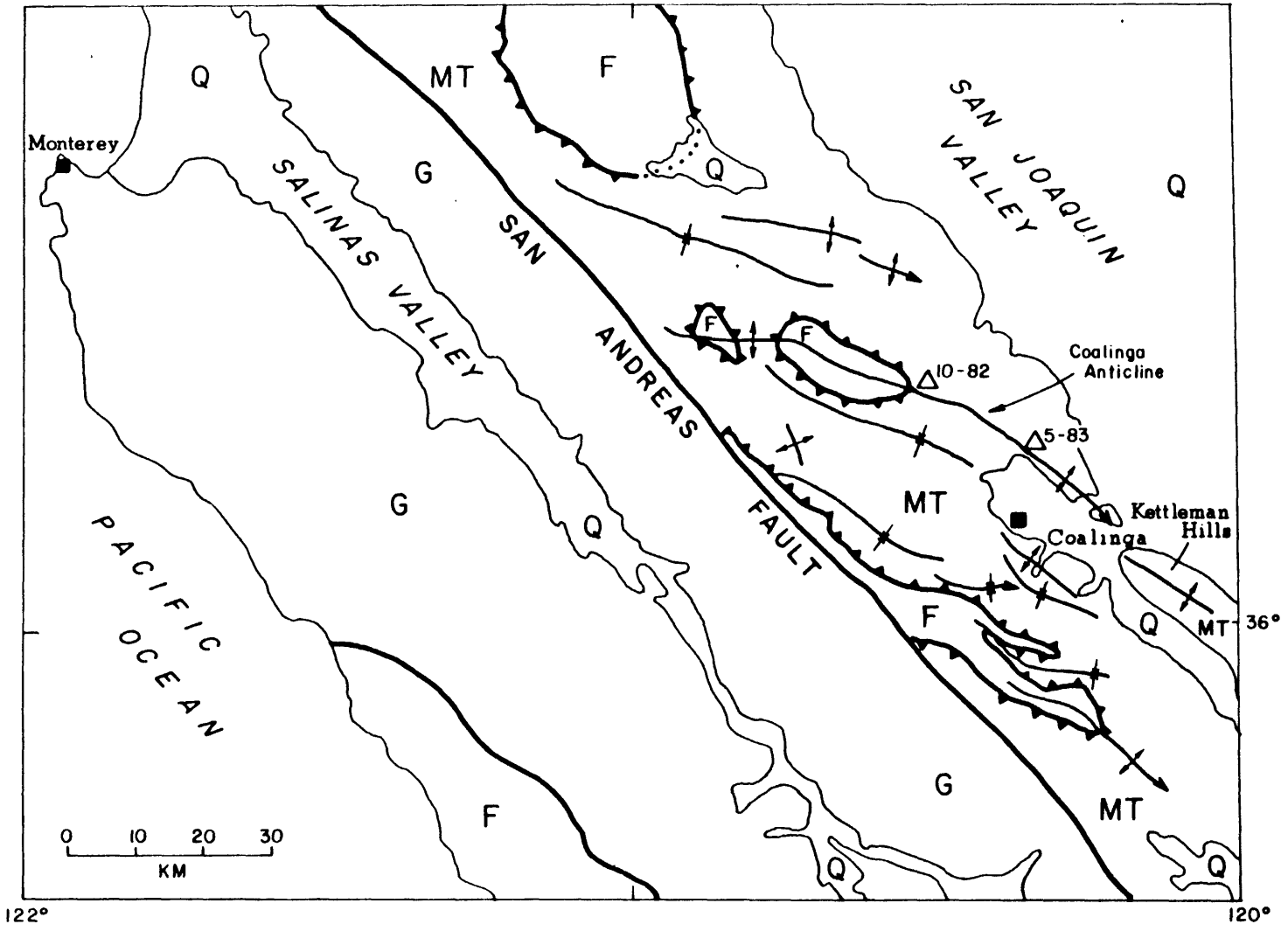

Figure 1. Tectonic sketch map of central California Coast Ranges. The Coast Range thrust, which encloses anticlinal cores of the Franciscan assemblage, is the pre-San Andreas structural boundary between western oceanic crust and eastern continental crust. Generalized from Jennings (1977).

Explanation

Q — Alluvial deposits of Quaternary age

MT — Marine sedimentary rocks of Mesozoic and Tertiary age; locally contains continental deposits and some strata of Quaternary age

F — Franciscan assemblage; intensely deformed marine sedimentary and volcanic rock; locally includes serpentinite; chiefy Jurassic and Cretaceous

G — Crystalline granitic and metamorphic rocks southwest of the San Andreas fault; Cretaceous and older; locally overlain by marine and continental deposits of Cretaceous and Tertiary age

Anticline, showing plunge

Syncline

Fault, high angle

Thrust fault, barbs on upper plate, dotted where concealed. Northeast of San Andreas fault, symbol identifies Coast Range thrust

△ 10-82 — Epicenter of earthquake, showing month and year

anticlinal cores, however, are an assemblage of sheared and cataclastically metamorphosed marine mudstone, sandstone, chert, and oceanic volcanic rocks. These rocks, collectively termed the Franciscan assemblage, are in part contemporaneous with the relatively undeformed Mesozoic strata in the anticlinal limbs, but they differ from those strata in their origin and in their subsequent structural history. In many places, these Franciscan cores are separated from the overlying rocks by a zone of intense shearing, lenses or tabular bodies of serpentinite, and tectonic masses of exotic rock; in the Coalinga anticline these relations are best described near the New Idria quicksilver mines (Eckel and Myers, 1946).

The contact of the Franciscan assemblage with folded but otherwise little-deformed pre-Tertiary rocks structurally above it is now recognized as a major detachment fault, the Coast Range thrust (Bailey and others, 1970). This fault--or others with remarkably similar structural and stratigraphic relations--can be traced throughout the Coast Ranges northeast of the San Andreas fault as a bedding-plane, or near bedding-plane, thrust fault; it has been folded with the overlying marine sequence of Mesozoic and Tertiary age and its present attitude thus changes from place to place depending on local geologic structure.

The Franciscan core of the Coalinga anticline and the folded thrust fault--the New Idria thrust fault of Eckel and Myers (1946)--are exposed 25 km northwest of Coalinga. They plunge southeasterly into the aftershock zones of the October 1982 and May 1983 earthquakes. The epicenter of the 1982 main shock, of magnitude 5.5, was located within a few kilometers of the surface trace of the fault, and both this earthquake and the main shock of the May 1983 sequence have yielded preliminary focal mechanisms (Eaton, this report and oral comm.). The two focal solutions are consistent with thrusting on either limb of the folded thrust fault. This agreement between geologic structure and focal mechanisms, however, must be viewed cautiously, because no direct geologic evidence of structural relations at hypocentral depths is available and because final analysis of the seismological data is still incomplete.

Whether the Coalinga earthquakes occurred on the Coast Range thrust, on structurally lower faults in the Franciscan core, or on an unrecognized fault higher in the anticlinal structure, they seem to identify the fold systems of the eastern part of the Coast Ranges and the western edge of the Great Valley as potential sources of damaging earthquakes. This should not be surprising for several of these folds exhibit evidence of deformation during late Tertiary and Quaternary time, a few show evidence of Holocene deformation, and many probably owe their present shape, size, and orientation to the same stress system that produced, and currently drives, the San Andreas fault.

REFERENCES CITED

Bailey, E. H., Irwin, W. P., and Jones, D. L., 1970, On-land Mesozoic oceanic crust in the California Coast Ranges: U.S. Geological Survey Professional Paper 700-C, p. C70-C81.

Dibblee, T. W., 1971, Geologic maps of the Coalinga, Joaquin Rocks, New Idria, and Priest Valley 15' quadrangles: U.S. Geological Survey Open-File Report 71-87 (sheets 5, 8, 10, and 15).

Dibblee, T. W., 1979, Geologic map of the central Diablo Range between Hollister and New Idria, San Benito, Merced, and Fresno Counties, California: U.S. Geological Survey Open-File Report 79-358.

Eckel, E. B., and Myers, W. B., 1946, Quicksilver deposits of the New Idria mining district, San Benito and Fresno Counties, California: California Journal of Mines and Geology, Report XLII of the State Mineralogist, p. 81-124.

Jennings, C. W., 1977, Geologic map of California: California Division of Mines and Geology, California Geologic Data Map Series, scale 1:750,000.

Kaplow, E. J., 1945, Coalinga oil field, in Summary of operations, California oil fields; thirty first annual report of the State Oil and Gas Supervisor: Department of Natural Resources, Division of Oil and Gas, vol. 31, no. 2, p. 5-22.

THE MAY 2, 1983 EARTHQUAKE AT COALINGA, CALIFORNIA: THE SEARCH FOR SURFACE FAULTING

Malcolm M. Clark, Katherine K. Harms, James J. Lienkaemper, James A. Perkins, Michael J. Rymer, and Robert V. Sharp[1]

U.S. Geological Survey
345 Middlefield Road
Menlo Park, CA 94025

This report briefly describes our efforts to determine whether surface faulting accompanied the May 2, 1983 earthquake at Coalinga. Our ground search for evidence of faulting began on the morning of May 3 and continued to May 7; other brief investigations were made on May 10 and May 24-25. Nearby parts of the San Andreas and other known faults were also ground checked to see if they sustained sympathetic movement due to shaking or stress changes.

An aerial search made on the morning of May 3 extended from the San Andreas fault near Mustang Ridge eastward to Interstate Highway I-5 and from Avenal northward to the Black Mountain vicinity (fig. 1). Rockfalls, landslides, slumps, and related secondary fractures were seen from the air, but no fault ruptures were identified.

Although fissures and cracks were found by ground search at many places within about 10 km of the instrumental epicenter, none appeared to represent new faulting. Indeed, the epicentral region is notable because of the absence of both previously identified faults and lineaments on the ground surface that could reflect pre-existing fault structures.

In interpreting the observed cracks we applied the following criteria to discriminate tectonic faulting from cracking due to other processes:

(1) That there be net displacement across the crack features, or alternatively, that purely extensional opening on steeply dipping cracks be insufficient evidence of faulting (which by definition requires displacement parallel to its surface);
(2) That the style of faulting or sense of displacement of suspected faults persist, or at least vary in some consistent way, along the length of the crack features;
(3) That the cracks not be readily explainable by other processes restricted to the near-surface (for example--slumps parallel to a free face of a nearby channel or an artificial fill).

Our ground search concentrated in the epicentral area because of the abundance of new fissures and cracks there (figs. 1 and 2 show paths followed in the investigation on the ground). A preliminary focal mechanism provided by U.S.G.S. seismologists at the beginning of our ground search suggested, however, that a far-ranging regional inspection should be made, particularly along the eastern margin of the Coast Ranges. As a consequence of the shallow

---

[1] Authors listed alphabetically.

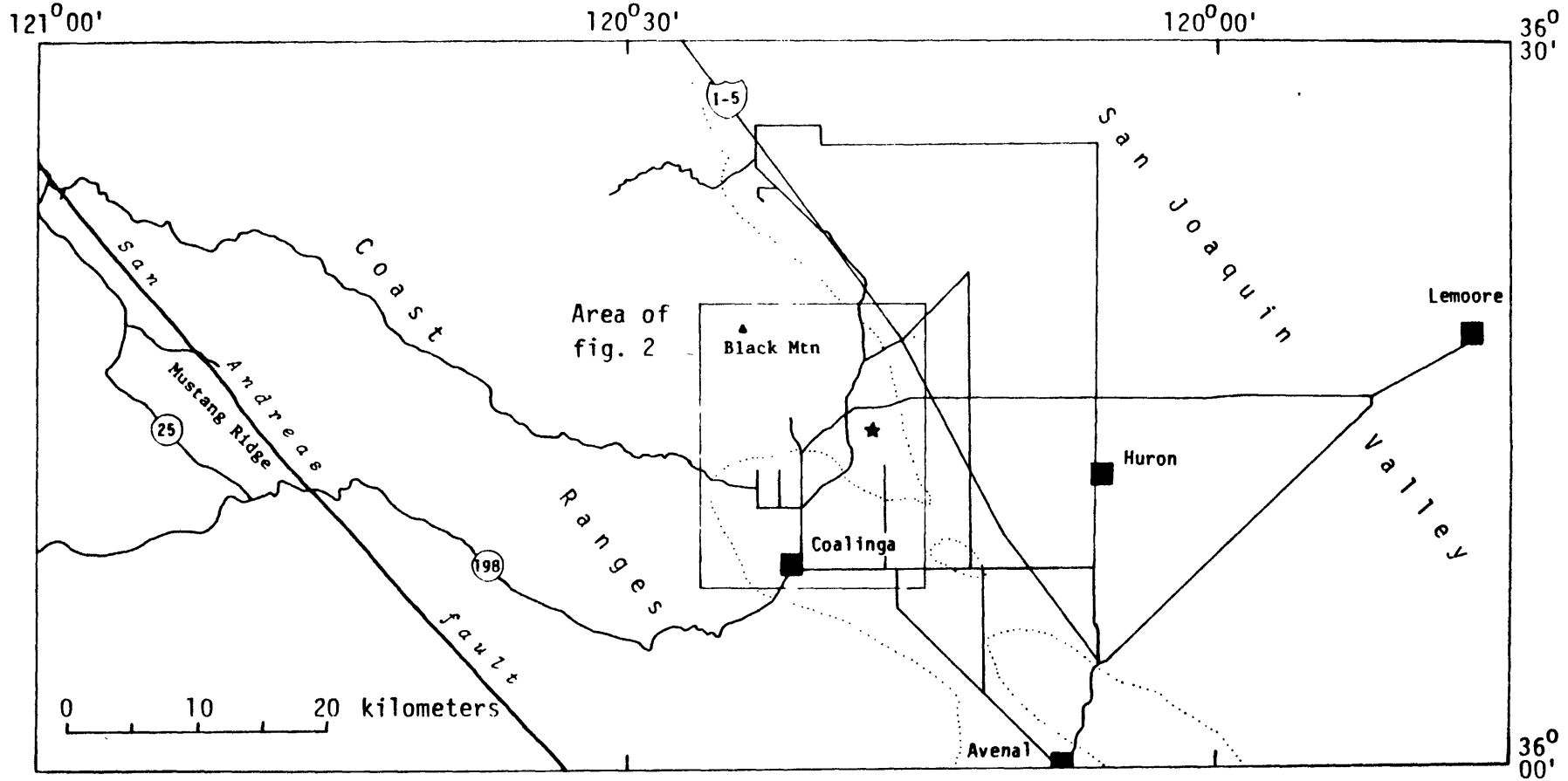

Figure 1. Map showing routes that were carefully inspected for surface rupture. Shown are only those roads that were inspected during this investigation. Dotted line represents approximate boundary between San Joaquin Valley and Coast Ranges. Star shows location of main shock epicenter.

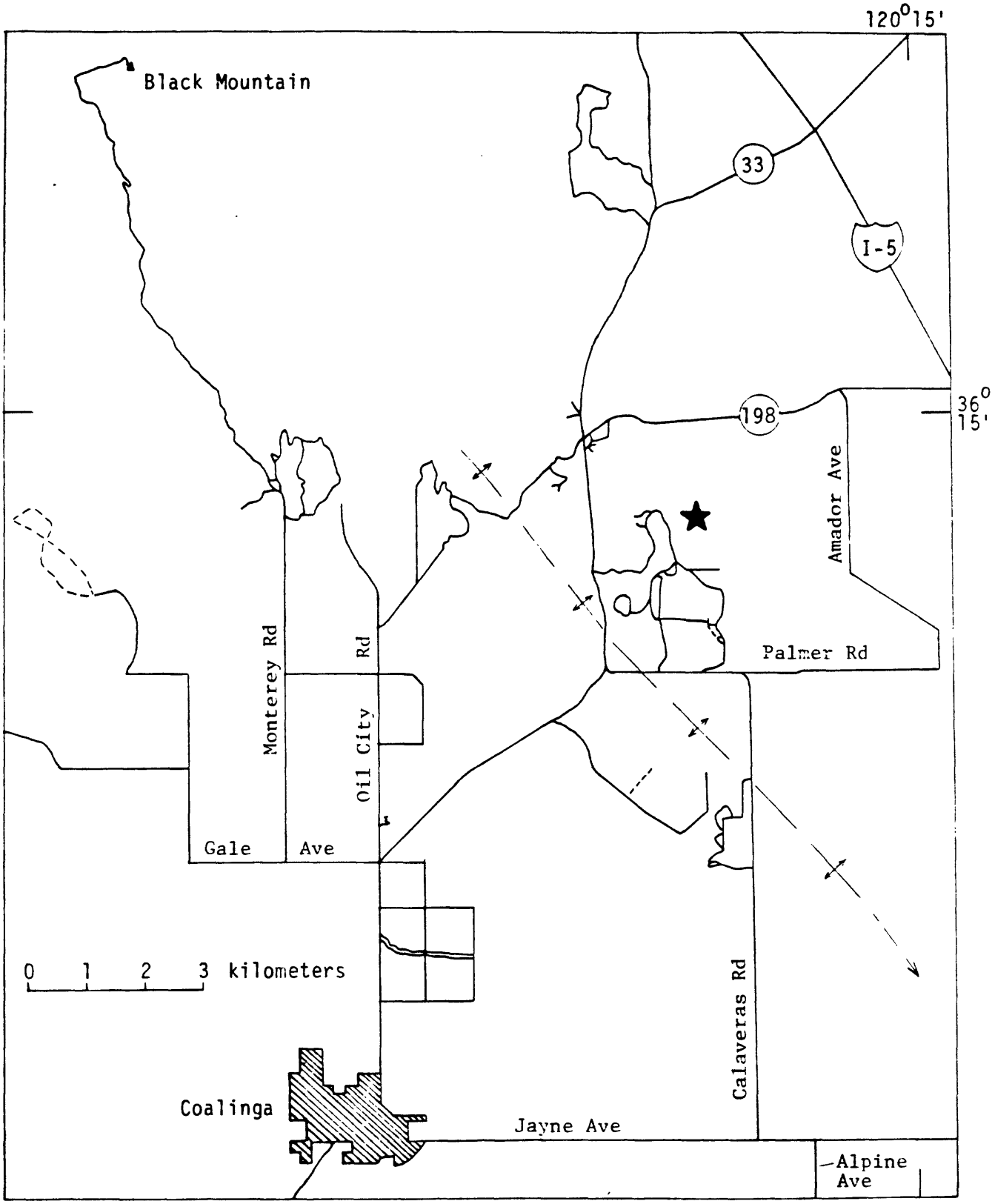

Figure 2. Map of epicentral region showing routes that were carefully inspected for surface rupture. Shown are only those roads that were inspected during this investigation. Roads traversed by vehicle are shown as solid lines; routes traversed by foot are shown by short dashed lines. Star shows location of main shock epicenter.

dip of one of the focal planes, ground checks along pavements were made to a considerable distance eastward into San Joaquin Valley.

One characteristic of many fissures and cracks that were found either in the epicentral area, which overlies an anticlinal structure, or on the alluviated surface immediately to the southwest deserves notice. The trends of many of these breaks were oriented in the northwest quadrant, approximately parallel to the nearby Coast Range regional strike and the limbs of the anticline. The consistent orientation of cracks might be explained in various ways--one of the most likely being that the preexisting structure of both buried and exposed sedimentary beds might have controlled the orientation of new breaks. Bedding-controlled topography buried under young alluvium also may have guided differential compaction boundaries expressed at the surface as fissures with downdropping on one side.

Several kinds of surficial processes combined with strong ground shaking probably account for the recently created fractures that were observed on the ground surface after the Coalinga earthquake. None of the fracturing, however, is considered by us to be caused by tectonic displacements on deeply rooted fault structures.

LANDSLIDES AND RELATED GROUND FAILURES

David K. Keefer, Edwin L. Harp, and Raymond C. Wilson

U.S. Geological Survey
345 Middlefield Road
Menlo Park, CA 94025

A reconnaissance for landslides and earthquake-related ground failure was conducted in the region near Coalinga, California on May 3 and 4, 1983. The routes through the mountains north and west of Coalinga along State Highway 198 and the Los Gatos Creek Road were investigated as well as portions of Interstate-5, State Highway 33 from I-5 south to Avenal, selected secondary roads in the San Joaquin Valley east of Coalinga, and some roads in the Anticline Ridge area. Location of earthquake-induced failures discussed in text are plotted (fig. 1).

Rock falls, rock slides, and soil falls in mountainous terrain

In the mountains north and west of Coalinga, the most numerous and widely distributed landslides were rock falls, rock slides, and soil falls. A reconnaissance flight on May 3 reported many rockfalls in the mountains northwest of Coalinga along Joaquin Ridge and adjacent hills to the northeast (Malcolm Clark; oral commun.).

State Highway 198: Along State Highway 198, no landslides attributable to the earthquake were seen west of the Fresno-Monterey County line (locality 1, fig. 1). A Caltrans worker told us that the earthquake had triggered a rock fall at locality 1, where we found a thin layer of dry rock and soil debris covering the highway. Many small rock falls with volumes less than 2 m^3 were visible from the road between localities 2 and 3. Rock falls and rock slides were larger and more numerous along the flanks of steep, high ridges between locality 3 and Coalinga. Figure 2 shows several typical rock slides in this area. The largest rock falls and rock slides in this area had volumes of several tens of cubic meters.

Los Gatos Creek Road: Several tens of rock falls with volumes of as much as several hundred cubic meters occurred in a massive cliff-forming sandstone of the Panoche Formation (fig. 3). This sandstone is weakly cemented and disintegrated readily on impact so that the rock-fall deposits contained a high proportion of individual sand grains. The largest rock falls seen were at locality 4 (fig. 1). Smaller rock falls from this sandstone and from a thinly-bedded fissile shale unit along Los Gatos Creek Valley were seen as far northwest as locality 5. Soil falls along the banks of Los Gatos Creek were common between localities 4 and 5. These soil falls involved weakly cemented alluvium containing a high proportion of gravel and cobbles.

Rotational slumps in Los Gatos Creek valley

A large slump (volume 200,000 m^3) occurred at locality 6 (fig. 4). Near-surface material in the slump was loose, dry, slightly cemented sand. The head scarp of the slump was 1 to 2 m high. The toe spilled into Los Gatos Creek at the outside of a meander. Cracks crossed the slope above the head scarp and the next ridge north. Slumps in highway fill occurred at locality 7 (fig. 5). A slump in the roadbed was reactivated at locality 8 by the earthquake.

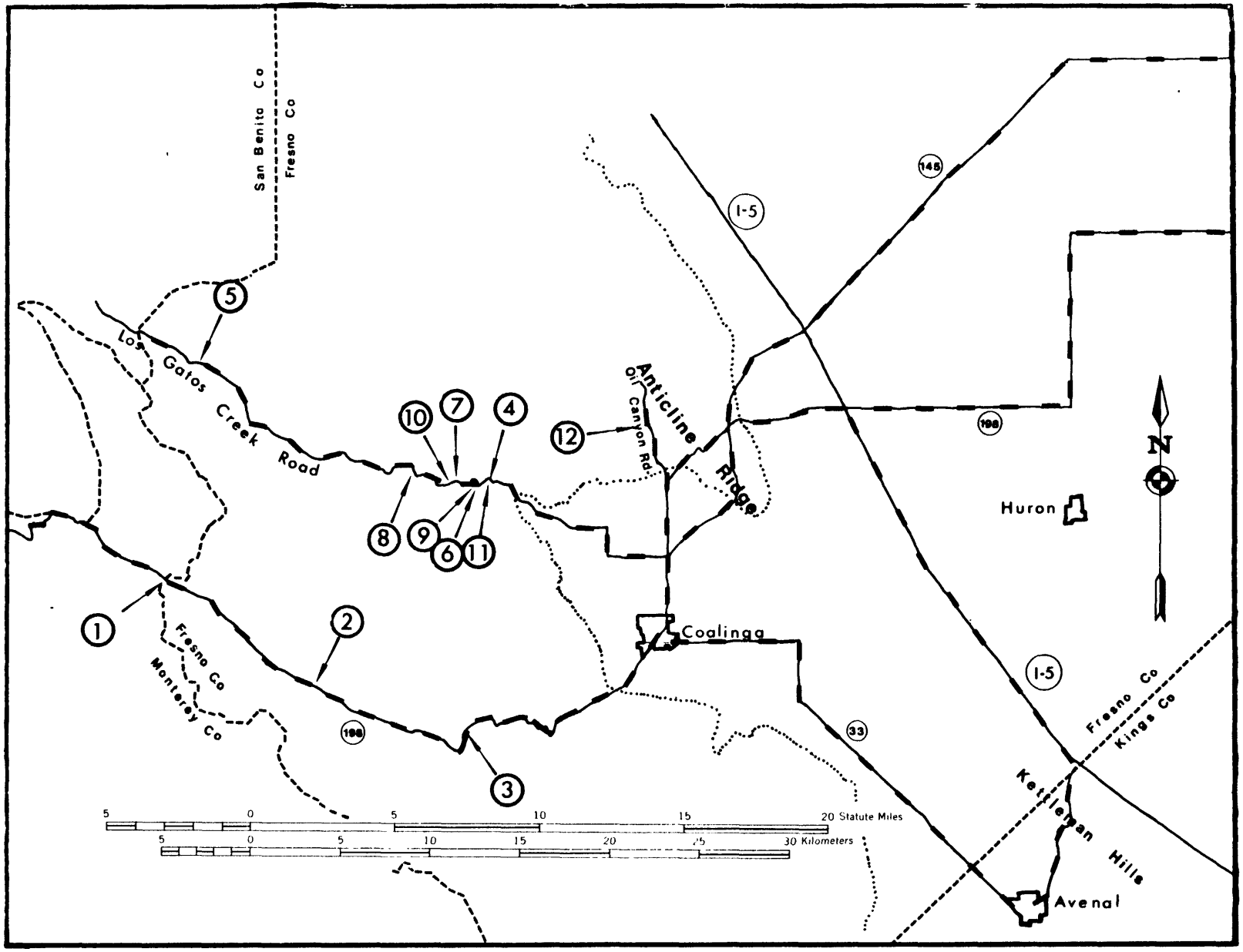

Figure 1: Location map showing sites of earthquake-induced ground failure (numbered circles and arrows), routes traveled on reconnaissance (bold dashes along highway) and approximate eastern limit of mountainous terrain (dotted line).

Figure 2. Rock slides along California State Highway 198 southwest of Coalinga.

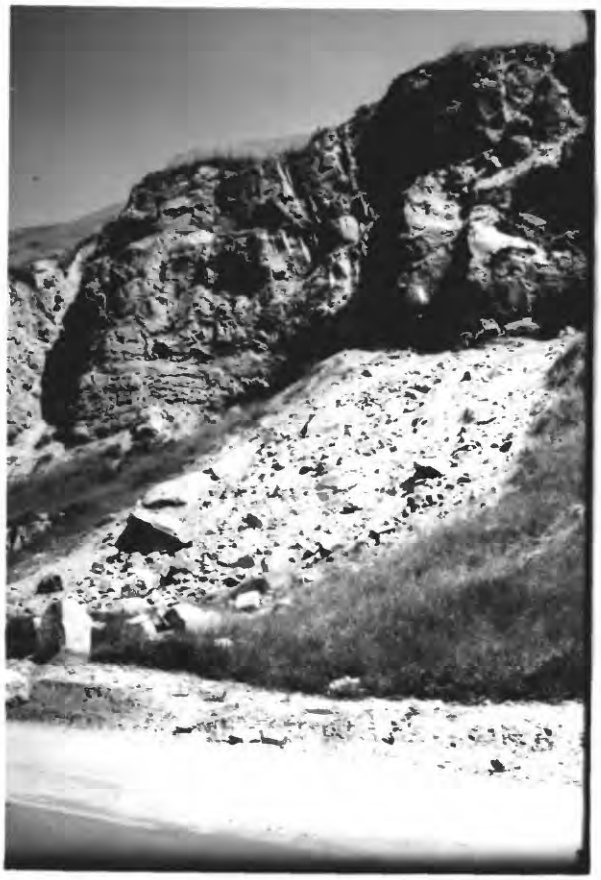

Figure 3. Rock fall from cliffs in massive, weakly cemented sandstone of Panoche Formation along Los Gatos Creek Road at locality 4.

Figure 4. Rotational slump of approximately 200,000 m^3 along Los Gatos Creek at locality 6.

Figure 5. Slump in highway fill, Los Gatos Creek Road, locality 7.

Lateral spreading in Los Gatos Creek

Lateral spreading cracks and associated sand boils occurred in a river bar in Los Gatos Creek at locality 9 (Fig. 6). The material there was silt and fine sand to a depth of approximately 15 cm; below that depth the material was gravel. The largest crack was about 10 cm wide and several meters long. Cracks also crossed river bars at localities 10 and 11, but no sand boils were present at those localities. At locality 11, a sand bar approximately 100 m long along the outside meander of Los Gatos Creek sustained extensive cracking accompanied by limited lateral spreading (fig. 7). The sand deposit is thin (up to 0.6 m); the cracks did not extend into the underlying gravel (fig. 8). Individual cracks were up to 3 m long and had up to 5 cm of extension.

Ground failures in Anticline Ridge area

Many cut-and-fill pads for oil wells and tanks were inspected in this region (locality 12). Typically, rock and/or soil fell from cut slopes (fig. 9), fill at the edges of pads cracked and slumped (fig. 10), and vibrational compaction produced small scarps and cracks around concrete pump aprons (fig. 11). These types of failures were abundant throughout the oil field.

Other areas

The only ground failures found east of Interstate 5 were minor cracks caused by vibrational compaction of roadbed fill.

Figure 6. Lateral spreading cracks in river-bar sand in Los Gatos Creek at locality 9.

Figure 7. Lateral spreading cracks in sand along Los Gatos Creek at locality 11.

Figure 8. Cracks in thin sand deposit overlying gravel along Los Gatos Creek at locality 11. Cracks are present only in overlying sand.

Figure 9. Rock and soil fall from cut slope above oil field pad at locality 12.

Figure 10. Slump in fill at edge of oil well pad.

Figure 11. Crack in margin of concrete oil pump apron. Scale divisions are 1 cm.

SEISMIC SETTING, LOCATION AND FOCAL MECHANISM OF THE MAY 2, 1983, COALINGA EARTHQUAKE

Jerry P. Eaton

U.S. Geological Survey
345 Middlefield Road
Menlo Park, CA 94025

Typical background seismicity in the central Coast Ranges is illustrated by the seismicity map of the region for 1982 (fig. 1). Concentrated activity along the creeping section of the San Andreas fault from Parkfield to San Juan Bautista and on the Paicines and Calaveras faults northwest of Bear Valley dominate the pattern. Scattered small earthquakes and occasional moderate earthquakes with dense clusters of aftershocks occur throughout the Coast Ranges between this section of the San Andreas fault and the Great Valley to the east.

From a single year's data it is difficult to discern any clear pattern in the seismicity east of the San Andreas. However, if a longer period of time is considered, a pattern does emerge. Seismicity in the region east of the San Andreas fault from January 1972 through April 1983 is shown in figure 2, where activity along the San Andreas, Paicines, and Calaveras faults has been excluded. In the northwest part of the region, clusters of events are generally small, scattered events are distributed rather uniformly between the clusters, and the density of events drops off sharply northeast of a line, with an azimuth of about N30^{o}W, along the longitudinal axis of the region. In the southeast half of the region, concentrations of epicenters from moderate earthquakes and their aftershocks are larger and most of the activity is northeast of the axial line described above.

Selected aftershocks of the Coalinga earthquakes for the period May 2 through May 7 are shown in figure 3. These aftershocks were located by the Menlo Park real-time processor and were screened according to hypocenter quality factors (number of stations, rms of residuals, and estimated epicenter and focal depth errors) to insure that only well-located events were plotted. The aftershock zone is approximately centered on the epicenter of the main shock benearth Anticline Ridge, about 10 km northeast of Coalinga. The aftershock zone is about 30 km long and 15 km wide, and its long axis has a strike of about N38^{o}W. The aftershock zone is several times larger than those of previous moderate earthquakes in the region, as would be expected from the larger magnitude of the Coalinga earthquake.

The relationship of the Coalinga aftershock zone to seismicity in the eastern central Coast Ranges from January 1972 through April 1983 is shown in figure 4, where an outline of the Coalinga aftershock zone (dashed line) and its dense central core (cross-hatched area) are superposed on the map for 1972-1983. Dates of occurrence of the more prominent earlier earthquakes and their aftershock swarms are also indicated on figure 4. The Coalinga aftershocks have filled a seismicity gap betwaeen aftershock clusters of 1976, 1980, and 1982. Several other gaps in the pattern of epicenters of figure 4 deserve further study.

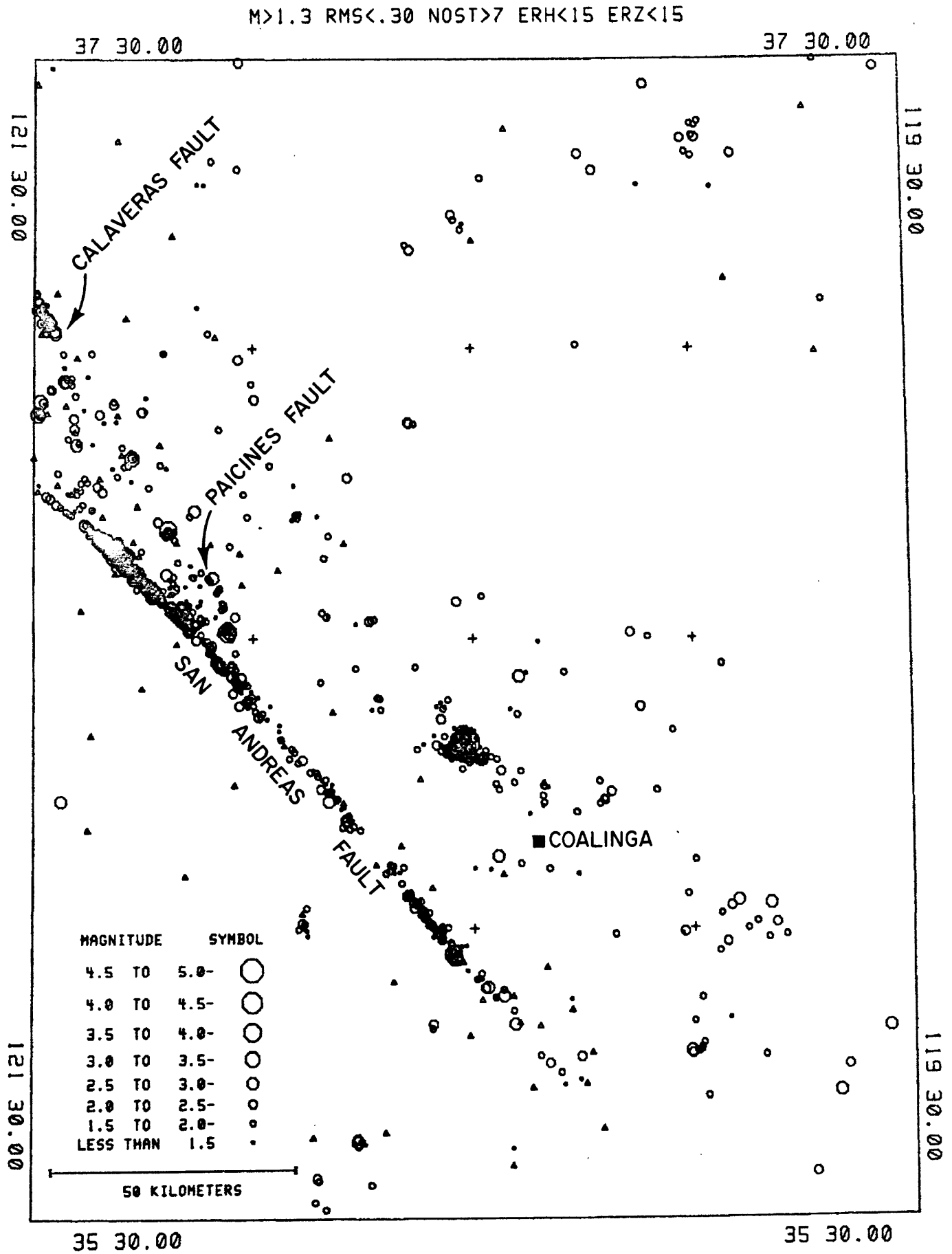

Figure 1: Central Coast Ranges seismicity: 1982.

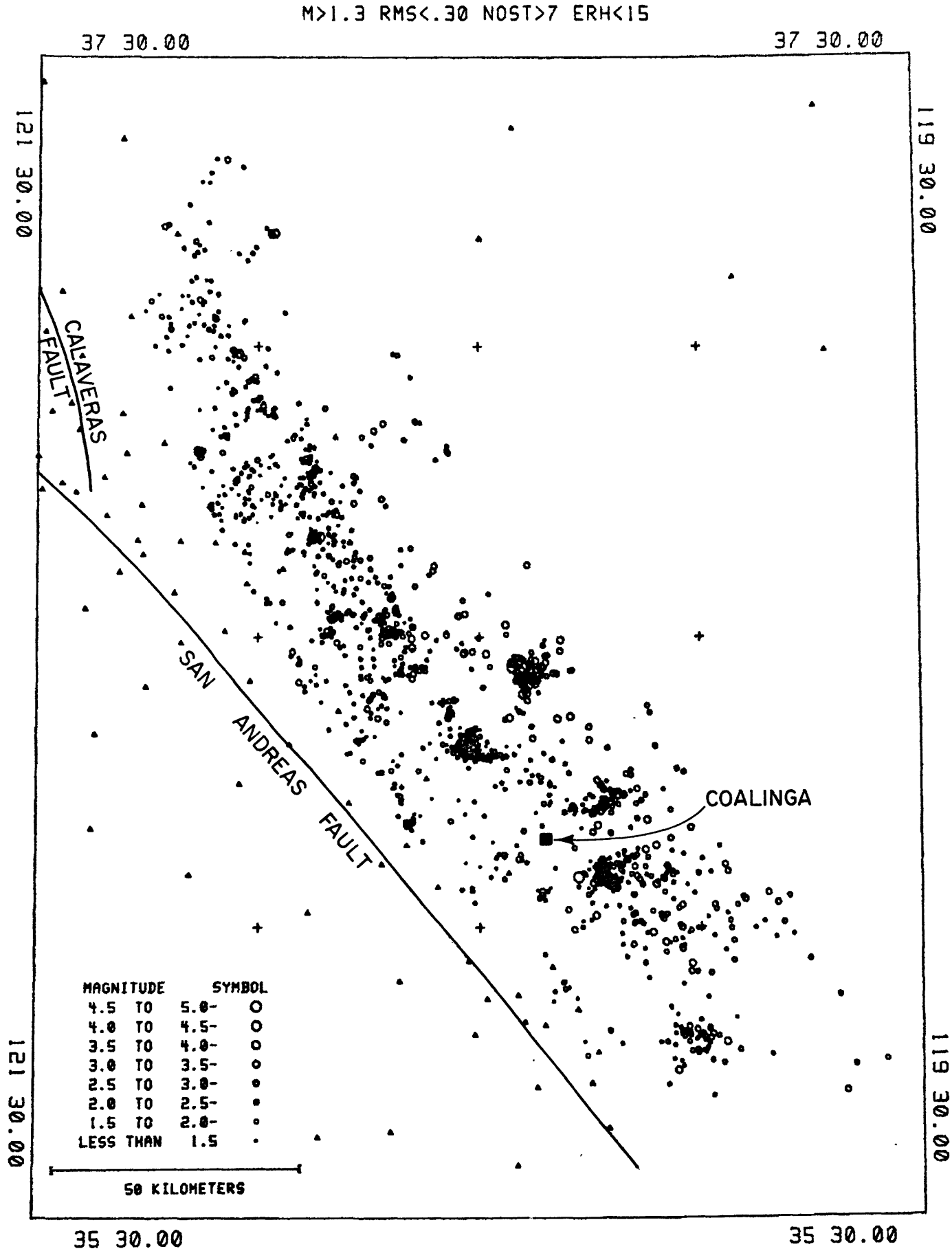

Figure 2: East central Coast Ranges seismicity: January 1972-April 1983.

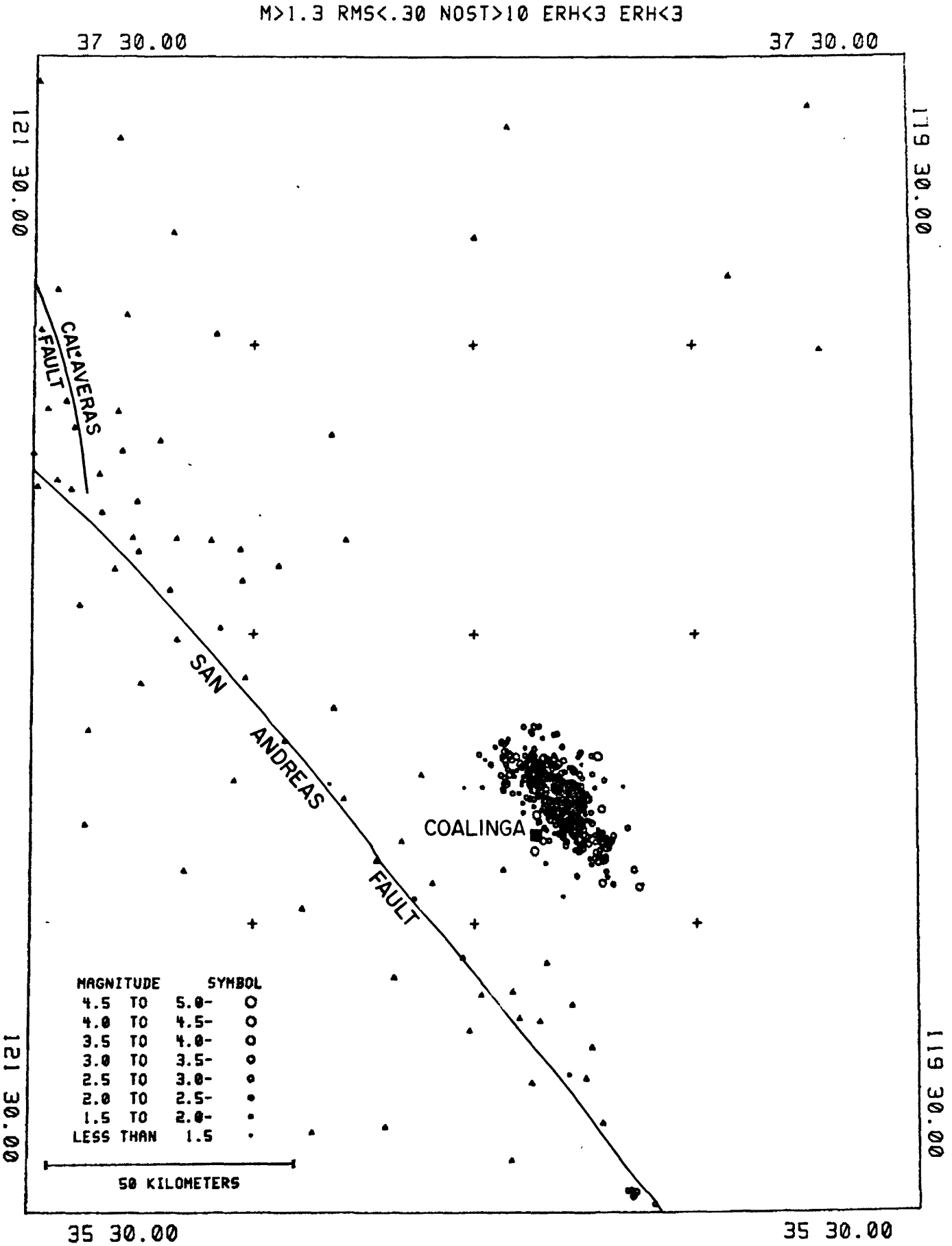

Figure 3: Coalinga aftershocks: May 2-7, 1983.

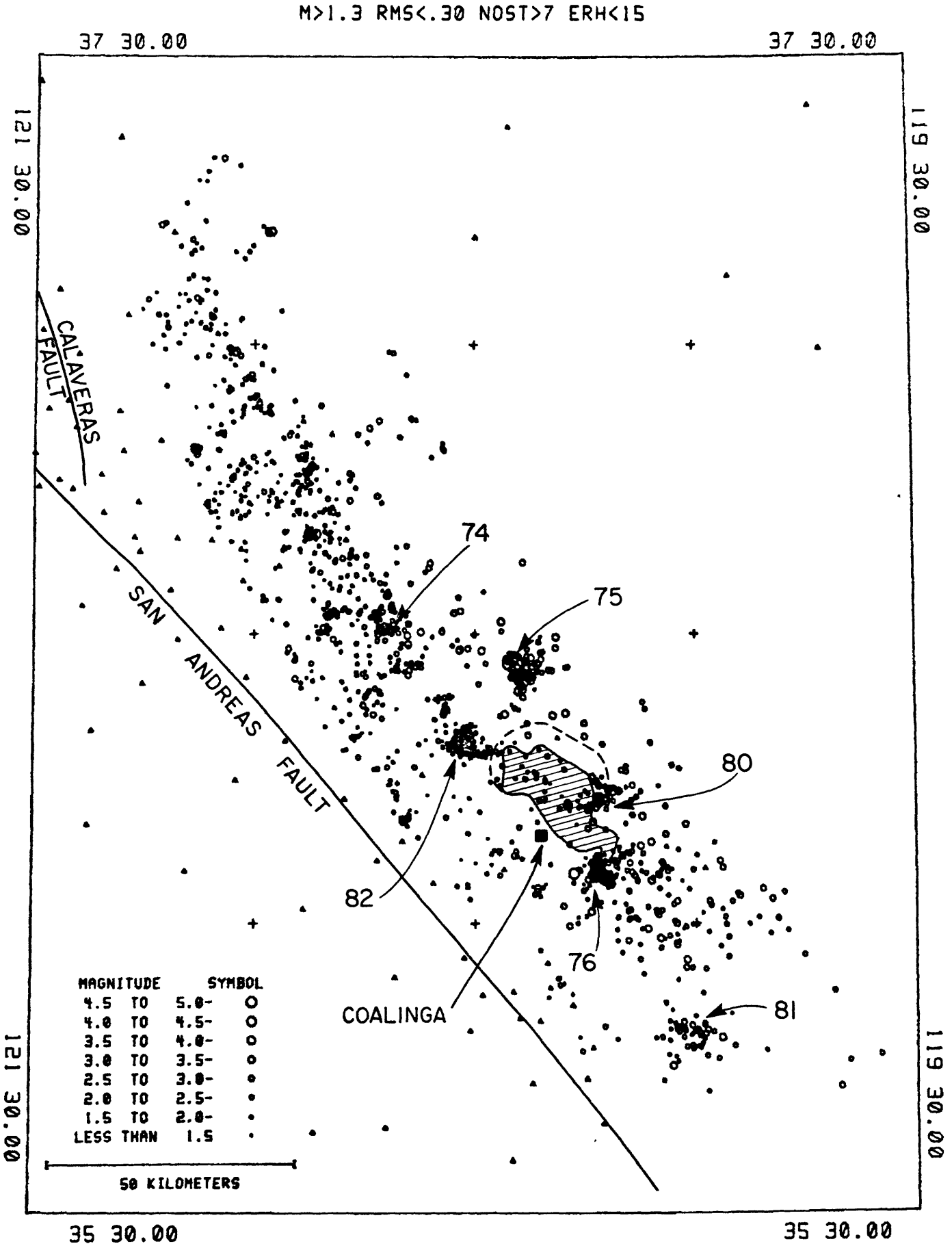

Figure 4: Coalinga aftershocks (May 2-7, 1983) and east central Coast Ranges seismicity (January 1972-April 1983).

To determine the hypocenter and focal mechanism of the main shock, data from more than 400 stations of the northern and southern California seismic networks were played back from magnetic tape and P-wave arrival times and polarities were measured. Station delays for stations within 100 km of the epicenter were adapted from an unpublished Pn time-term-difference study of the central California network region. Starting with the standard crustal model used for routine processing of central California network data, layer velocities and depths were varied during a succession of relocations of the Coalinga earthquake to minimize the rms of the residuals at stations nearer than 100 km and to permit separation of the fields of dilations and compressions on a plot of first-motion directions. The favored model thus produced is:

2.5 km/s	0.0-2.0 km
5.50 km/s	2.0-9.0 km
5.70 km/s	9.0-14.0 km
6.40 km/s	14.0-28.0 km
7.90 km/s	28.0 km.

The hypocenteral parameters of the main shock are:

Time: 23h 42m 37.8s GCT May 2, 1983
Location: 36^{o}13.99'N 120^{o}17.59'W
Depth: 10.5 km
Magnitude: 6.5
Number of station in solution: 39
Distance to nearest station: 4.7 km
RMS of residuals: 0.14 s
ERH (estimated error in epicenter): 0.7 km
ERZ (estimated error in depth): 0.4 km.

The error estimates ERH and ERZ are unrealistically small because of uncertainties in the velocity model and station delays used in the hypcenter determination.

A plot of first-motion directions from the main shock, projected onto the lower hemisphere of the focal sphere, is shown in figure 5. The only seriously discordant first motion is at station PMR, circled on figure, but that station is very near the crossover distance for direct and refracted arrivals.

One nodal plane is constrained very well by the data. It strikes $N53^{o}W$ and dips 67^{o} toward the northeast. The dip of the second nodal plane is constrained to between 23^{o} and 26^{o}, but its strike is determined only to the range about $N20^{o}W$ to about $N80^{o}W$. If the strike of the second plane is chosen to match that of the first, the second plane strikes $N53^{o}W$ and dips 23^{o} toward the southwest. If the first plane represents the fault, it is a high angle reverse fault with the northeast side up. If the second plane represents the fault, as seems more probable, it is a low angle thrust fault with the southwest side up.

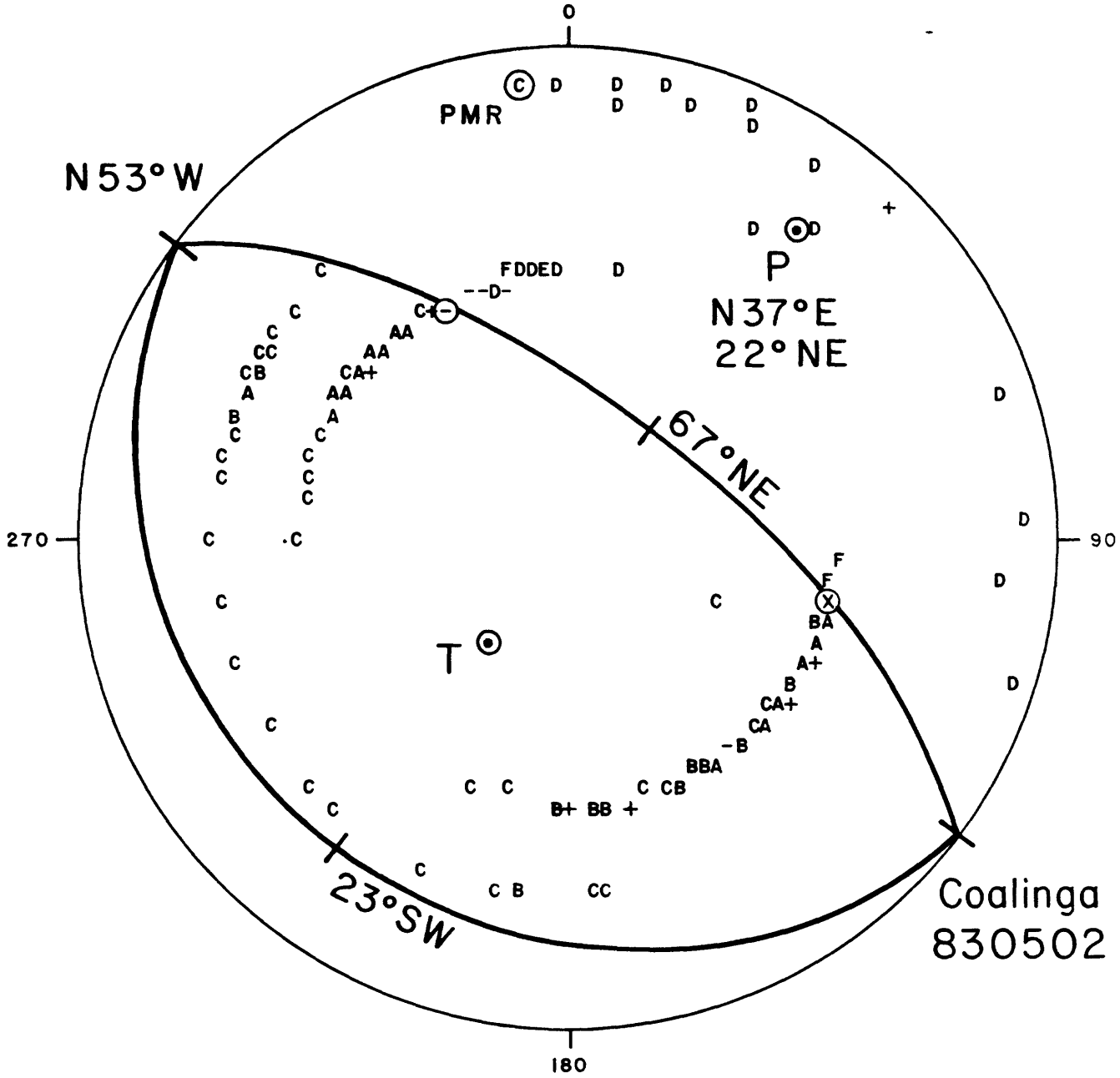

Figure 5: First motion direction plot for the May 2, 1983, Coalinga earthquake. C, B, and A represent 1, 2, and 3 or more compressional first motions; D, E, and F represent 1, 2, and 3 or more dilatational first motions; + represents an uncertain compressional first motion; - represents an uncertain dilatational first motion; X represents a conflict in first motion directions.

PRELIMINARY VIEWS OF THE AFTERSHOCK DISTRIBUTION OF THE MAY 2, 1983, COALINGA, EARTHQUAKE

Paul Reasenberg, Donna Eberhart-Phillips, and Paul Segall

U.S. Geological Survey
345 Middlefield Road
Menlo Park, CA 94025

The May 2, 1983 Coalinga earthquake occurred about 30 km northeast of the San Andreas fault, in the eastern Diablo Range of central California. The epicenter is located on the eastern edge of the U.S. Geological Survey's telemetered microseismic network (fig. 1). Data from this network are telemetered to, and recorded and analyzed at the U.S. Geological Survey in Menlo Park, California. Constantly monitoring this network in real-time is a microprocessor system, recently developed by R. Allen and J. Ellis (Allen, 1982), that automatically identifies and picks P-wave arrivals as they occur. Computer determination of the earthquake hypocenters automatically follows, usually within a few minutes, thus providing early and accurate information on the location and progress of an earthquake sequence while it is occurring. As a result, the U.S. Geological Survey was able to respond quickly to the developing aftershock sequence, installing portable seismograph stations and four additional telemetered stations around the earthquake zone beginning 25 hr after the mainshock. Data from the portable stations will be used in more detailed studies of this earthquake, during the months to come. All the data presented here, however, are from the microprocessor-picked phases from the telemetered network.

While the automated system has enabled an extremely early analysis of earthquake data that previously would have taken several months to accomplish, its performance did reveal, during this sequence, one shortcoming. It was found that during the first several hours of the aftershock sequence the rate of aftershock occurrence was so great, with reverberations from one event literally running into the onset of the next, that the automatic picker was unable to keep up with, or distinguish among, the hundreds of aftershocks per hour that occurred. Consequently, the resulting set of hypocenters is known to be incomplete, with the earlier part of the sequence significantly under-represented. This deficiency will be mitigated when the time-consuming job of hand-processing the network data fills in the missing events. It is also expected that arrival time errors in the present data set, introduced by the automatic picker, will be corrected as the hand-processing procedes, thus improving the location precision.

This preliminary report shows aftershock hypocenters for the 10-day period ending 12 May (2251 GMT). Nine hundred thirty-nine earthquakes in this period were relocated, using the procedure described below. From these, 543 were selected for spatial display on the basis of location quality estimates (shown are HYP071 qualities A through C, Lee and Lahr, 1975). Location uncertainties are typically less than 1.5 km (epicenter) and 2.0 km in depth. The magnitudes indicated by the symbol sizes in the hypocenter plots are approximate estimates. Earthquakes with coda magnitudes larger than 3 are represented here as magnitude 3's (except for the mainshock and some of the larger aftershocks).

In map view (fig. 2) the distribution of aftershock epicenters is an elongate zone striking approximately N30°W, with approximate length 32 km and breadth 16 km. The zone is wider in the northwest portion than in the southeast. The epicenters of both the mainshock and the largest aftershock (9 May, 0249 GMT; M_L 5.1) are located near the center of the zone, beneath Anticline Ridge (fig. 3). The strike of the aftershock zone parallels the regional strike of the Diablo Range to the west, and more locally, of the anticlinal structure composed of Anticline Ridge and Kettleman Hills. The aftershock epicenters are essentially confined to the anticline.

Vertical cross sections AA' and BB' (fig. 4) show the depth distribution of hypocenters in vertical planes along and transverse to the strike of the zone, respectively. The depth of the mainshock (approximately 10 km) and that of the largest aftershock (approximately 12 km) are near the bottom of the aftershock zone. The deeper aftershocks are confined to a volume near the mainshock hypocenter, within 5-7 km distance along the strike, and predominantly southwest of the mainshock. Aftershocks above 4 km depth are confined to the northwest portion of the aftershock zone. The densest concentration of aftershocks occurs between 6 and 9 km depth, near the mainshock hypocenter. In transverse cross section (BB') a weakly defined linear trend apparently dips toward the southwest, somewhat above the mainshock hypocenter. The possibility of inferring a steeply northeast-dipping plane passing through the densest part of the distribution is also noted. The location of the M 5.1 aftershock relative to the mainshock hypocenter would support the northeast-dipping plane if this aftershock were a continuation of the main rupture. However, resolution of any planar features in the aftershock pattern is poor in this hypocenter set.

In figure 5, subsets of aftershocks occurring in the first 21 hours of the sequence with lower magnitude thresholds of 1.5, 2.0, 2.5 and 3.0 are shown in transverse cross section (BB'). The larger magnitude events suggest a southwest-dipping plane. The temporal development of the sequence during the first 24 hours (fig. 6) suggests that during the first 18 hours aftershocks defined a southwest-dipping structure. The first four days of the sequence are shown in figure 7 according to magnitude threshold, and in figure 8 in four sequential time intervals. While not as clear as the trend revealed during the first few hours, these plots also favor a southwest-dipping structure in cross section.

Hypocenter Determination Procedure

The hypocentral solutions shown were obtained with P-wave arrivals from 22 of the 24 stations in the USGS Central California seismograph network shown in figure 1. Stations PHB and PWM, which improve the azimuthal coverage, were added to the network on May 9. A comparison of location sets obtained with and without these additional stations revealed no systematic difference in hypocentral distribution. For the sake of continuity, locations presented here for the entire 10-day period were obtained without data from stations PHB or PWM. Arrival times were picked automatically by the Real Time Processor (Allen, 1982). Hypocenters were determined with a velocity model determined by Walter and Mooney (1980) from refraction data from a (presumed) structurally similar area 40 to 300 km north-northwest of Coalinga. Station corrections were determined by inversion of a subset of the P-wave data. Hypocenters determined with this model fit the data with typical rms residual

of 0.1 seconds. The locations are undoubtedly more precise in relation to each other than in an absolute sense. In particular, the absolute depth of the solutions is not well constrained.

REFERENCES CITED

Allen, R. V., 1982, Automatic phase pickers: Their present use and future prospects: Bulletin, Seismological Society of America, v. 72, no. 6, p. 5225-5242.

Fowkes, E. J., 1982, An Educational Guidebook to the Geologic Resources of the Coalinga District, California, Westhills College, Coalinga, CA.

Lee, W. H. K., and Lahr, J. C., 1975, HYP071 (Revised): A computer program for determining hypocenter, magnitude and first motion pattern of local earthquakes: U.S. Geological Survey Open-File Report 75-311.

Walter, A. W., and Mooney, W. D., 1980, Crustal structure of the Diablo and Gabilan Ranges, central California: a reinterpretation of existing data: Bulletin, Seismological Society of America, v. 72, no. 5, p. 1567-1590.

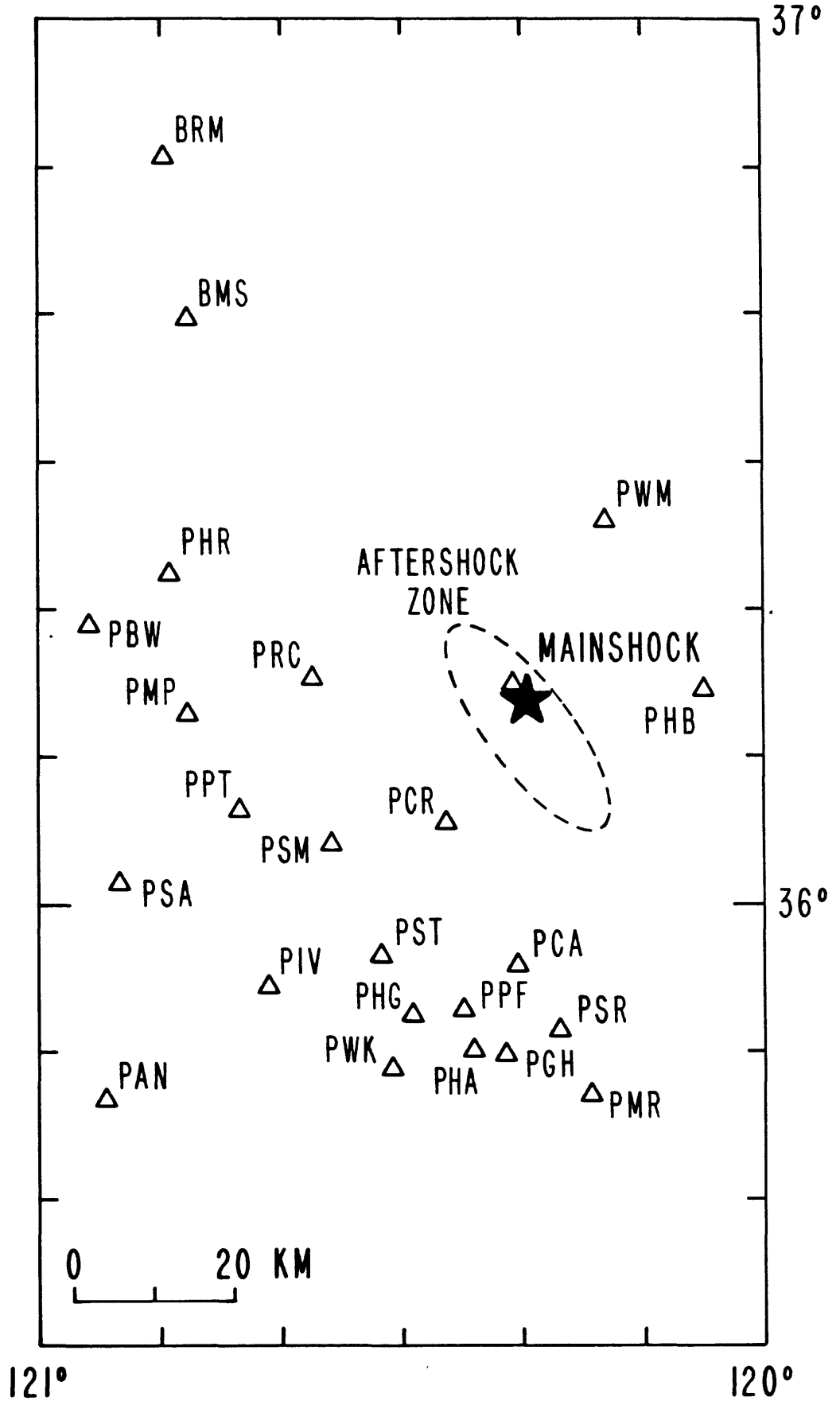

Figure 1: U.S. Geological Survey telemetered microearthquake network in the Coalinga region. The approximate locations of the aftershock zone and mainshock are indicated.

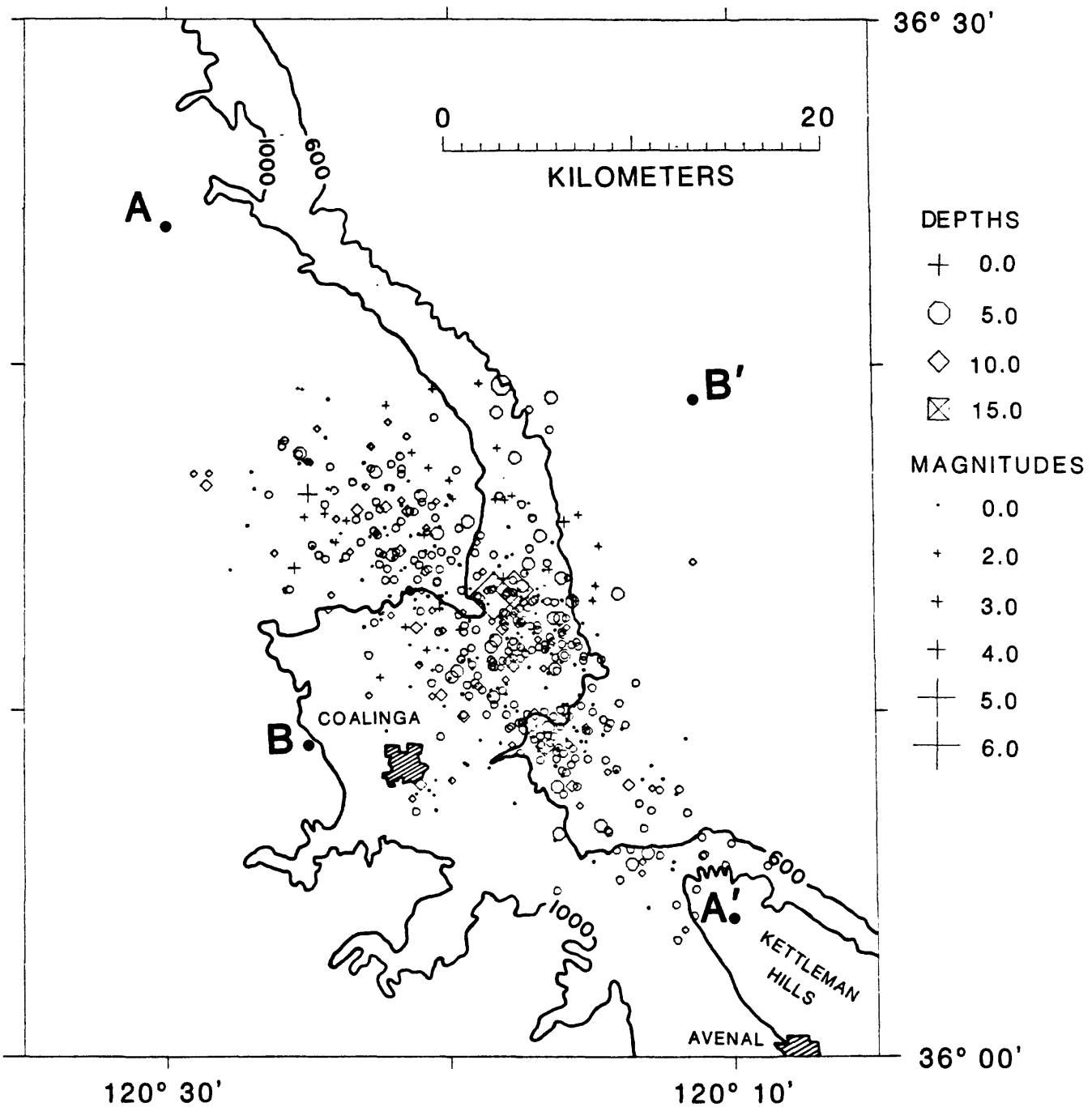

Figure 2: Epicenters of the mainshock (largest diamond symbol) and selected aftershocks for the period May 2-12, 1983. Aftershocks selected were observed on at least 10 of the seismograph stations shown in figure 1. Symbol type represents hypocentral depth range as indicated in key. Generalized 600-foot and 1000-foot elevation contours are shown.

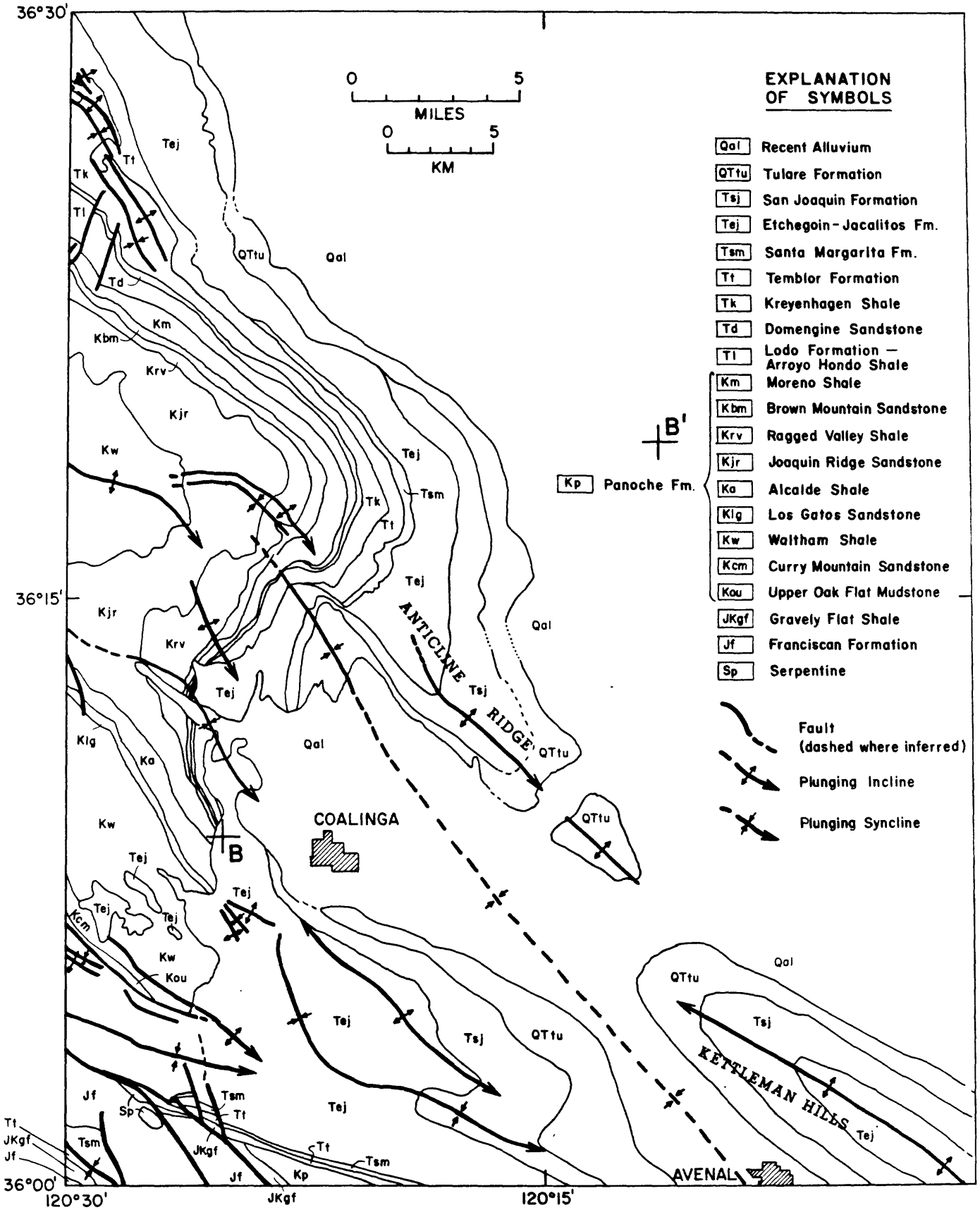

Figure 3: Simplified geologic map of the Coalinga area generalized from E. J. Fowkes, An Educational Guidebook to the Geologic Resources of the Coalinga District, California, Westhills College, Coalinga, CA (1982).

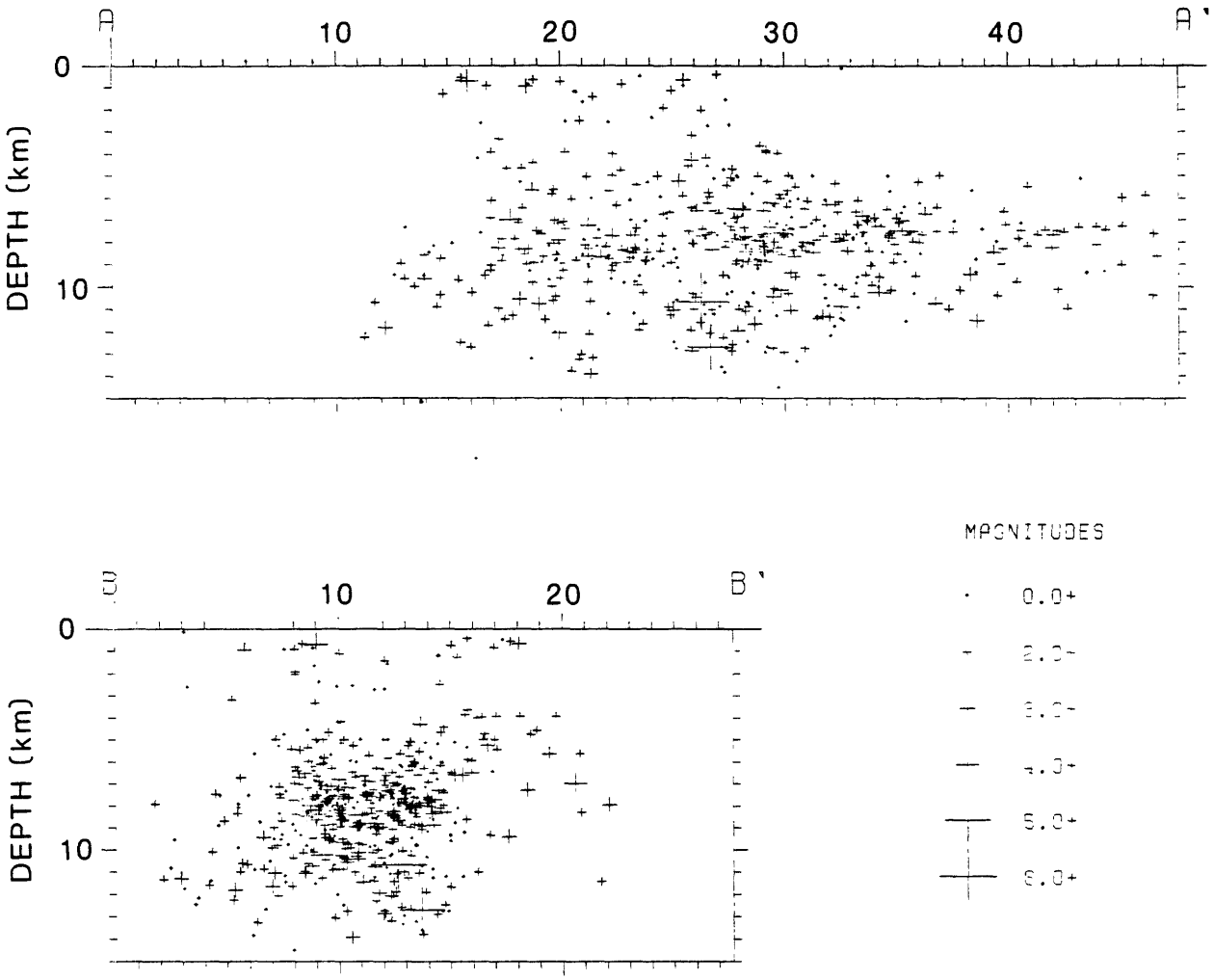

Figure 4: Cross-sectional views without vertical exaggeration of the earthquake set shown in figure 2. Hypocenters are projected onto vertical planes defined by the endpoints shown in figure 2.

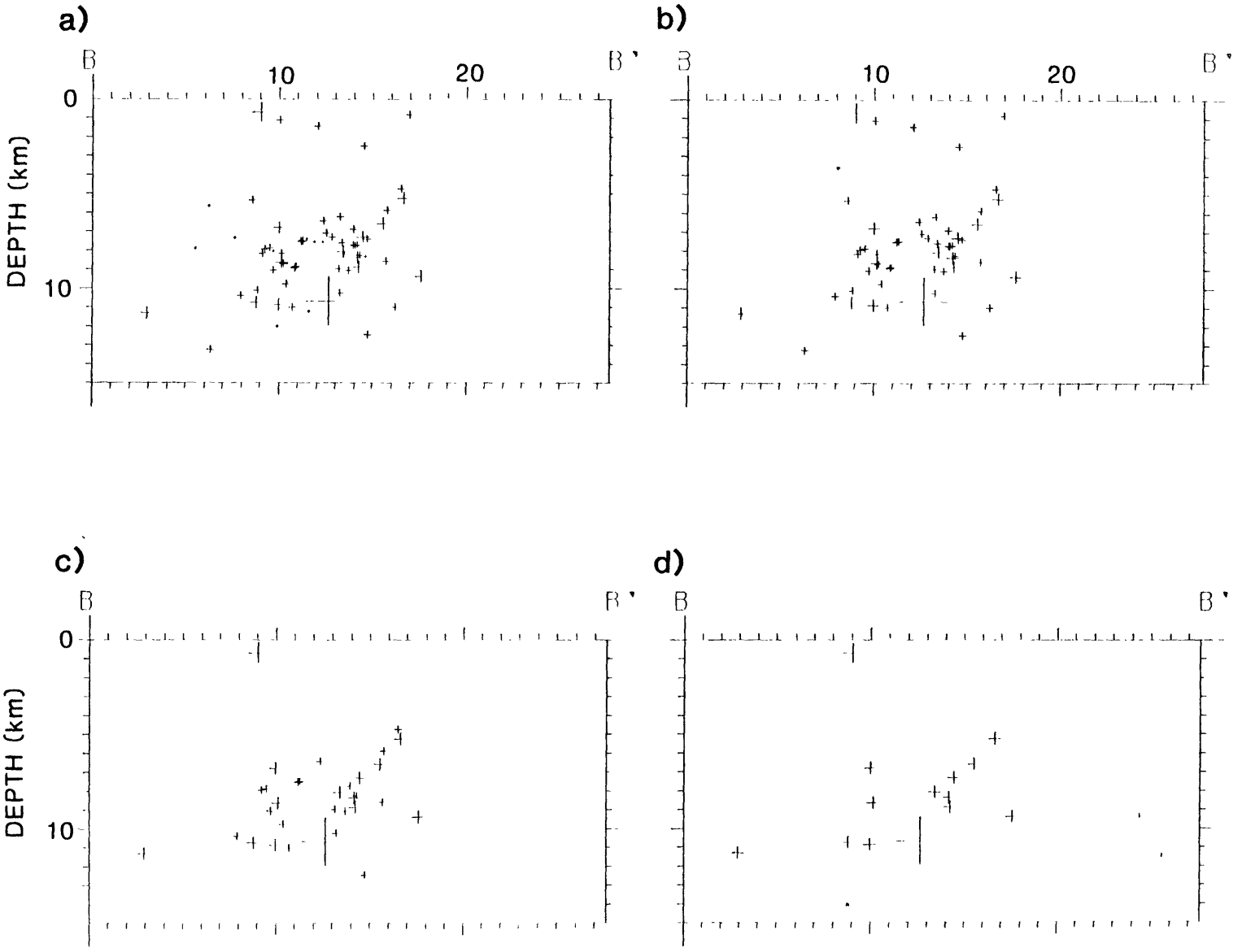

Figure 5: Transverse cross-sectional view of aftershocks for the first 21 hours of the sequence, for selected lower magnitude thresholds. (a) $M \geq 1.5$; (b) $M \geq 2.0$; (c) $M \geq 2.5$; (d) $M > 3.0$.

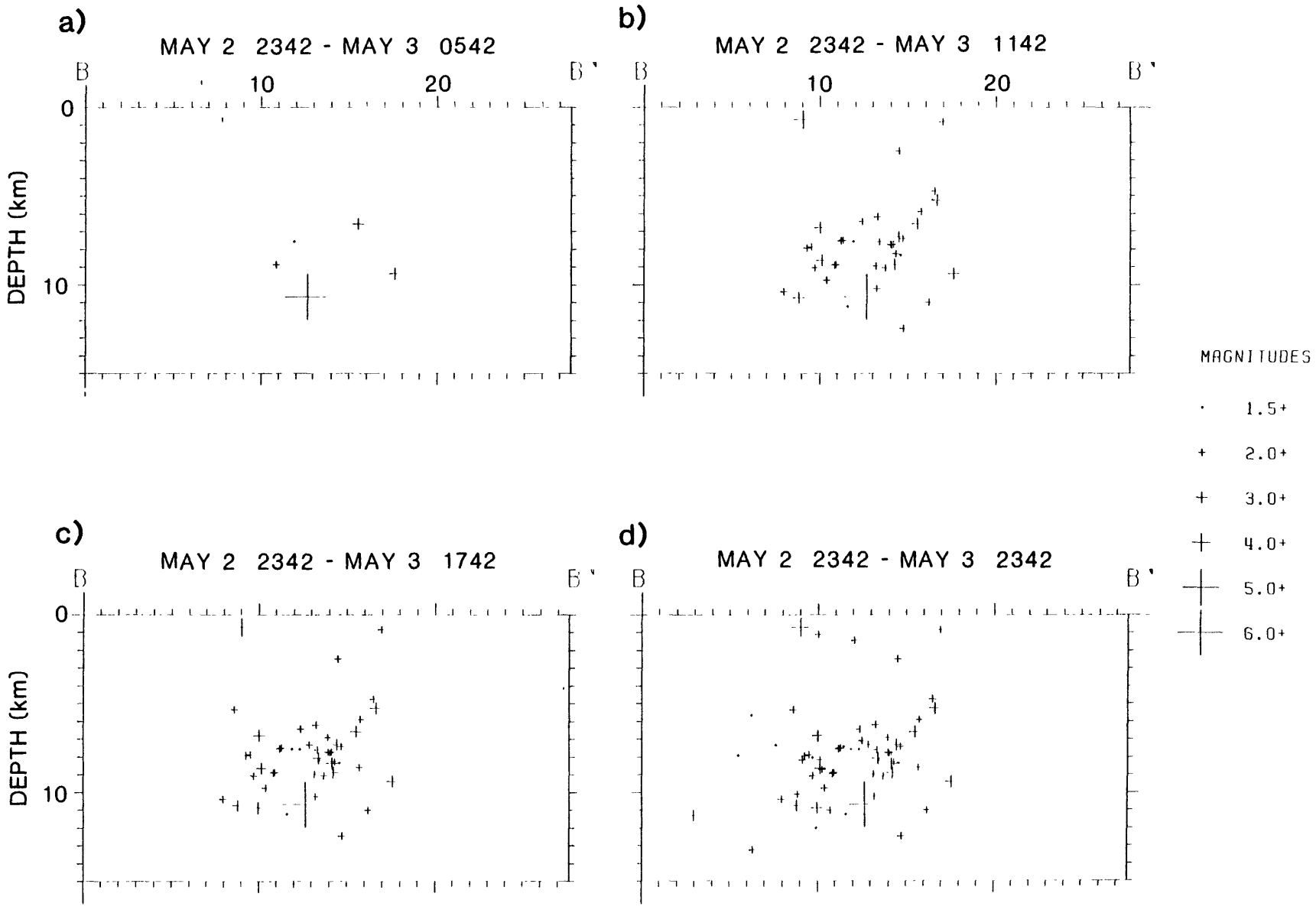

Figure 6: Transverse cross-sectional views of aftershocks ($M \geq 1.5$) during the first 24 hours of the sequence. (a) first 6 hours; (b) first 12 hours; (c) first 18 hours; (d) first 24 hours.

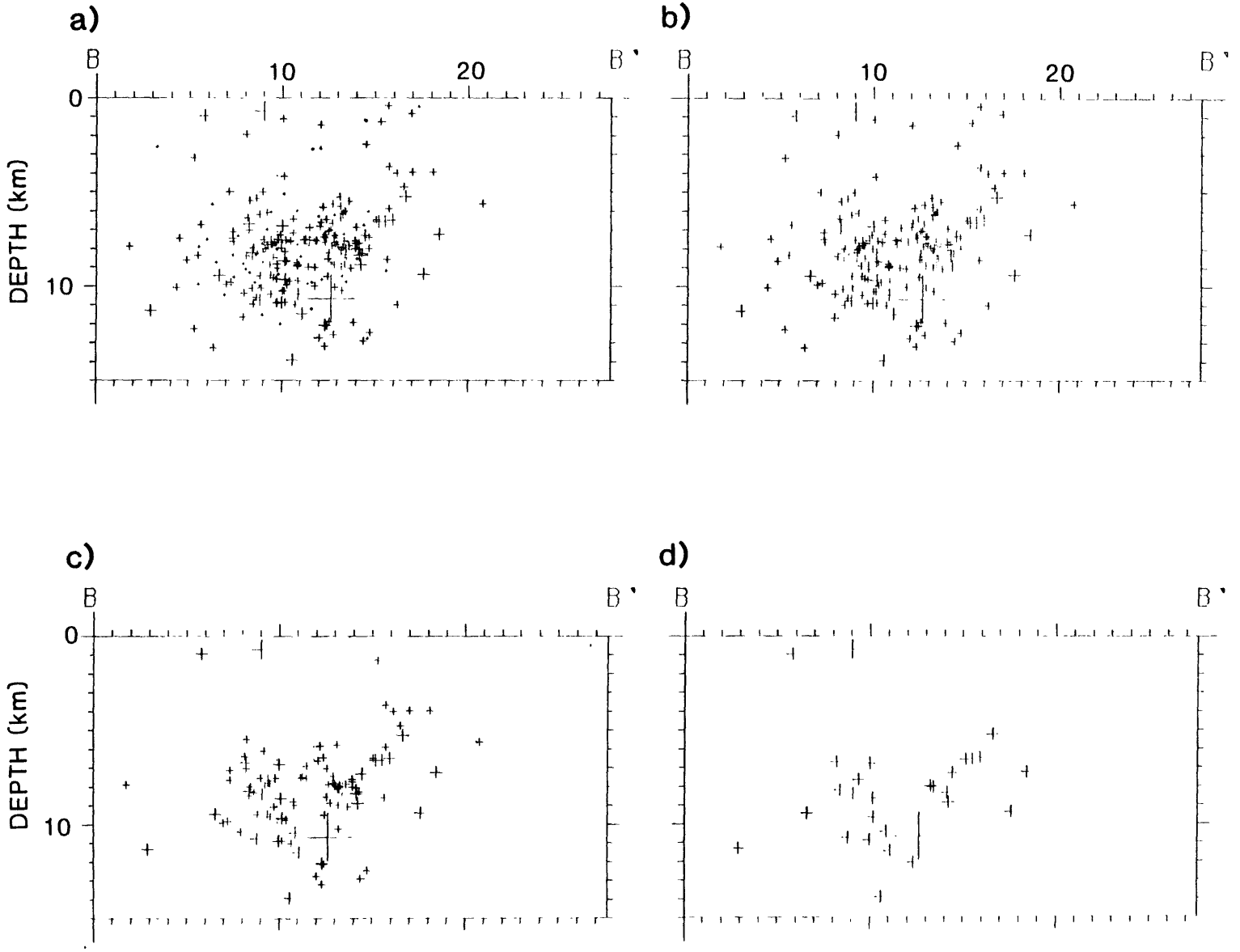

Figure 7: Transverse cross-sectional views of aftershocks for the first 4 days of the sequence, for selected lower magnitude thresholds (a) M $\geq$ 1.5; (b) M $\geq$ 2.0; (c) M $\geq$ 2.5; (d) M $\geq$ 3.0

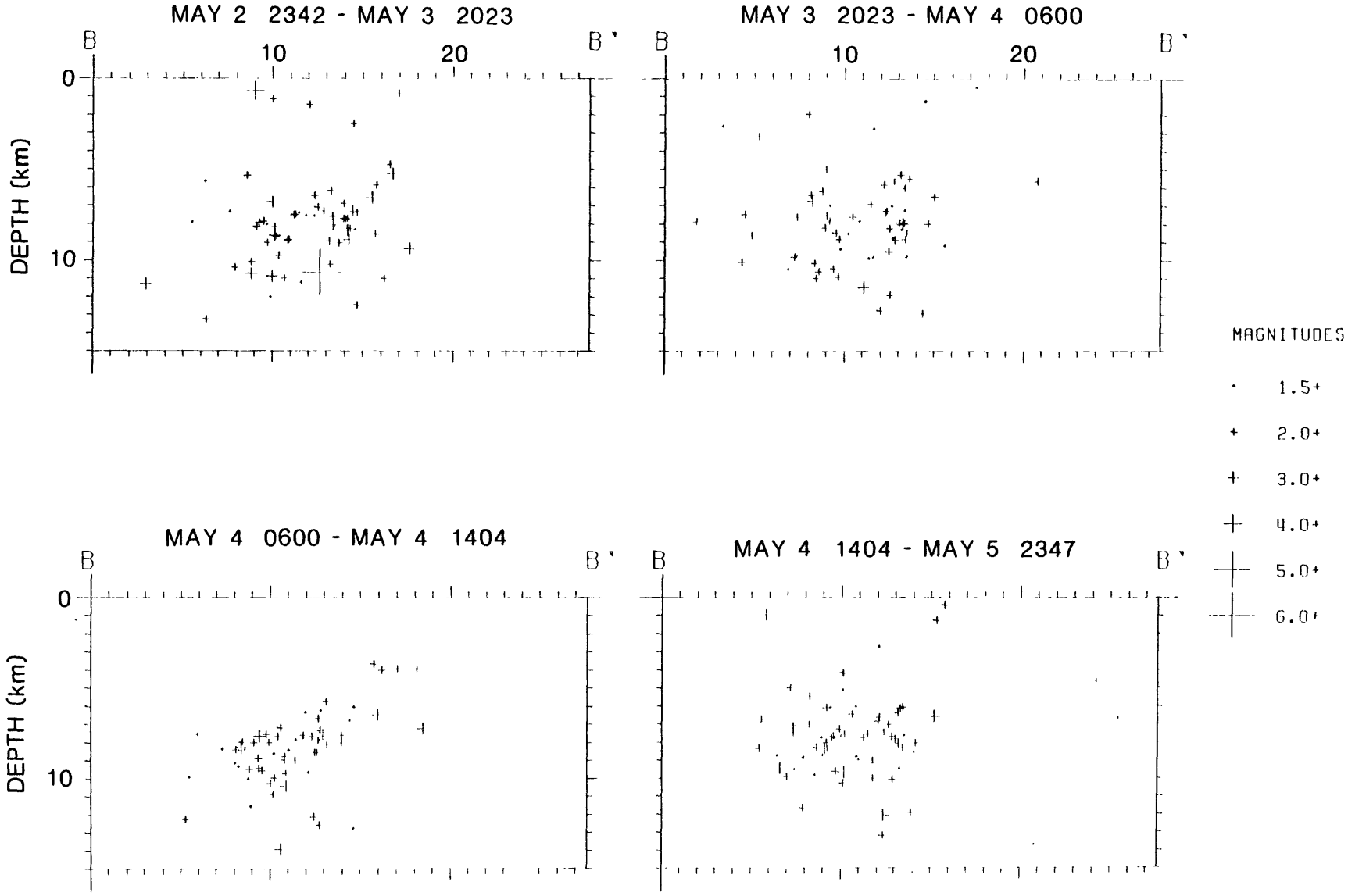

Figure 8: Transverse cross-sectional views of aftershocks for the first 4 days of the sequence, for four sequential intervals with equal number of events in each interval.

ANALOG STRONG MOTION DATA AND PROCESSED MAIN EVENT RECORDS OBTAINED BY U.S. GEOLOGICAL SURVEY NEAR COALINGA, CALIFORNIA

R. Maley, G. Brady, E. Etheridge, D. Johnson, P. Mork, and J. Switzer

U.S. Geological Survey
345 Middlefield Road
Menlo Park, CA 94025

The moderate earthquake of May 2, 1983 near Coalinga, California (M = 6.5) triggered some 37 strong-motion accelerographs maintained as part of the national strong-motion network operated by the U.S. Geological Survey. The accelerographs closest to the epicenter were those at the Pleasant Valley pump plant. This array of accelerographs, purchased by the U.S. Bureau of Reclamation and installed by the U.S. Geological Survey, recorded the main event at an epicentral distance of about 9 km. Other accelerograph stations triggered at greater distances include those located at: Bear Valley, Veterans Administration Hospital in Fresno, Dos Amigos pump plant, and several dams associated with the Army Corps of Engineers and the U.S. Bureau of Reclamation.

Following the earthquake eight aftershock accelerographs were installed in the epicentral area and in the city of Coalinga. As of May 12, 1983, more than 50 records were obtained from these temporary instruments including recordings of the magnitude 5.1 earthquake of May 9, 0249 UTC. Numerous aftershocks were also recorded at the Pleasant Valley pump plant.

Main Event Data

The nearest accelerograph records were recovered 9 km from the earthquake epicenter at the Pleasant Valley Pump Plant, a facility that takes water from a feeder line of the California Aqueduct for transfer into the Coalinga Canal (fig. 1). Records were obtained from instruments on the basement floor, approximately 17 ft (5.2 m) below grade of the building site, and at the switchyard (ground site) which is 280 ft (85.3 m) southwest of the plant at the top of a slope about 70 ft (21.3 m) above the plant grade. The switchyard instrument is mounted on a 4 ft x 4 ft concrete pad with a small metal shelter 120 ft (36.6 m) northwest of the discharge pipeline.

Peak accelerations were 0.54 g horizontal and 0.37 g vertical at the switchyard and 0.33 g horizontal and 0.22 g vertical in the basement of the pump plant (Table 1 and fig. 2). This ratio of corresponding acceleration values at the two sites was consistent for larger aftershocks as well as for the Three Rocks earthquake of 3 August 1975, 0635 UTC. Note in figure 2 that four upward peaks on the 075° component from the switchyard were slightly clipped due to mis-alignment of the accelerometer mass resulting in subsequent large deflections being restricted by the transducer frame. Comparison of this record with that from the basement indicates little data was lost. Reconstruction of these peaks will be carried out during computer processing.

The instrumentation was interconnected for starting and timing signals and although the WWVB radio signal failed during the strong shaking, a real-time base was recovered by extrapolation from a clear radio signal recorded 60 s after triggering. From this radio code, trigger time for the two

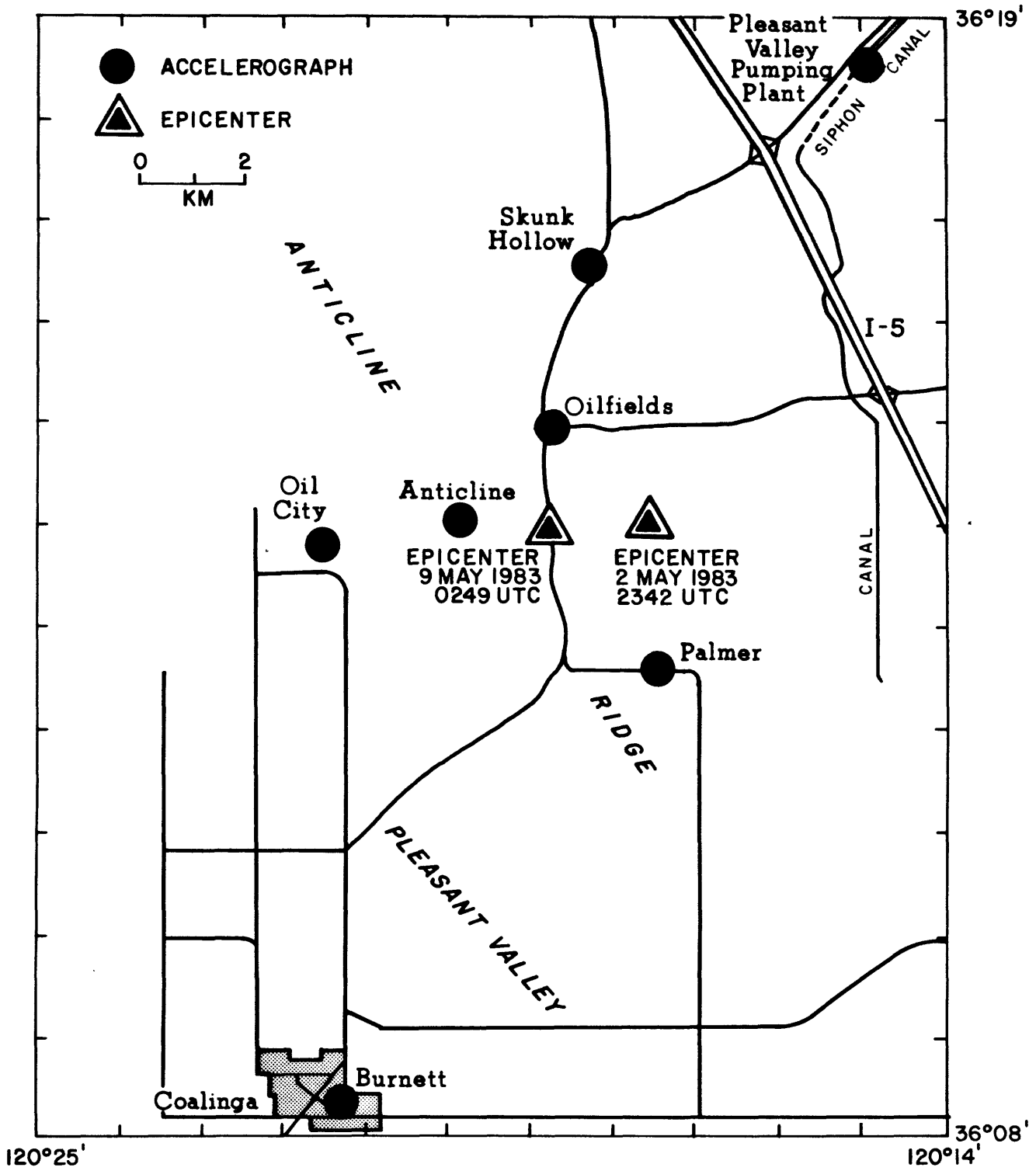

Figure 1: Map showing instrument locations and epicenters of the main shock (M_L = 6.5) and large aftershock (M_L = 5.1).

Table 1. Near-field accelerograph records from the Coalinga earthquake.

Station	Coordinates	Hypocentral distance (km)	Direction	Peak Acceleration (g)
Pleasant Valley pump plant	36.308° lat. 120.249° long.	14.0		
Switchyard			135°	0.54
			Up	.37
			045°	.45
Basement			135°	.28
			Up	.22
			045°	.33

Table 2. Distant accelerograph records fro the Coalinga earthquake.

Station	No. of records	Approximate distance (km)
Bear Valley array		75-100
Bear Valley fire station	1	
James Ranch	1	
Stone Canyon west	1	
Webb Ranch	1	
Williams Ranch	1	
VA Hospital (Fresno)	1	75
Dos Amigos pump plant	2	90
Buchanan Dam	5	95
Hidden Dam	4	95
New Melones Dam	6	185
Pine Flat Dam	3	110
Lake Success Dam	6	125
Terminus Dam	3	120

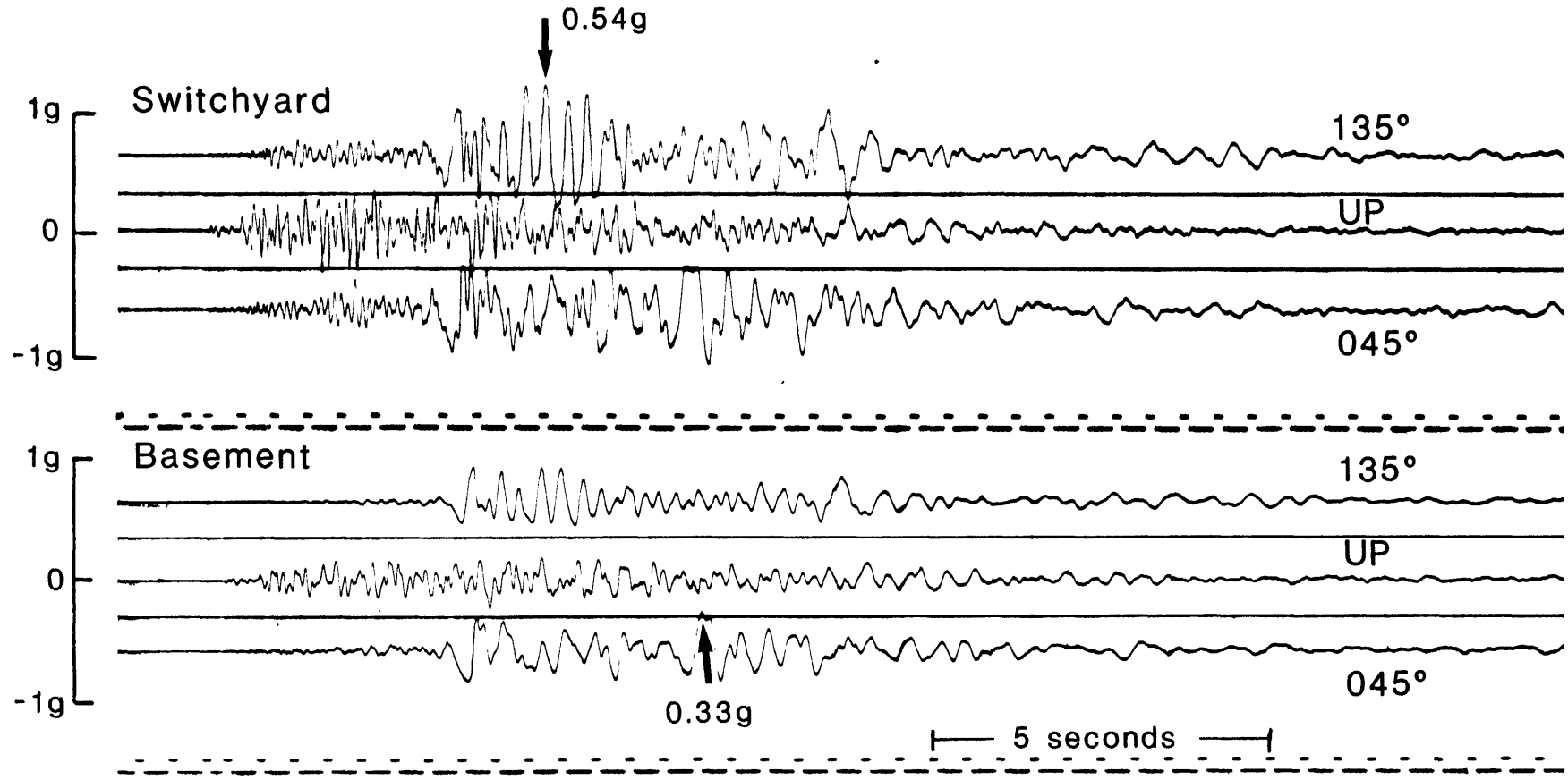

Figure 2: Strong-motion records from Pleasant Valley pump plant: Main shock.

accelerographs was calculated at 42 m 42.04 ± .03 s approximately 3.44 s after origin time. The hypocentral distance was about 14 km and S-wave minus trigger time was 4.24 s.

Strong-motion instruments were also located at the first floor level and on the roof at the pump plant but due to numerous false triggerings prior to the earthquake no recordings were obtained from these units. This station has had a long history of serious operational problems due to obsolete instrumentation, consequently the Bureau of Reclamation supplied four new units following the 25 October, 1982 earthquake near Coalinga. The new accelerographs were installed in late February. Internal crane operations caused numerous false triggerings of the instruments (roof accelerations as large as 0.09 g were generated). These false triggers generated by crane operations and some "electronic" triggers resulted in no records from two upper level instruments. Table 2 lists other stations in the network operated by the U.S. Geological Survey that generated records of the main shock.

Processed (Preliminary) Main Event Data

Preliminary digitization and processing has been completed for the main-event records obtained at the Pleasant Valley pump plant. Additional processing of the records will be completed subsequent to this report. Acceleration, velocity, and displacement time histories (figs. 3 and 4) and corresponding response spectra (figs. 5 and 6) are included.

The records obtained from the basement and the switchyard of the Pleasant Valley pump plant were commercially digitized (IOM-TOWILL, Santa Clara, CA) on a trace-following laser scanner. The digitizer's least count is one micrometer (10^{-6} m) and its RMS error in digitizing traces of the photographic quality of these records is approximately 10 μm (Fletcher and others, 1980). Peak-to-peak excursions on the original record reached 1.8 cm. Each record was digitized in six sections, or frames, of about 9.5 cm length, and subsequently reassembled to recover the record of 58 s total duration (Porter and others, 1978). Each trace was digitized at approximately 600 samples per second (sps).

Computer processing carried out at the National Strong-Motion Data Center in Menlo Park included linear interpolation to obtain equally spaced samples at 600 sps, time domain convolution to remove instrument response and prevent aliasing errors, and decimation to 200 sps. A low-cut, or high-pass, Butterworth filter, bidirectional, of order 8, with corner frequency of 0.1 Hz, was selected to remove all periods longer than 10 s. The selection of the long-period cut-off of 10 s was based on a desire to include all periods associated with the faulting duration of approximately 7 s (estimated from the strong-motion duration of the records). The displacement and spectral plots indicate the presence of 7-8 s content, which at this stage is not considered long-period noise. There is no evidence of any 10-s content which might have indicated an incompatability between the records, the 10-s content therein, and the 10-s corner frequency of the Butterworth filter.

The long-period content in the displacements between triggering and S-wave arrival 3-1/2 s later have, in the past, been considered as indicating the presence of noise, or an incompatibility between record and filter. Two items help to remove this concern. One is the similarity between the

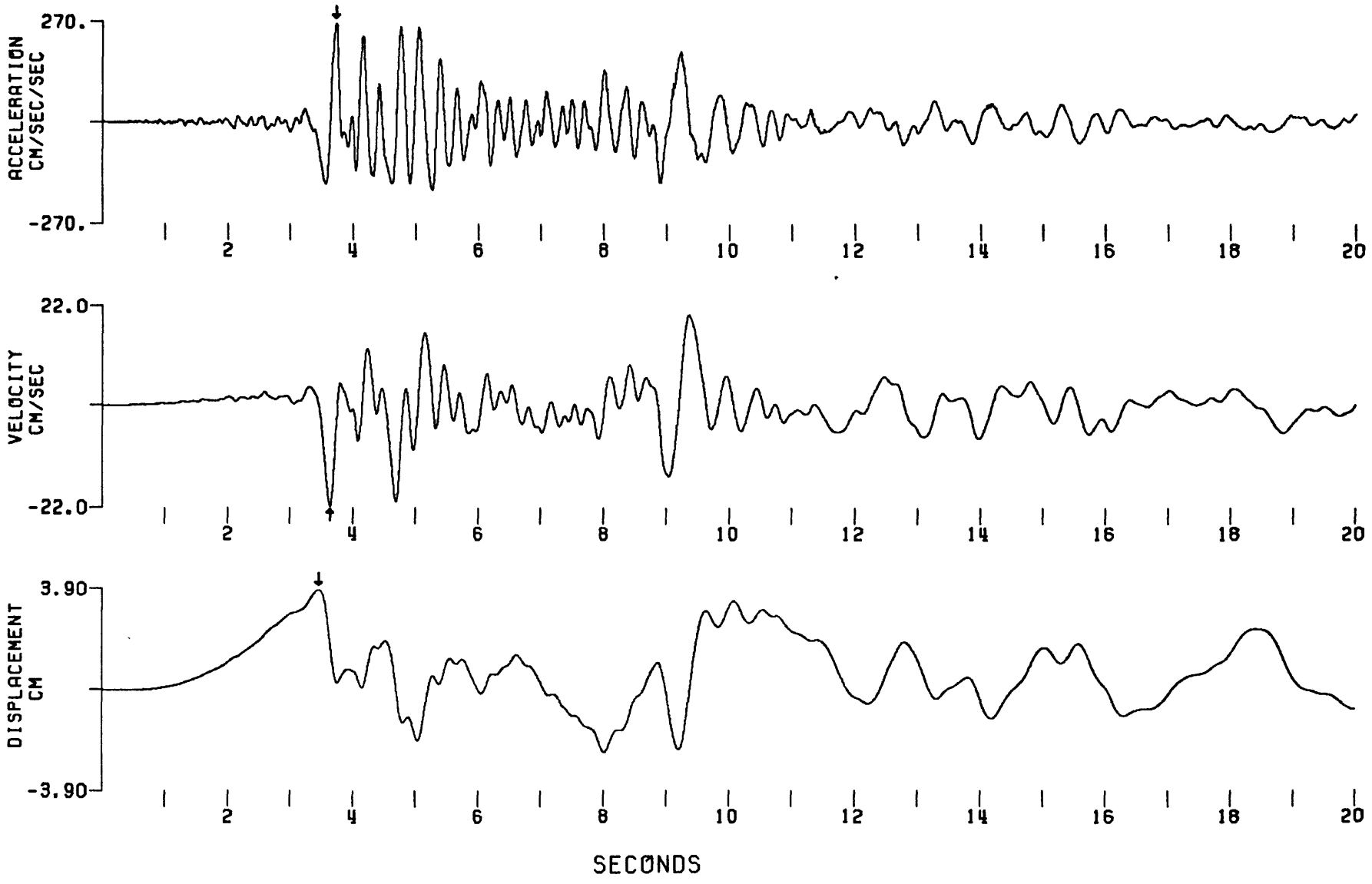

Figure 3a: Corrected acceleration, velocity and displacement time histories (200 sps) for earthquake of 2 May 1983, (2342 UTC) as recorded on 135^{0} horizontal component at Pleasant Valley pumping plant (basement). Peak values are: acceleration = 267.28 cm/s^{2}, velocity = 21.71 cm/s, displacement = 3.86 cm (band pass filtered 0.1 to 50 Hz, Butterworth order 8 lowcut, cosine taper 50 Hz highcut).

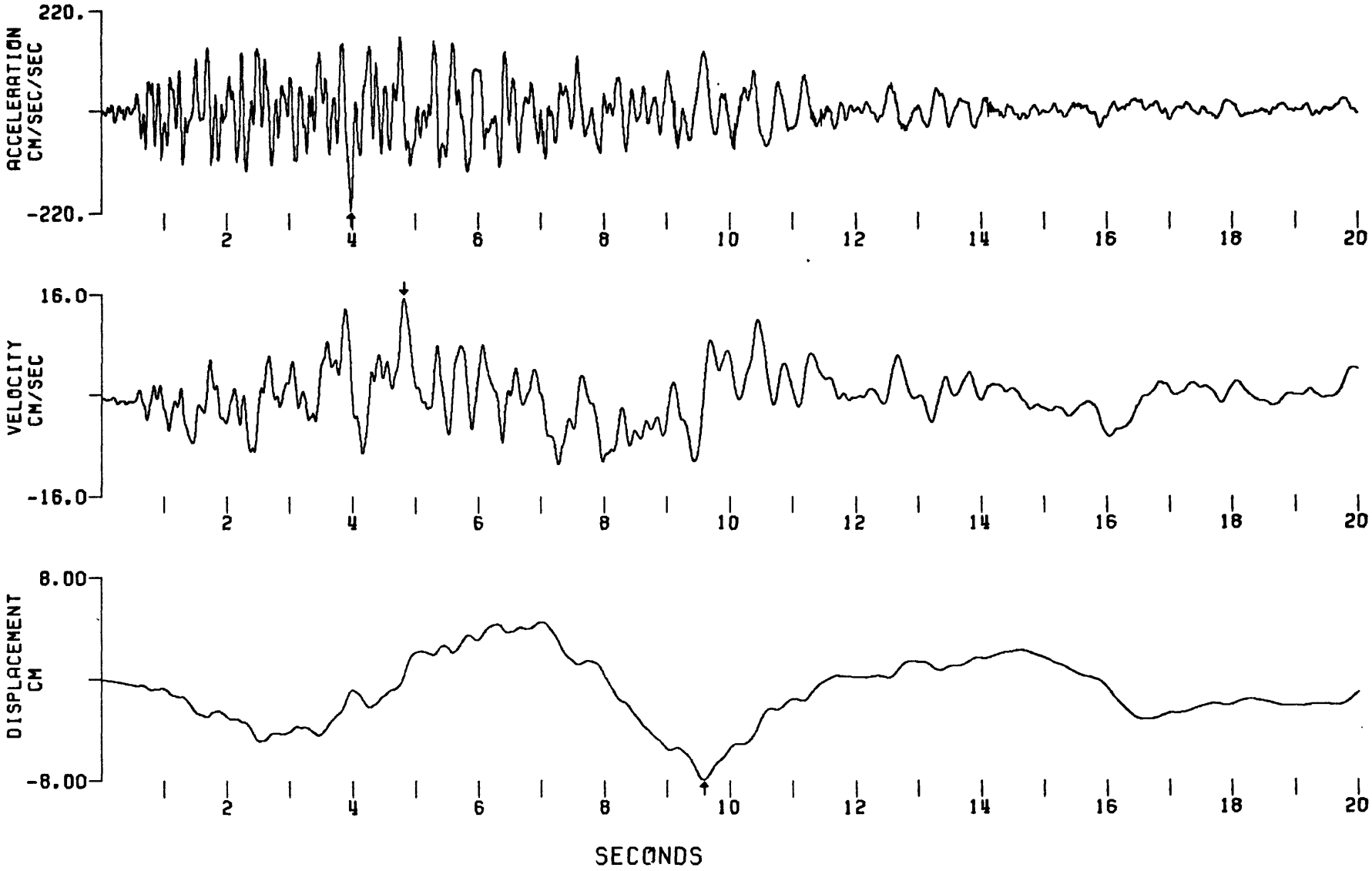

Figure 3b: Corrected acceleration, velocity and displacement time histories (200 sps) for earthquake of 2 May 1983, (2342 UTC) as recorded on vertical component at Pleasant Valley pumping plant (basement). Peak values are: acceleration = 216.26 cm/s^2, velocity = 15.53 cm/s, displacement = 7.94 cm (band pass filtered 0.1 to 50 Hz, Butterworth order 8 lowcut, cosine taper 50 Hz highcut).

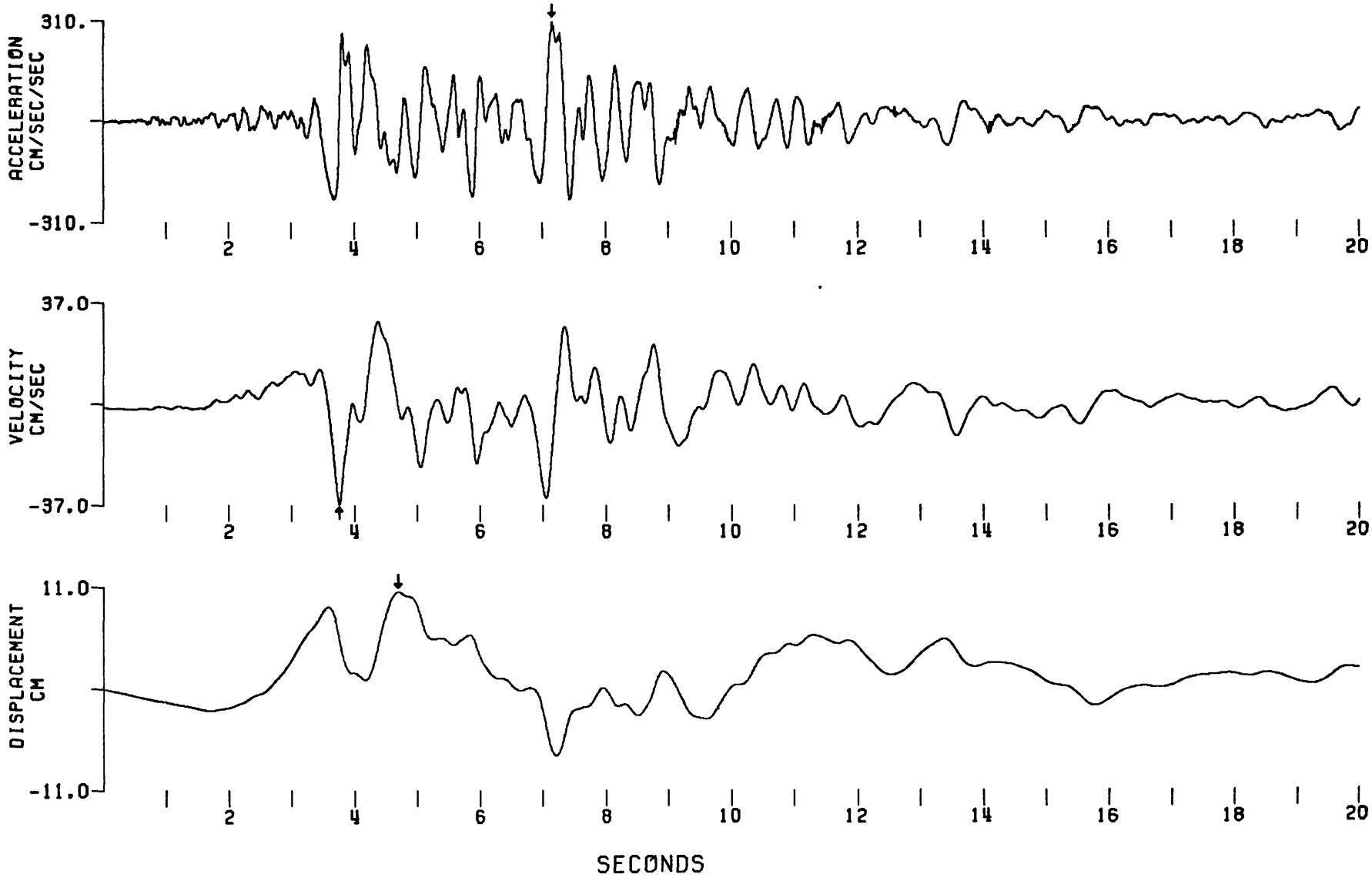

Figure 3c: Corrected acceleration, velocity and displacement time histories (200 sps) for earthquake of 2 May 1983, (2342 UTC) as recorded on 045^{0} horizontal component at Pleasant Valley pumping plant (basement). Peak values are: acceleration = 306.69 cm/s^{2}, velocity = 36.74 cm/s, displacement = 10.54 cm (band pass filtered 0.1 to 50 Hz, Butterworth order 8 lowcut, cosine taper 50 Hz highcut).

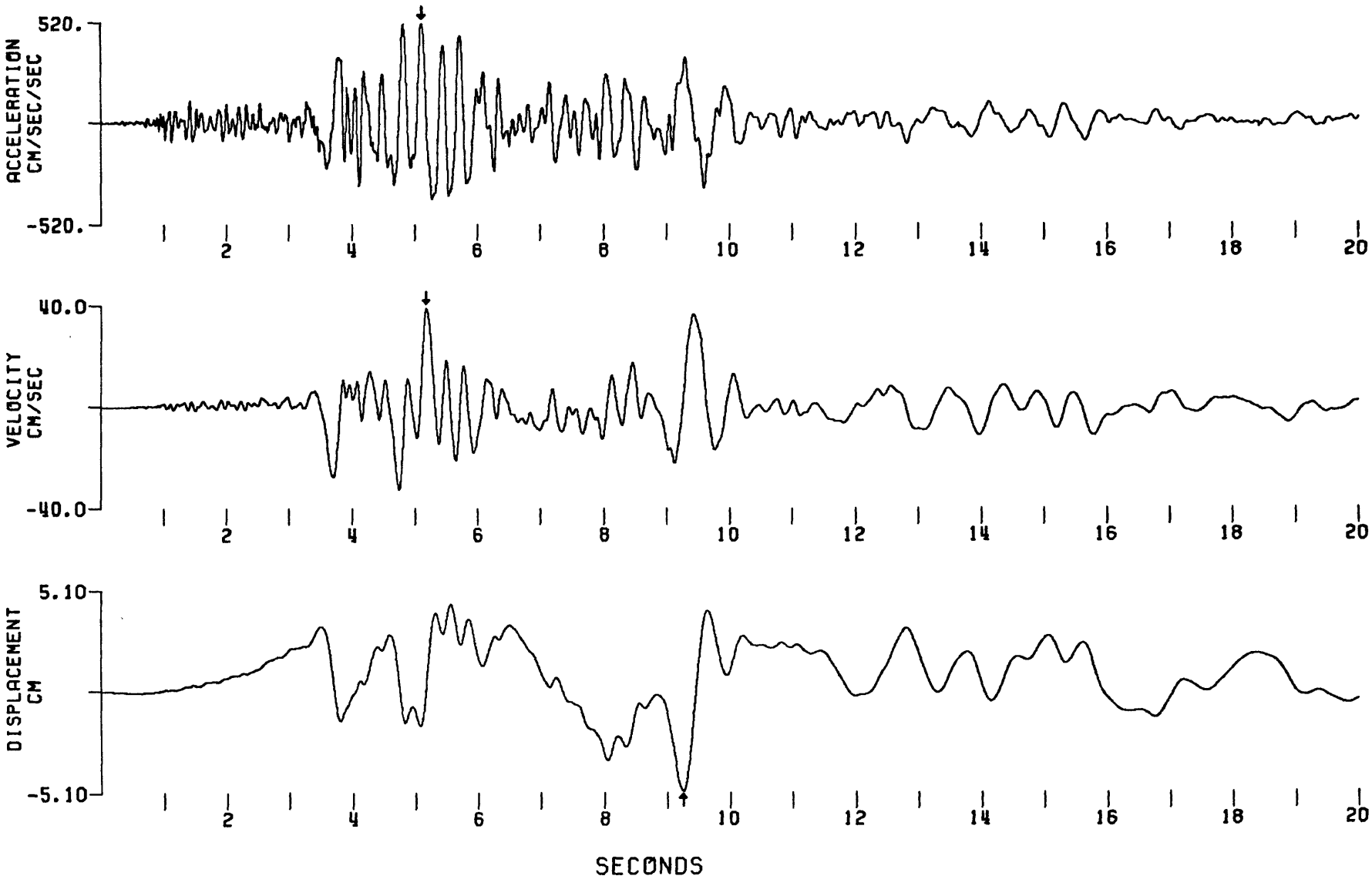

Figure 4a: Corrected acceleration, velocity and displacement time histories (200 sps) for earthquake of 2 May 1983, (2342 UTC) as recorded on 135° horizontal component at Pleasant Valley pumping plant (switch-yard). Peak values are: acceleration = 514.43 cm/s^2, velocity = 39.22 cm/s, displacement = 5.05 cm (band pass filtered 0.1 to 50 Hz, Butterworth order 8 lowcut, cosine taper 50 Hz highcut).

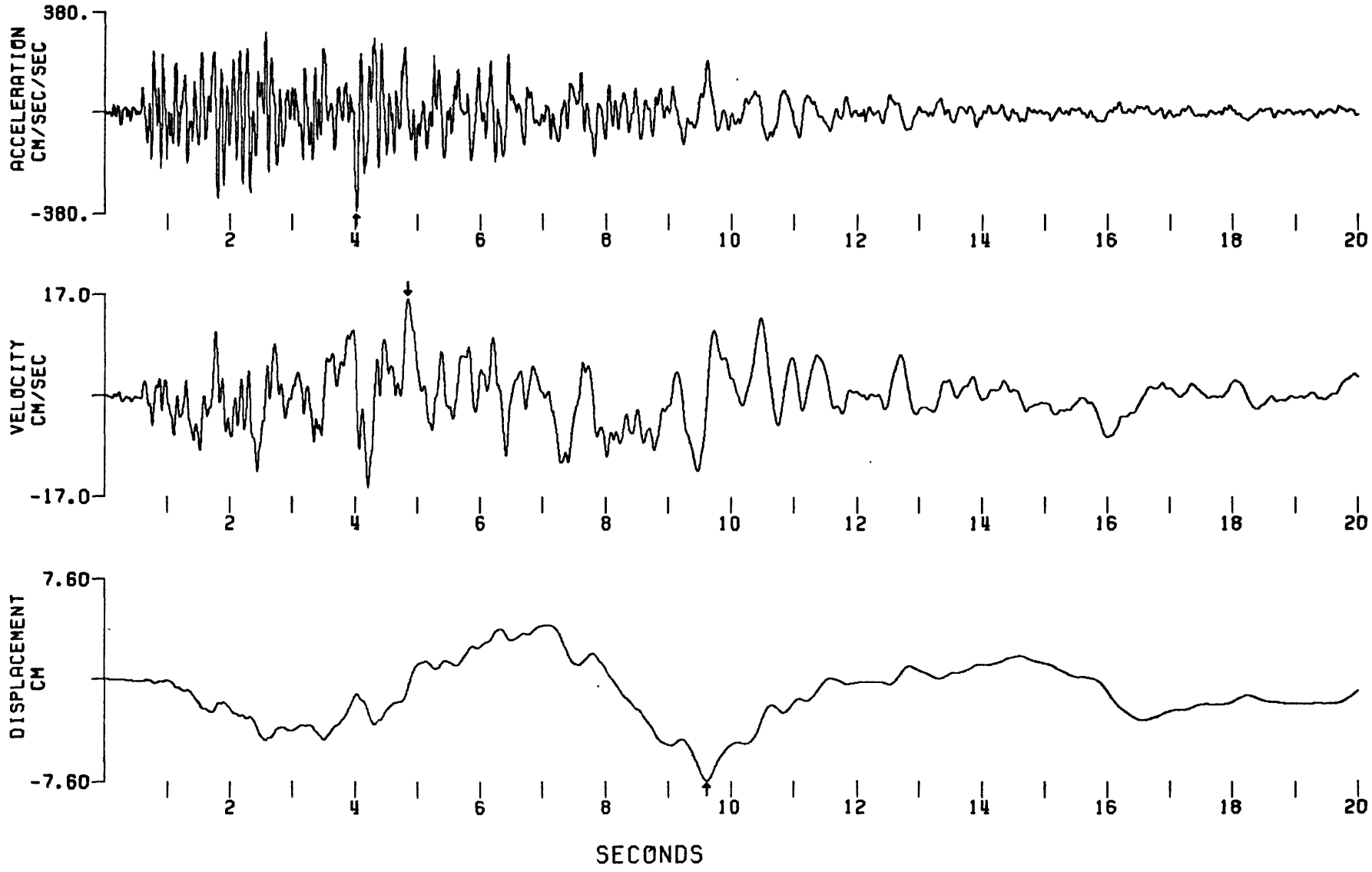

Figure 4b: Corrected acceleration, velocity and displacement time histories (200 sps) for earthquake of 2 May 1983, (2342 UTC) as recorded on vertical component at Pleasant Valley pumping plant (switchyard). Peak values are: acceleration = -371.13 cm/s^2, velocity = 16.40 cm/s, displacement = -7.58 cm (band pass filtered 0.1 to 50 Hz, Butterworth order 8 lowcut, cosine taper 50 Hz highcut).

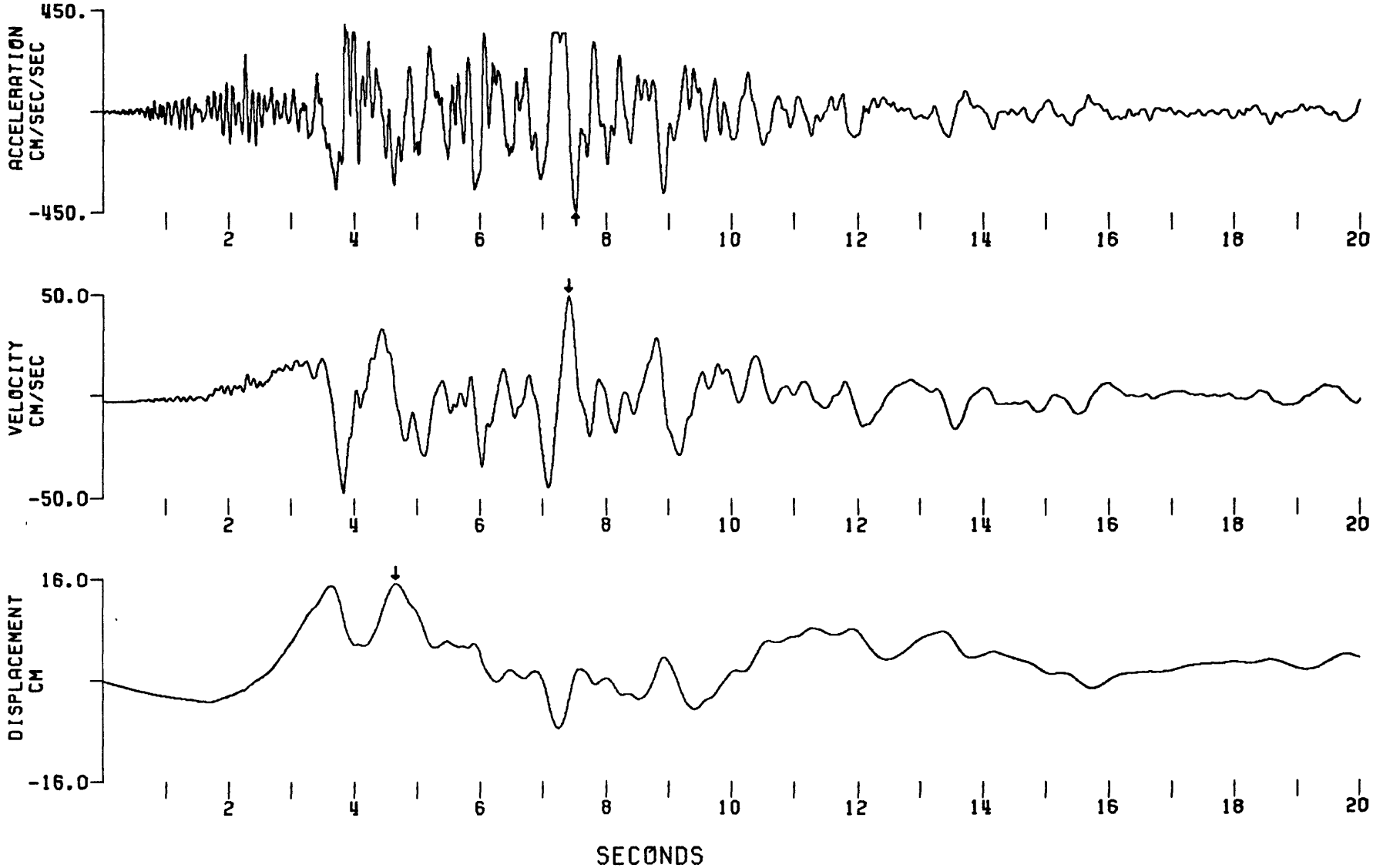

Figure 4c: Corrected acceleration, velocity and displacement time histories (200 sps) for earthquake of 2 May 1983, (2342 UTC) as recorded on 045° horizontal component at Pleasant Valley pumping plant (switch-yard). Peak values are: acceleration = -440.56 cm/s^2, velocity = 49.96 cm/s, displacement = 15.46 cm (band pass filtered 0.1 to 50 Hz, Butterworth order 8 lowcut, cosine taper 50 Hz highcut).

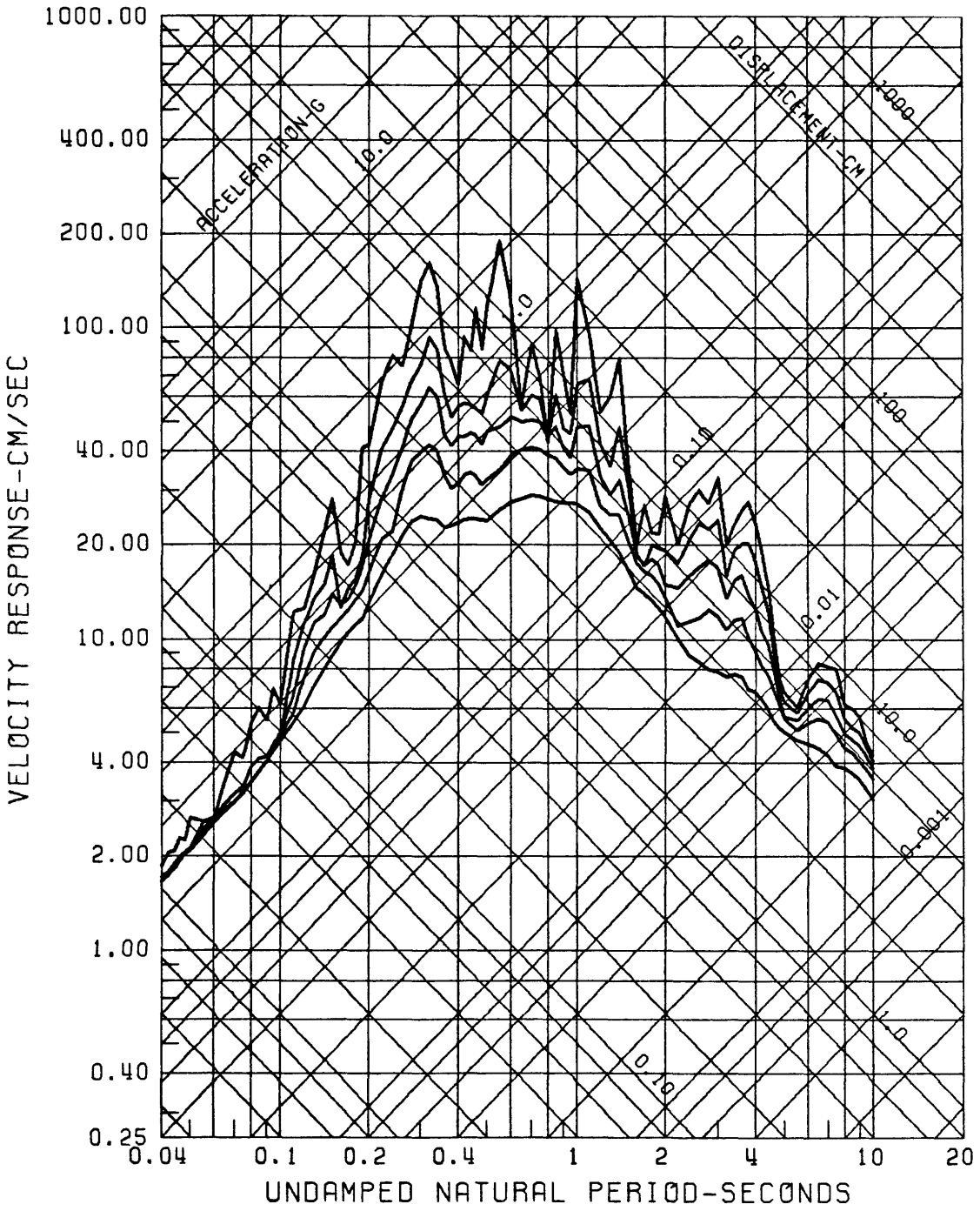

Figure 5a: Pseudo-velocity response curves (0, 2, 5, 10, 20 percent critical damping) computed for earthquake of 2 May 1983 (2342 UTC) as recorded on 135° horizontal component at Pleasant Valley pumping plant (basement). (Band pass filtered 0.1 to 50 Hz, Butterworth order 8 lowcut, cosine taper 50 Hz highcut, U.S. National Strong-Motion Data Center).

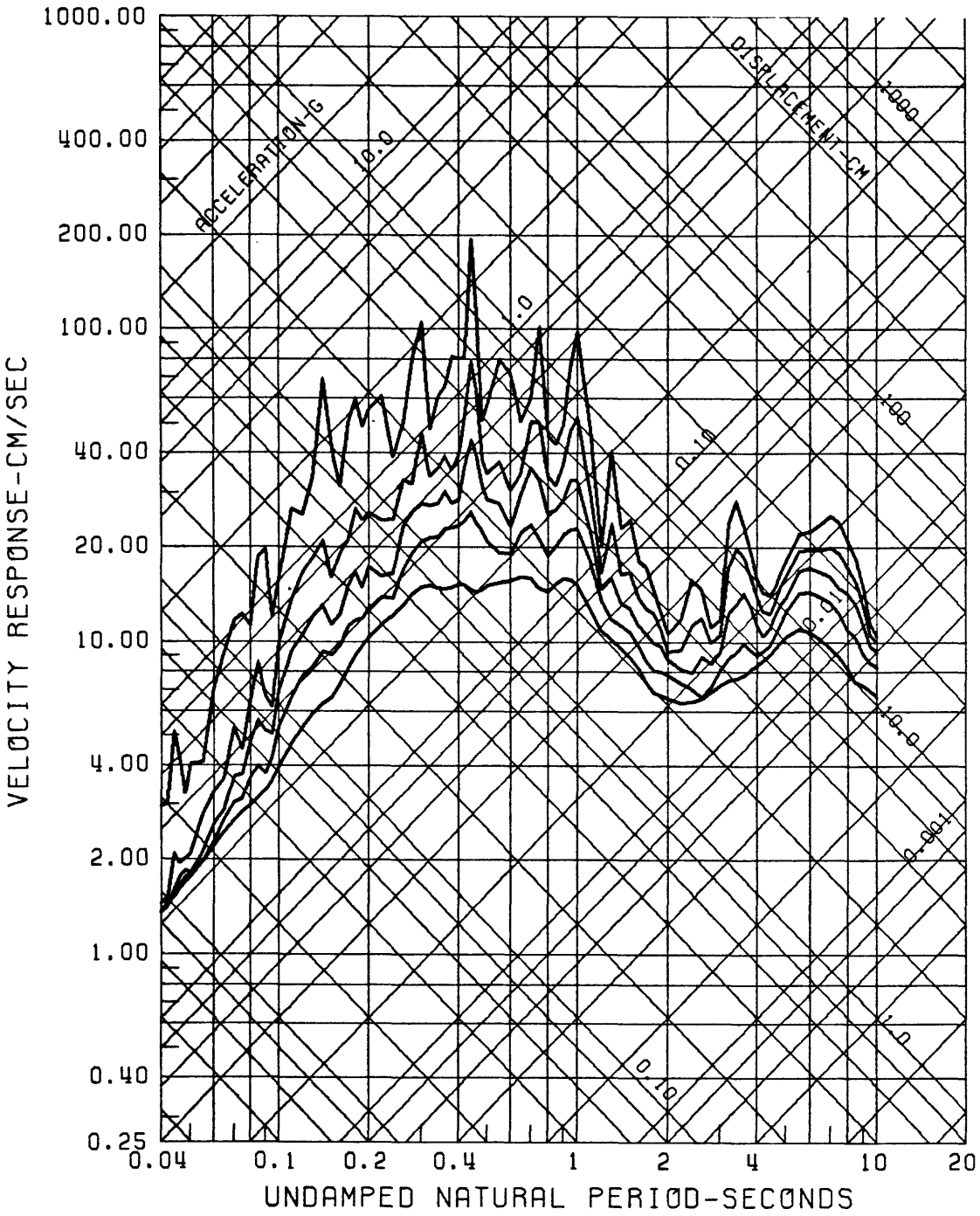

Figure 5b: Pseudo-velocity response curves (0, 2, 5, 10, 20 percent critical damping) computed for earthquake of 2 May 1983 (2342 UTC) as recorded on vertical component at Pleasant Valley pumping plant (basement). (Band pass filtered 0.1 to 50 Hz, Butterworth order 8 lowcut, cosine taper 50 Hz highcut), U.S. National Strong-Motion Data Center).

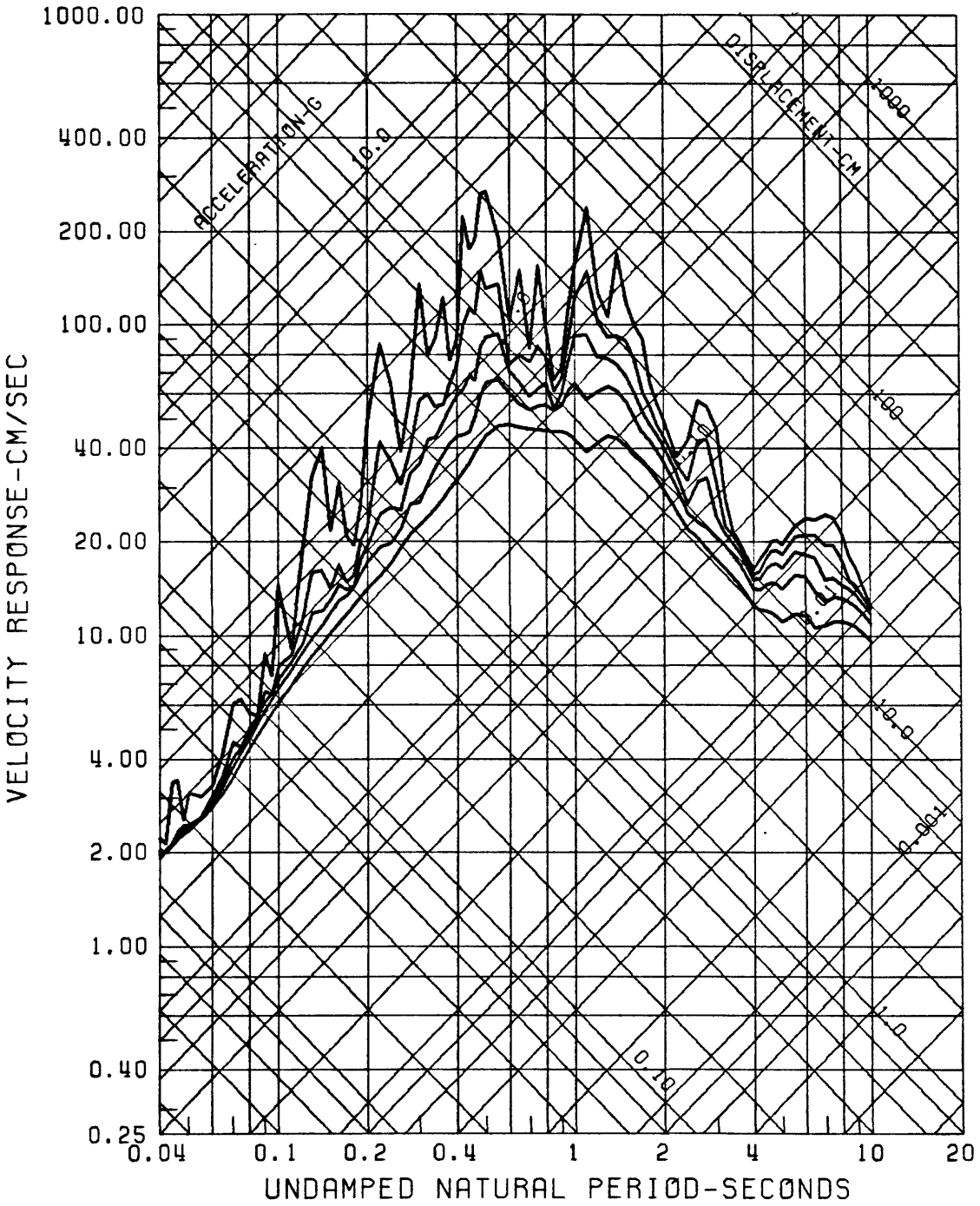

Figure 5c: Pseudo-velocity response curves (0, 2, 5, 10, 20 percent critical damping) computed for earthquake of 2 May 1983 (2342 UTC) as recorded on 045° horizontal component at Pleasant Valley pumping plant (basement). (Band pass filtered 0.1 to 50 Hz, Butterworth order 8 lowcut, cosine taper 50 Hz highcut, U.S. National Strong-Motion Data Center).

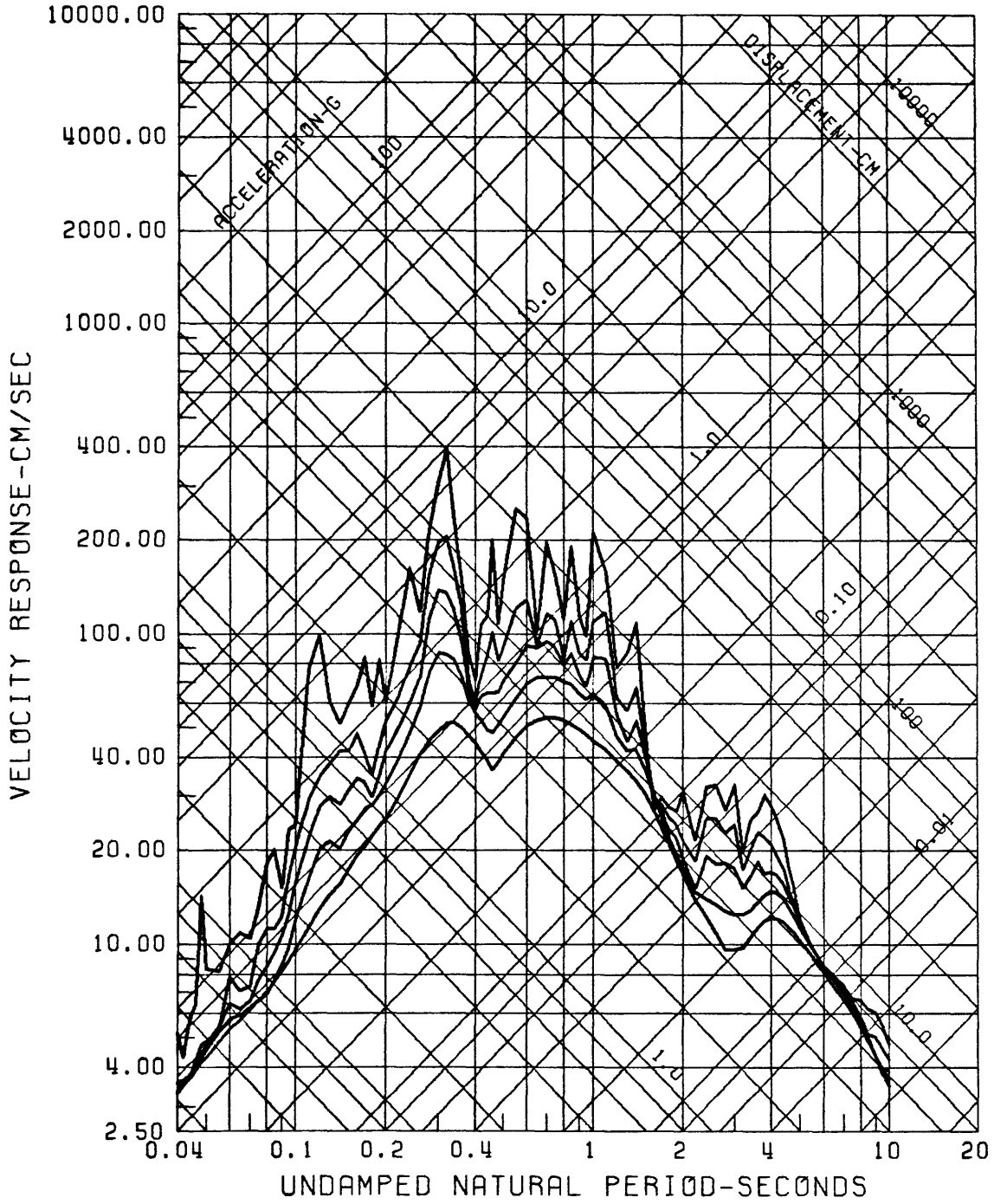

Figure 6a: Pseudo-velocity response curves (0, 2, 5, 10, 20 percent critical damping) computed for earthquake of 2 May 1983 (2342 UTC) as recorded on 135° horizontal component at Pleasant Valley pumping plant (switchyard). (Band pass filtered 0.1 to 50 Hz, Butterworth order 8 lowcut, cosine taper 50 Hz highcut, U.S. National Strong-Motion Data Center).

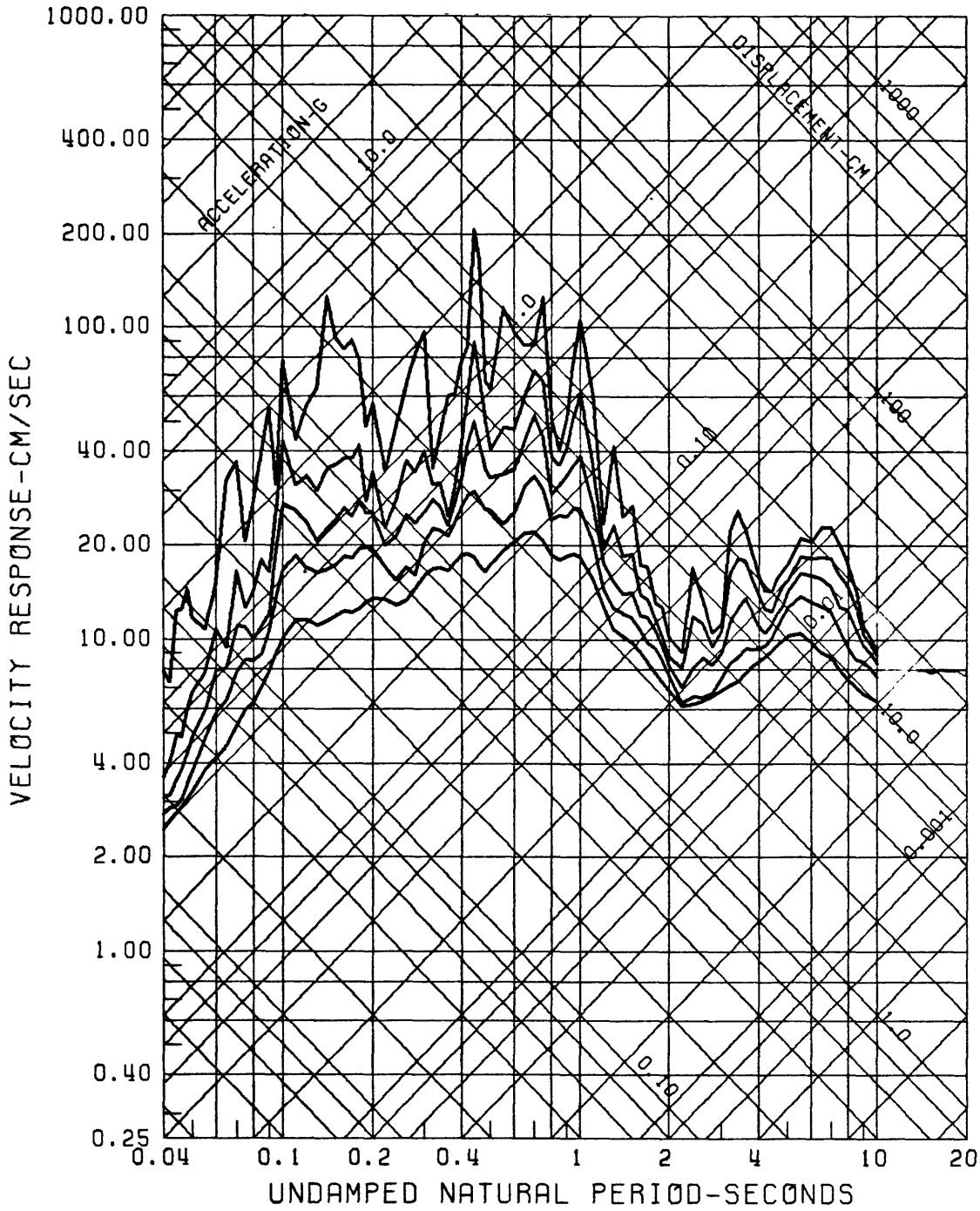

Figure 6b: Pseudo-velocity response curves (0, 2, 5, 10, 20 percent critical damping) computed for earthquake of 2 May 1983 (2342 UTC) as recorded on vertical component at Pleasant Valley pumping plant (switchyard). (Band pass filtered 0.1 to 50 Hz, Butterworth order 8 lowcut, cosine taper 50 Hz highcut, U.S. National Strong-Motion Data Center).

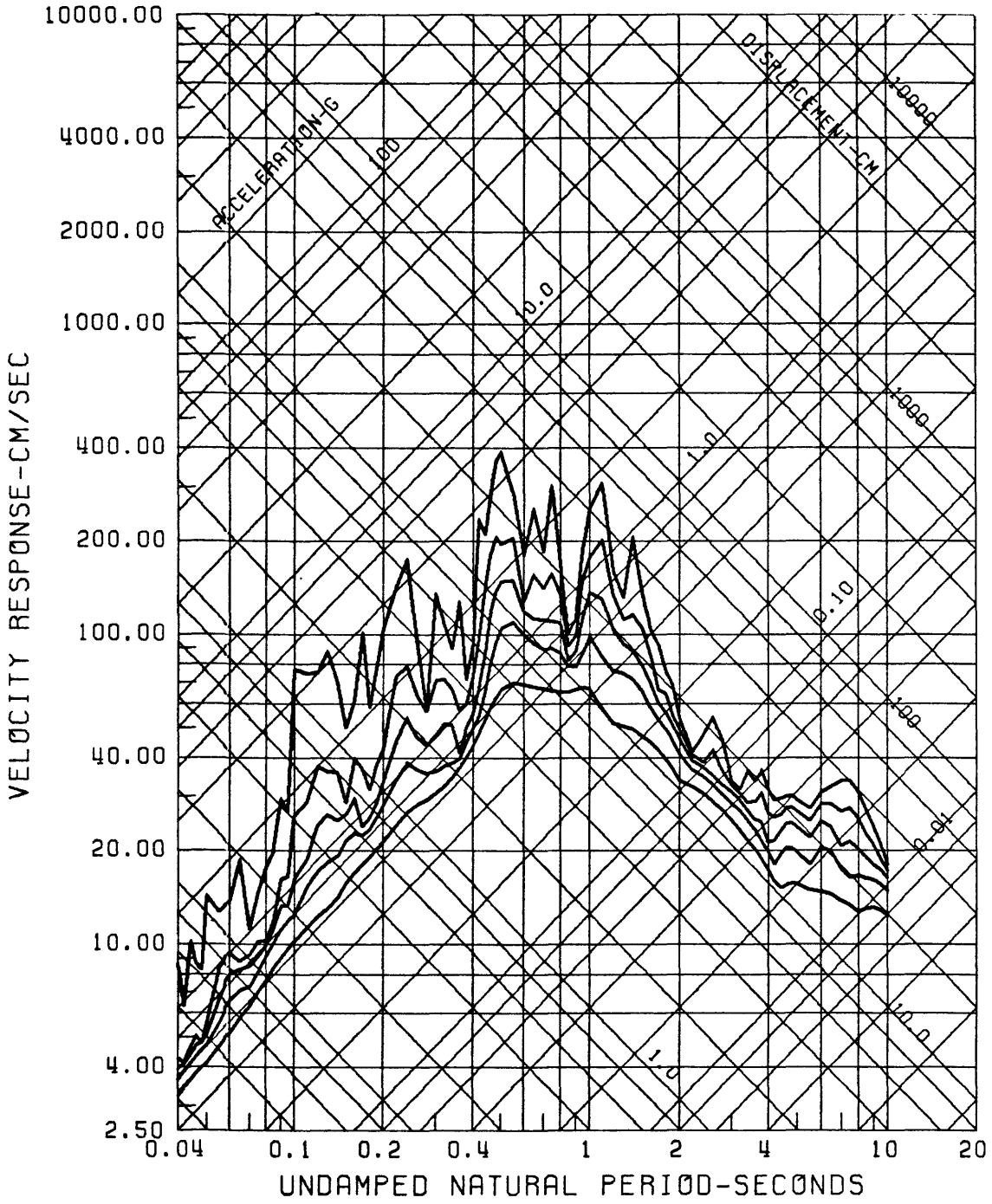

Figure 6c: Pseudo-velocity response curves (0, 2, 5, 10, 20 percent critical damping) computed for earthquake of 2 May 1983 (2342 UTC) as recorded on 045° horizontal component at Pleasant Valley pumping plant (switchyard). (Band pass filtered 0.1 to 50 Hz, Butterworth order 8 lowcut, cosine taper 50 Hz highcut, U.S. National Strong-Motion Data Center).

calculated displacements at each of the two sites, for each of the three pairs of components. The long-period content of these signals, as portrayed by displacement, should be similar, and such is the case. The possibility that noise, of any origin, affected both records identically is remote. The second item is that similar long-period components have been observed on other instruments from the main event and some of the larger aftershocks (Lindh, oral commun., Borcherdt and others, this report).

No attempt to correct for the four occasions of "clipping" in the switchyard 45^{o} component is reported here. Ongoing investigations of possible trace position details include; comparing the switchyard and basement records for the main shock and the largest aftershock on 9 May 0249 UTC. Only slight alteration to the appearance of spectral plots and calculated peak values, is expected.

A trial processing of the data with no long-period filter resulted in serious long-perod sinusoidal noise problems at a period of about 60 s, corresponding closely to the record length. Displacement amplitudes of 20 to 64 cm were reached. This corresponds to small acceleration amplitudes of 0.2 to 0.7 cm/s^2, or amplitudes on the original film of 4 to 13 micrometers. This is the same order of magnitude as the RMS error of the digitizing; namely, 10 μm. Processing of the aftershock records was not complete for inclusion in this report.

Aftershock Data

Shortly after the main shock eight aftershock accelerographs were installed at six sites, five in the epicentral area and one in Coalinga (see fig. 1 for locations). The following is a brief description of the stations:

Anticline Ridge:	SMA-1 bolted to a concrete pump pad (pump removed) on the top of a ridge about 50 ft (15.2 m) above Shell Road. A second SMA-1 located 10 ft (3.0 m) off the pad held in position by several bags of soil laid over the top of the unit. The two instruments are interconnected for starting and WWVB radio signals.
Burnett Construction:	SMA-1 anchored to a large concrete pad (base for a parking shelter) at 5th and Glenn in Coalinga, approximately one block southeast of the border of the heavily-damaged downtown area.
Oil City:	SMA-1 bolted to the pad of a small (garage size), light weight wood frame building located at Shell Oil's West Coalinga unit production laboratory.
Oil Fields Fire Station:	SMA-1 mounted at the end of a long, narrow pad used as a base for a light weight hose drying rack. A second SMA-1 located 10 ft (3.0 m) away on natural ground, anchored, and interconnected in the same manner as Anticline Ridge.

Palmer Avenue: SMA-1 installed on a concrete pad formerly used as a derrick footing (according to an unknown source at Union Oil).

Skunk Hollow: SMA-1 mounted on an old pump pad (pump removed).

The most significant aftershock, a magnitude 5.1 event that occurred on 9 May 0249 UTC, was recorded by all eight aftershock instruments as well as the complete structural array located at the pump plant. Peak accelerations from this shock are listed in Table 3 and copies of the records displayed in figures 7a, 7b, and 7c.

All stations had hypocentral distances of nominally 13 to 17 km, with peak accelerations ranging from 0.09 g in Coalinga, to 0.15 g to 0.56 g in the epicentral area. The high accelerations of 0.56 g, free-field, and 0.48 g, concrete pad, were measured at Anticline Ridge. It was pointed out by Malcolm Clark (oral communication, 1983) that surficial shatter effects were evident on the far side of the ridge, about 20-30 ft (6.1-9.1 m) from the accelerograph site. Accelerations at other stations at approximately the same distance from the preliminary epicenter are on the order of half that observed at Anticline Ridge.

The set of records from Pleasant Valley pump plant (fig. 7) show, as expected, a peak acceleration at the switchyard that is substantially higher, 0.22 g, compared to the basement, 0.14 g. As mentioned previously, this relationship held true for the main shock and prior earthquakes. Note that data traces from the basement and first floor are nearly identical, a phenomenon noted in prior earthquakes and credited to the monolithic nature of the underground portion of the pump plant. The roof record exhibits a dominant 0.55 s period (accelerations about 0.25 g) in a northeast-southwest direction across the limber axis of the structure. One can only surmise the nature of the record that would have been recorded at the roof level during the main shock, but in comparing the basement records obtained from the two larger events in this series, accelerations well in excess of 0.5 g would be anticipated, perhaps as large as 1 g.

REFERENCES CITED

Fletcher, J. B., Brady, A. G., and Hanks, T. C., 1980, Strong-motion accelerograms of the Oroville, California, aftershocks: data processing and the aftershock of 0350 August 6, 1975: Bulletin, Seismological Society of America, v. 70, p. 243-267.

Porter, L. D., Brady, A. G., and Roseman, W. R., 1978, Computer reassembly of multiframe accelerograms [abs.]: Earthquake Notes, v. 49, p. 13.

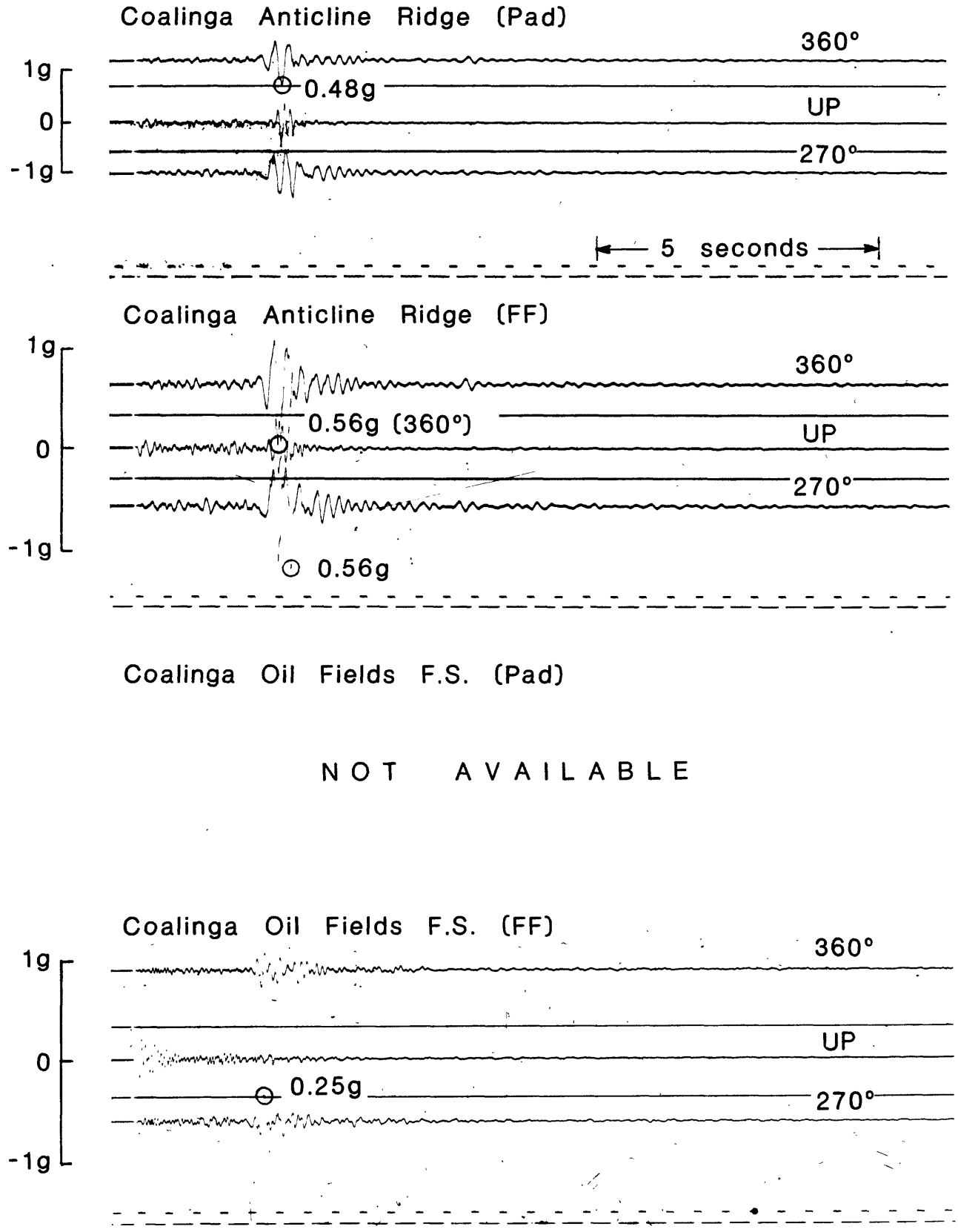

Figure 7a: Strong-motion records from temporary Coalinga stations: Anticline Ridge (Pad), Anticline Ridge (free-field), and Oil Fields Fire Station; for the aftershock 9 May 1983, 0249 UTC.

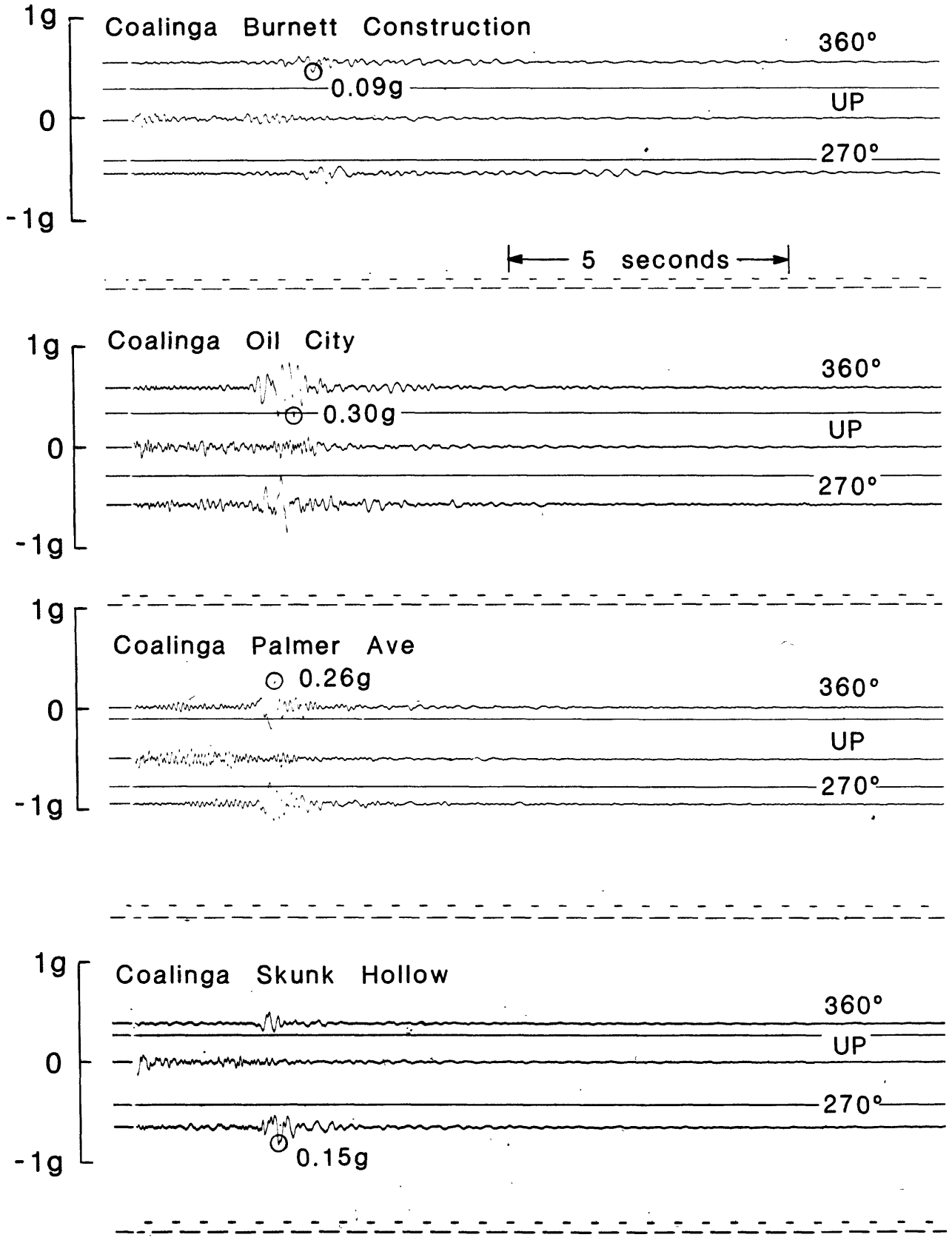

Figure 7b: Strong-motion records from temporary Coalinga stations: Burnett Construction, Oil City, Palmer Avenue and Skunk Hollow; for the aftershock 9 May 1983, 0249 UTC.

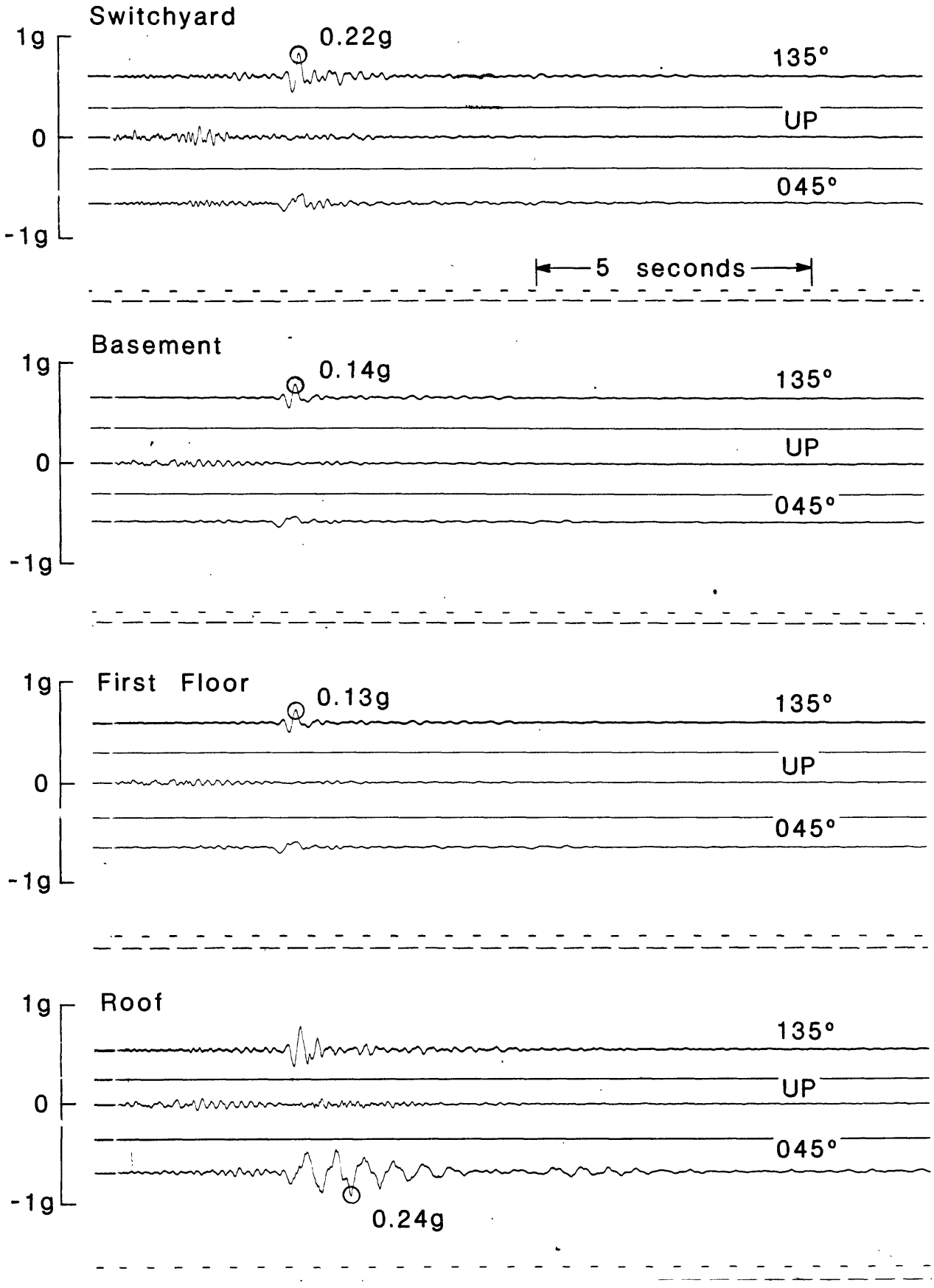

Figure 7c: Strong-motion records from the Pleasant Valley pump plant for the aftershock 9 May 1983, 0249 UTC: switchyard, basement, first floor, and roof.

Table 3. Near-field accelerograph records from the aftershock of 9 May 0249 UTC

Station	Coordinates	Hypocentral Distance (km)	Direction	Peak Acceleration (g)
Coalinga				
Anticline Ridge	36.233° 120.333°	12.9		
Free-field			360°	.56
			Up	.30
			270°	.56
Pad			360°	.48
			Up	.37
			270°	.47
Burnett Construction	36.138° 120.357°	16.9	360°	.09
			Up	.07
			270°	.08
Oil City	36.229° 120.360°	13.4	360°	.30
			Up	.10
			270°	.24
Oil Fields Fire Sta.	36.247° 120.314°	12.9		
Free-Field			360°	.18
			Up	.16
			270°	.25
Pad			360°	.19
			Up	.15
			270°	.22
Palmer Avenue	36.209° 120.292°	13.2	360°	.26
			Up	.10
			270°	.22
Skunk Hollow	36.275° 120.306°	13.6	360°	.12
			Up	.12
			270°	.15
Pleasant Valley pump plant	36.308° 120.249°	16.4		
Switchyard			135°	.22
			Up	.11
			045°	.10
Basement			135°	.14
			Up	.04
			045°	.05
1st Floor			135°	.13
			Up	.05
			045°	.06
Roof			135°	.23
			Up	.06
			045°	.24

DIGITAL STRONG-MOTION DATA RECORDED BY U.S. GEOLOGICAL SURVEY NEAR COALINGA, CALIFORNIA

R. Borcherdt, E. Cranswick, G. Maxwell, C. Mueller, R. McClearn, G. Sembera, and L. Wennerberg

U.S. Geological Survey
345 Middlefield Road
Menlo Park, CA 94025

The Coalinga earthquake of May 2, 1983 and subsequent aftershocks yielded an extensive set of on-scale strong-motion recordings. The main event was recorded on two accelerographs at the Pleasant Valley pump plant approximately 9 km northeast of the epicenter, the 40-station Parkfield array at distances of 28-40 km operated by the California Division of Mines and Geology, and numerous other accelerograph stations at more distant locations. Subsequent aftershocks with magnitudes as large as 5 were recorded at many of these stations as well as 26 additional digital and analog stations installed in the epicentral region of the aftershock zone. A majority of the aftershock recordings obtained in the epicentral region have been made at hypocentral distances less than 20 km.

Strong-motion instrumentation deployed by the U.S. Geological Survey to record the aftershock sequence includes: a set of ten wide-dynamic range digital recorders (GEOS), an eight-element two-dimensional short baseline array of digital recorders (DR-100), and a set of eight analog strong-motion recorders (SMA-1). Field experiments and corresponding data sets collected on the digital strong-motion instrumentation are discussed herein. Strong-motion data collected on the analog instrumentation and preliminary results from digital processing of the main shock records are presented by Maley and others (this report).

Installation of digital strong-motion recorders in the Coalinga region began the evening of May 2, 1983. An array of 10 GEOS stations and an eight-element two-dimensional short-baseline array of DR-100 recorders were established in the epicentral region of the aftershock zone. The stations yielded an extensive and relatively complete set of on-scale recordings for aftershocks ranging in magnitude from 1 to 5+. The digital stations operated during the time interval May 2-25. The digital data discussed in this report were collected during the time interval May 2-10. Transfer of the remaining data to computer disc has not been completed as of this report.

Locations of the instrumentation installed for strong-motion seismological and engineering studies in the epicentral region of the aftershock zone are shown in figures 1 and 2. Data from station SUB (fig. 1) was collocated with the SMA-1 that recorded the main event in the switchyard of the Pleasant Valley pump plant. The stations indicated were occupied continuously through May 19 at which time six of the GEOS stations were moved to collect information on soil response in the Coalinga area and at the Pleasant Valley pump plant. The soil response array in the Coalinga area (fig. 2) was installed on May 19 and 20 and operated through May 23. On May 23 the array was moved to the area of the Pleasant Valley pump plant (fig. 2) and operated until May 25 at which time all of the digital instrumentation was removed from the field. Computer playback of the recordings in the field from

these two arrays indicate that events greater than magnitude 4 and several smaller events were recorded on each of the arrays. The two-dimensional short-baseline array of DR-100 recorders (fig. 3) was operated at station OLF (fig. 1) from May 4 to May 24.

Each GEOS recorder (Borcherdt and others, 1979) was set up to record the output of six sensors, one three-component set of force-balance accelerometers and one three-component set of velocity transducers. System trigger parameters were selected such that events with amplitudes greater than about 4 times that of the seismic background noise were recorded. In general, these settings were selected to record all events in the epicentral region with magnitudes greater than about 1. Events with magnitudes as small as 0 were recorded at some of the stations with low seismic background noise.

Events recorded on at least three GEOS stations through May 10 are indicated on figure 1. Preliminary locations for the events were determined from the "Real-Time Picker" described by Reasenberg and others (this report). The events are represented by circles of source radius plotted to map-scale calculated from a Brune model using moments determined from the Thatcher-Hanks moment-magnitude relation and a prescribed stress-drop of 50 bars. Events of magnitude greater than 3.5 recorded on at least three of the GEOS stations during the time period of May 3-10 are shown on figure 4 and identified with particular stations (Table 1). The recorder at Station ANT was moved to location VEW after the first few hours because of a portable TV transmission tower discovered after sunrise. Stations JUN, YUB, ALP, and TRA were installed on May 4, 1983 and station SGT on May 6.

The two-dimensional short-baseline digital array established with the DR-100 recorders was operational during the period of May 4 to 24. The location, orientation, and station spacing is indicated on figure 3. The location of the array vertex corresponds to station location OLF as shown on figure 1. Station OLF was occupied by a GEOS recorder through May 4, at which time the recorder was used to establish a new station. Four of the recording systems in the short-baseline array were equipped with force-balanced accelerometers and four were equipped with velocity transducers with site AR1/AR8 (fig. 3) being occupied simultaneously by both types of sensors.

The largest aftershock recorded on the digital strong-motion arrays was the event on May 9 (M 5.1; 0249 GMT). Six seconds of output of the force-balanced accelerometers as recorded on the GEOS array are shown in figures 5a, 5b, and 5c. Recordings of the velocity transducers were also obtained at each of these sites, with some of the larger amplitudes being clipped due to dynamic range of the sensor.

Data recorded on the DR-100 array for the event of May 9 (M 5.1; 0249 GMT) is shown plotted at a normalized amplitude scale in figures 6a, 6b, and 6c. The recordings at sites AR1, ARA, AR9, and AR7 correspond to ground acceleration, and the remainder correspond to ground velocity. An interesting feature of the GEOS and DR-100 data sets (figs. 5 and 6) is the relatively long-period onset pulse apparent at each of the stations. A similar long-period component appears to exist on the main shock displacement records (Maley and others, this report) and the digital records recorded in the

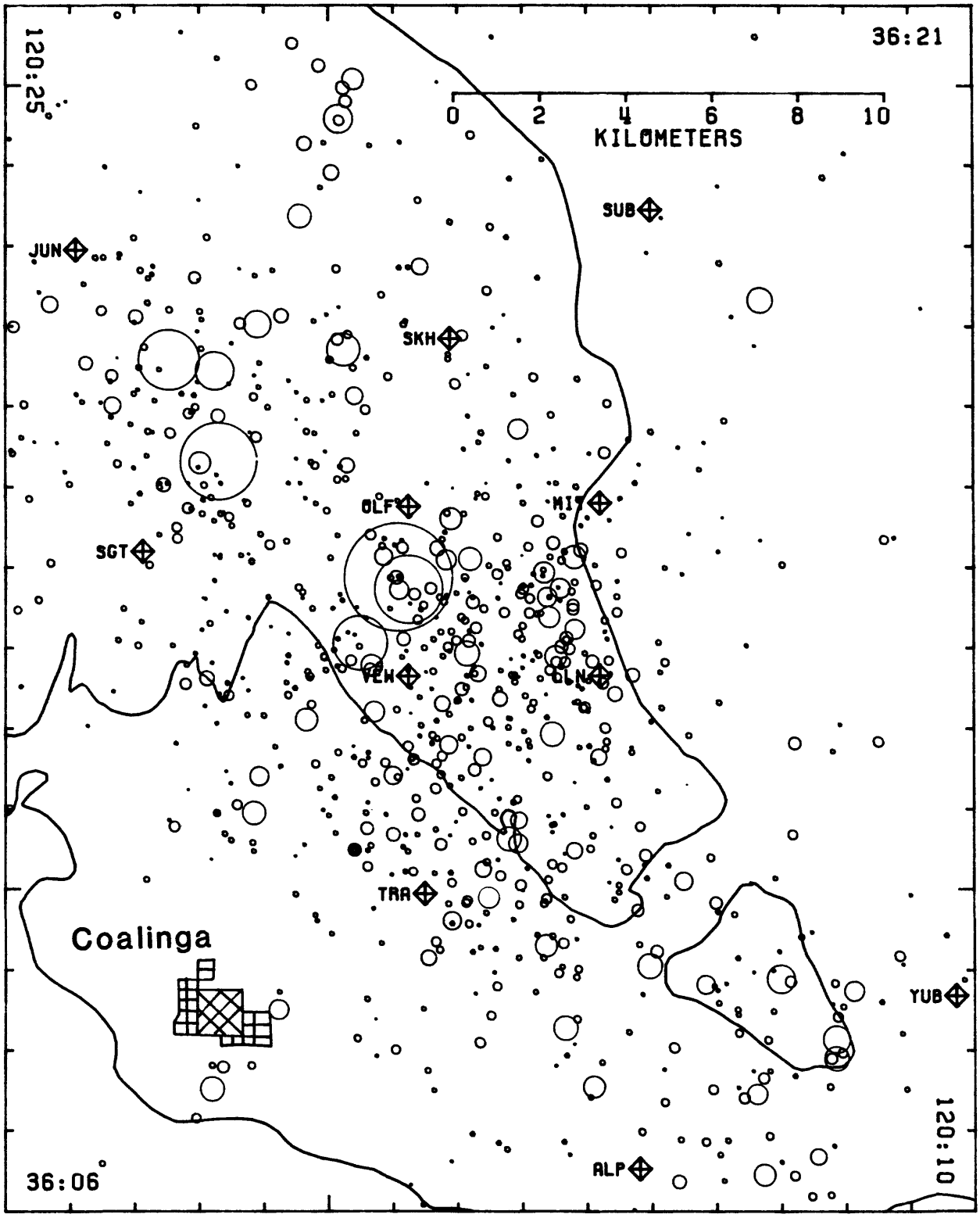

Figure 1: Locations for digital recording stations (GEOS) and seismicity near Coalinga during time period May 2-10, 1983. (See Eaton, this report for location of main event; see text for representation of source size). Outcrop-alluvium boundary is indicated by solid line.

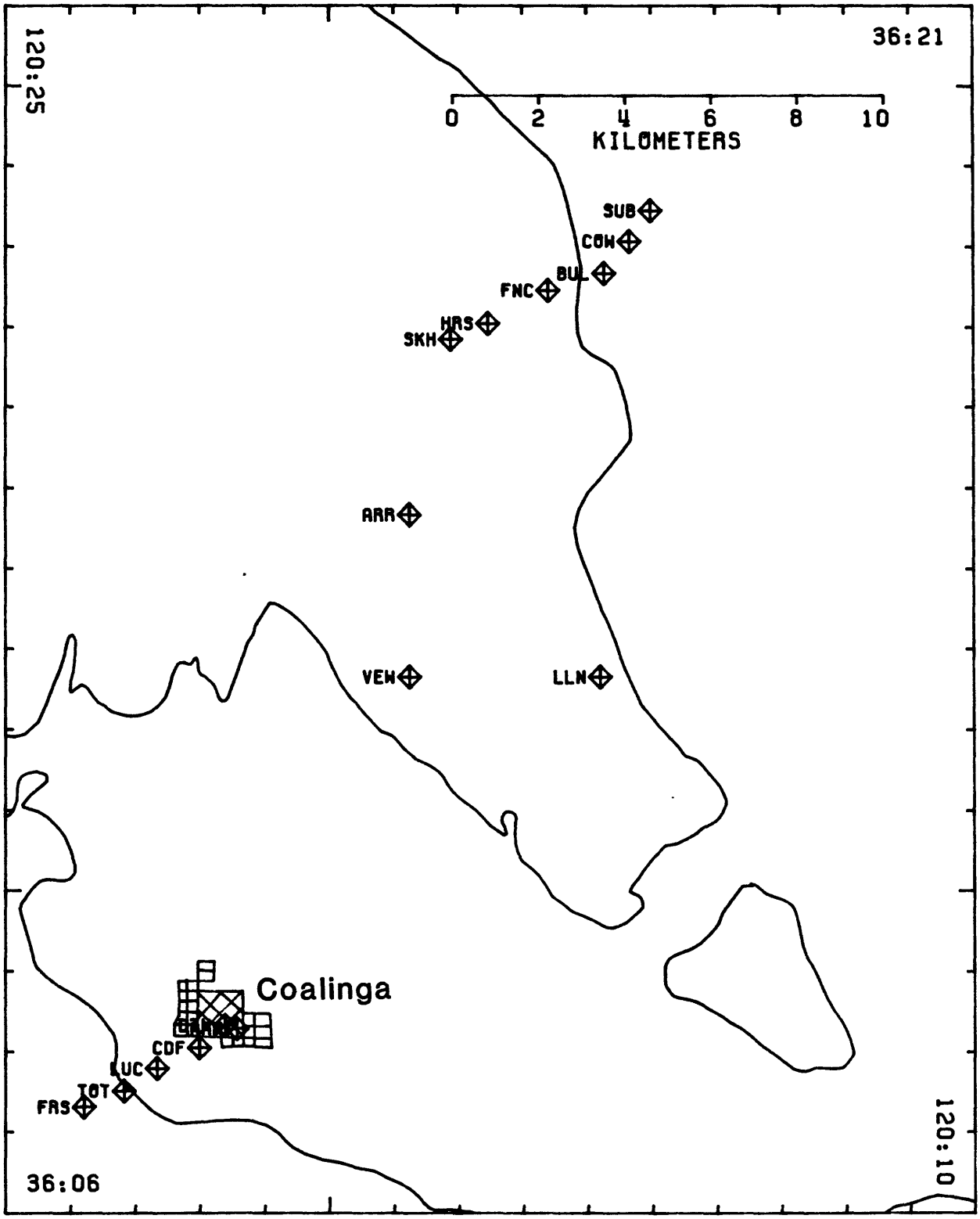

Figure 2: Locations for digital recording stations (GEOS) and digital two-dimensional short-baseline array (ARR) occupied during time period May 19-25. The soil-response array near Coalinga was moved to Pleasant Valley pump plant on May 23.

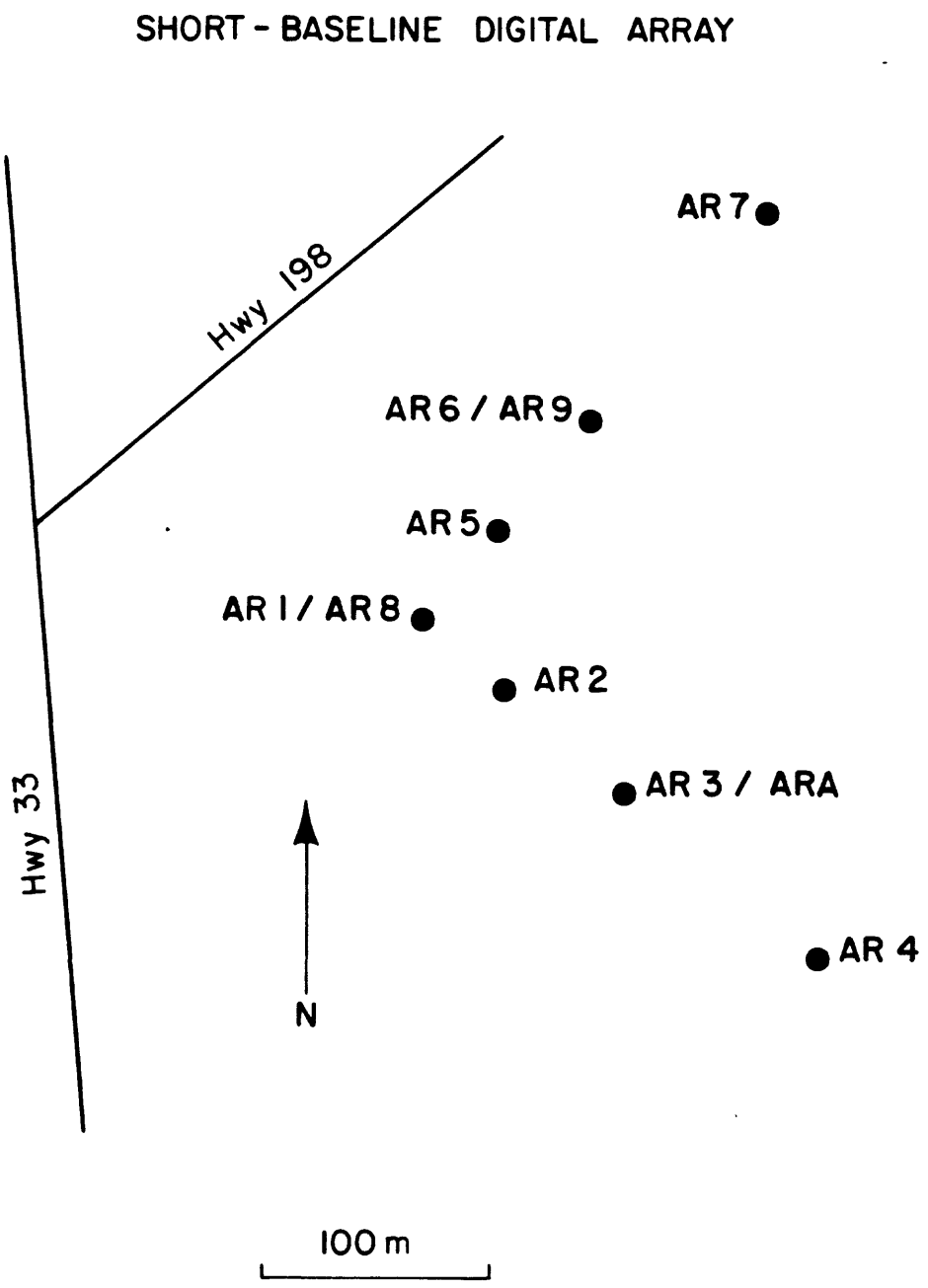

Figure 3: Locations plotted to scale for elements of two-dimensional short-baseline array operated during time period May 4-25 using digital DR-100 recorders. Location ARI/AR8 corresponds to location OLF (fig. 1).

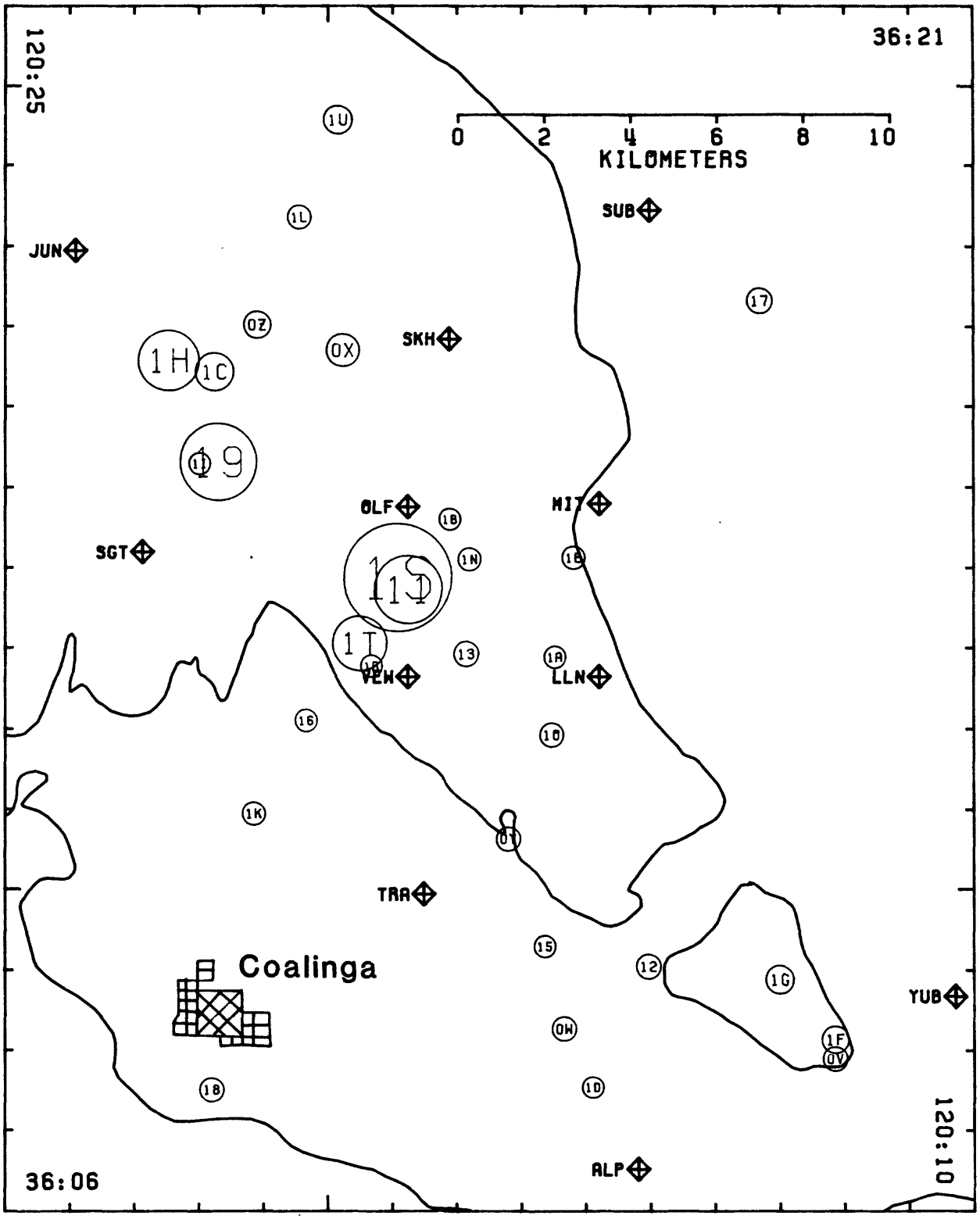

Figure 4: Epicentral locations for aftershocks with magnitudes greater than 3.5 recorded on GEOS stations during the time period May 3-10, 1983. Stations that recorded each of the events are identifiable using event code and Table 1.

Table 1. Matrix showing the GEOS stations that recorded aftershocks with magnitudes $\geq$ 3.5 during May 3-10, 1983.

EVENT ID	TIME	SUB	SKH	OLF	ANT	LLN	MIT	VEW	JUN	YUB	ALP	TRA	SGT
0V 123	1257		*	*		*							
0W 123	1309	*		*		*	*						
0X 123	1426	*		*		*	*						
0Y 123	1450	*		*		*	*						
0Z 123	1510	*		*		*	*						
11 123	1541	*			*	*	*						
12 123	1617	*				*	*						
13 123	1701	*		*		*	*						
15 123	2136	*				*	*						
16 123	2229	*		*		*	*	*					
17 123	2345			*		*		*					
19 124	0728	*	*			*	*	*		*	*		
1B 124	1559	*	*			*	*					*	
1C 124	1611	*	*			*	*					*	
1E 125	0027	*				*				*		*	
1F 125	0437					*			*	*		*	
1G 125	0806								*	*		*	
1K 126	0943		*			*	*	*	*	*		*	*
1L 127	0017					*		*	*	*		*	
1N 127	0543		*					*	*	*			
1R 128	2025	*				*	*	*			*	*	*
1S 129	0249	*	*			*	*	*	*	*	*	*	*
1T 129	0326	*	*			*	*	*	*		*	*	*
1U 130	1326					*			*		*	*	

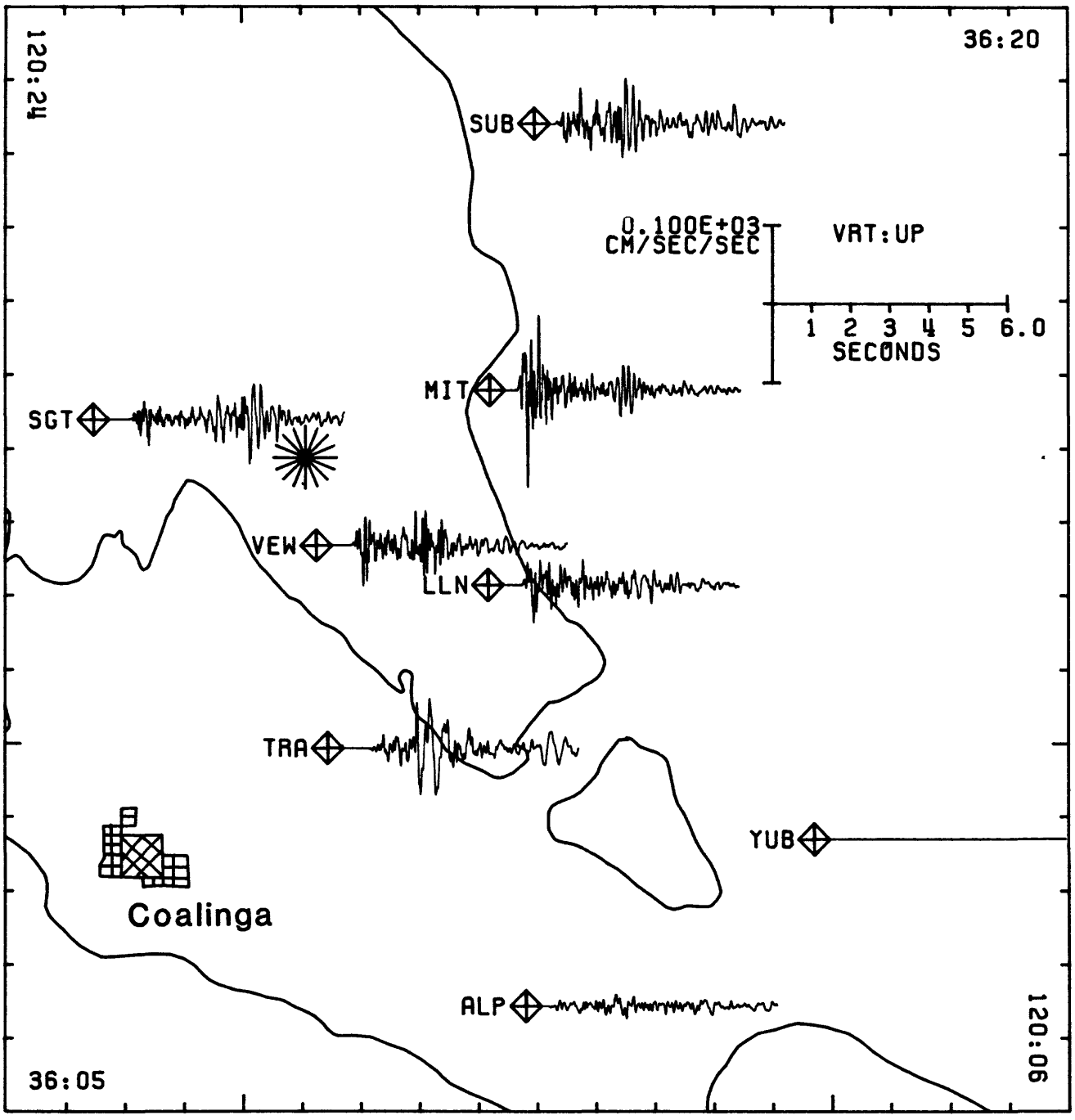

Figure 5a: Six seconds of acceleration time histories from the aftershock of May 9, 1983 (M 5.1) as recorded on eight of the GEOS stations. (Map format did not permit illustration of recordings obtained at stations JUN and SKH.) Three components of ground acceleration are shown (vertical, fig. 5a; east-west, fig. 5b; north-south, fig. 5c).

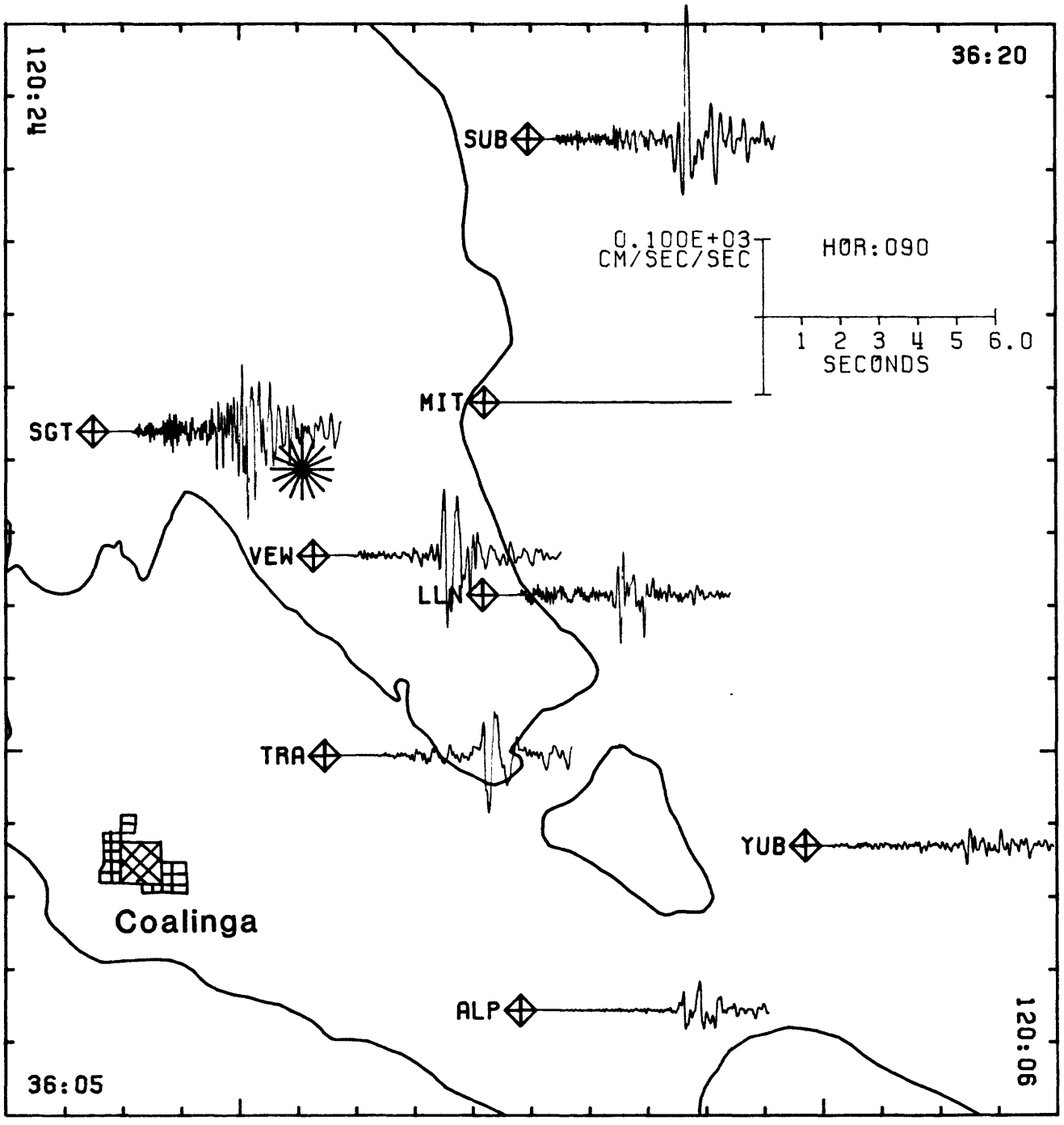

Figure 5b: Six seconds of acceleration time histories from the aftershock of May 9, 1983 (M 5.1) as recorded on eight of the GEOS stations. (Map format did not permit illustration of recordings obtained at stations JUN and SKH.) Three components of ground acceleration are shown (vertical, fig. 5a; east-west, fig. 5b; north-south, fig. 5c).

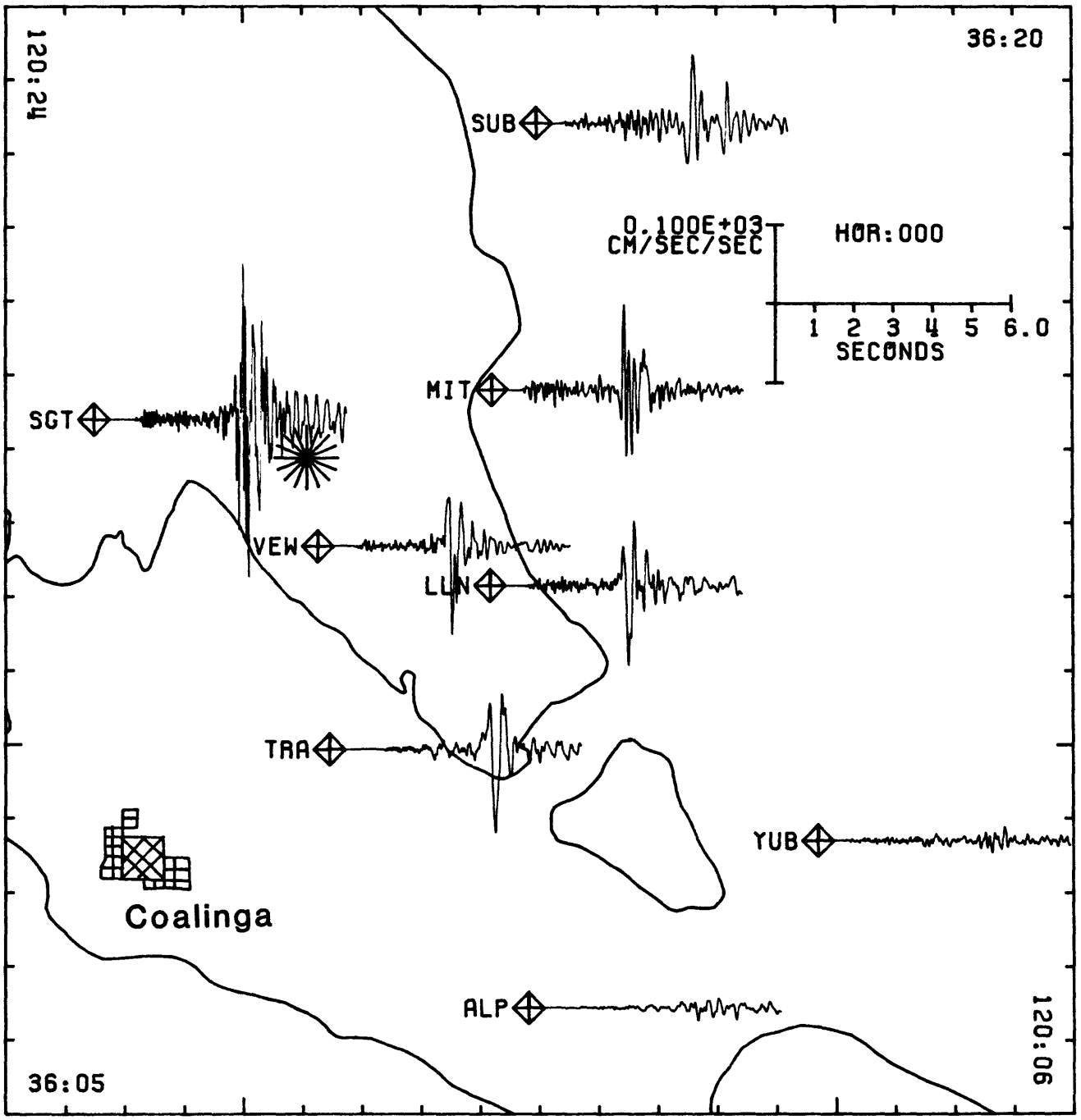

Figure 5c: Six seconds of acceleration time histories from the aftershock of May 9, 1983 (M 5.1) as recorded on eight of the GEOS stations. (Map format did not permit illustration of recordings obtained at stations JUN and SKH.) Three components of ground acceleration are shown (vertical, fig. 5a; east-west, fig. 5b; north-south, fig. 5c).

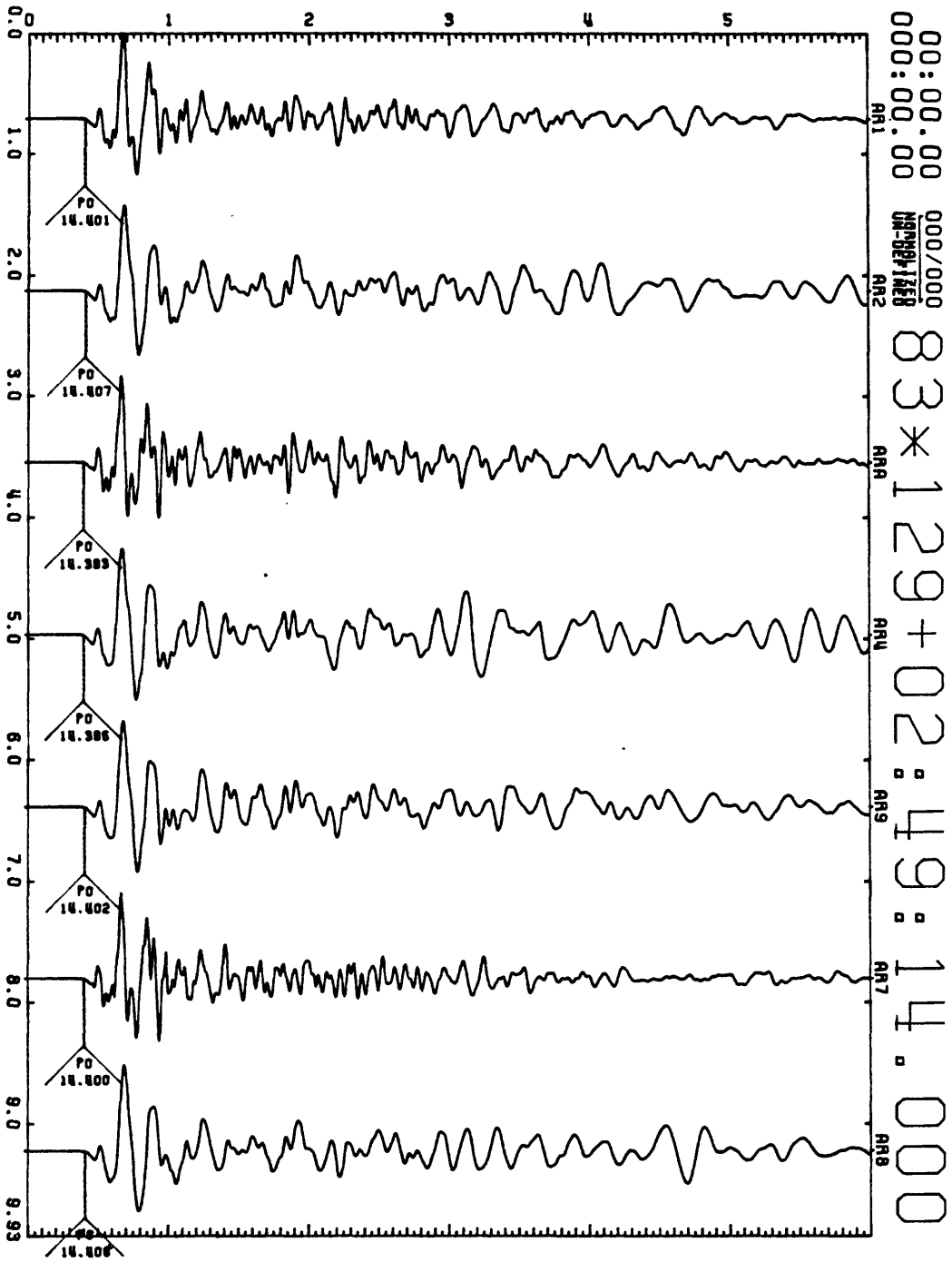

Figure 6a: Six seconds of normalized acceleration and velocity time histories from the aftershock of May 9, 1983 (M 5.1) as recorded on the two-dimensional short-baseline array of DR-100 recorders. Velocity transducers were used at locations AR2, AR4, AR9, AR8, and force-balanced accelerometers were used at locations AR1, ARA, AR7. Three components of ground motion are shown (vertical, fig. 6a; east-west, fig. 6b; north-south, fig. 6c).

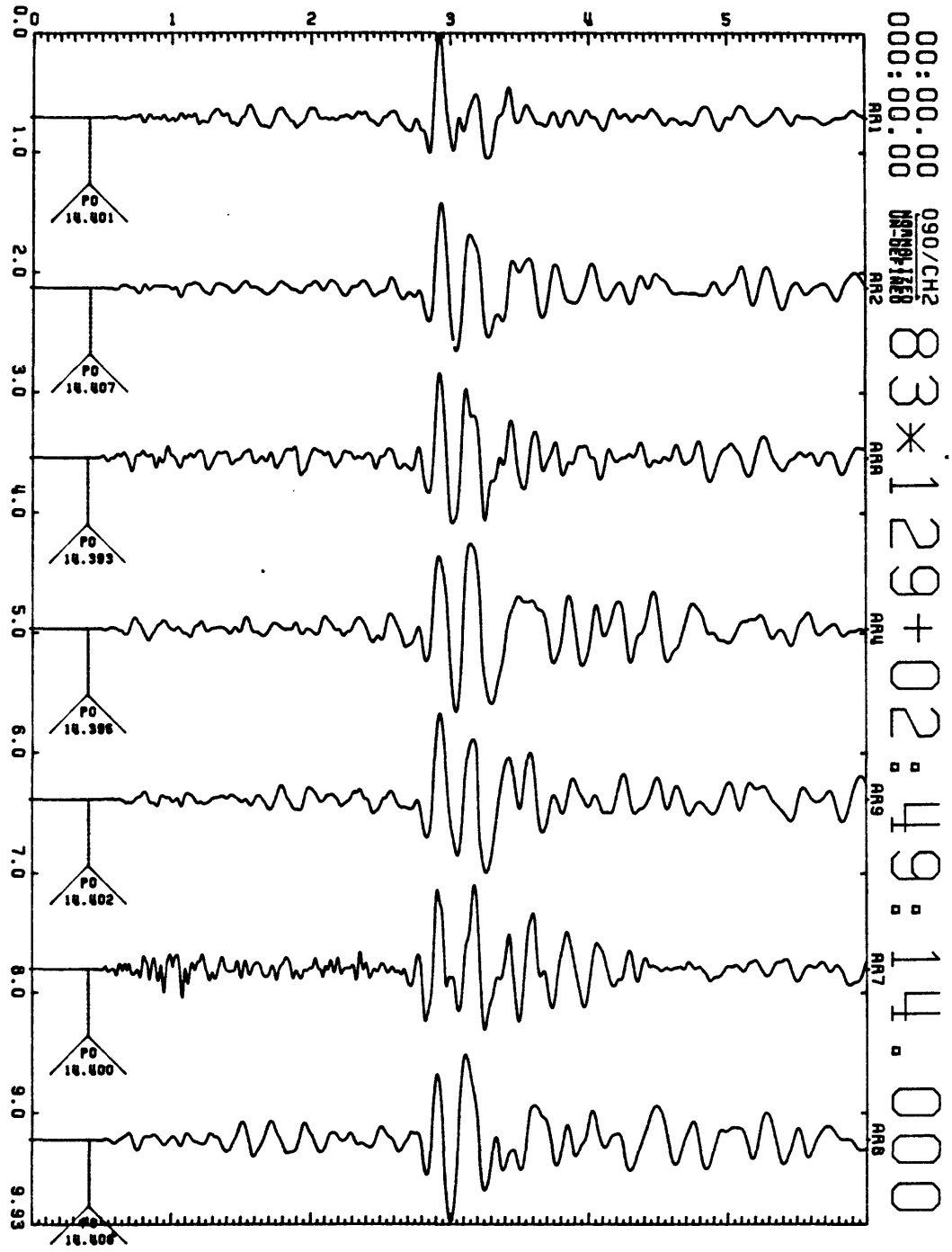

Figure 6b: Six seconds of normalized acceleration and velocity time histories from the aftershock of May 9, 1983 (M 5.1) as recorded on the two-dimensional short-baseline array of DR-100 recorders. Velocity transducers were used at locations AR2, AR4, AR9, AR8, and force-balanced accelerometers were used at locations AR1, ARA, AR7. Three components of ground motion are shown (vertical, fig. 6a; east-west, fig. 6b; north-south, fig. 6c).

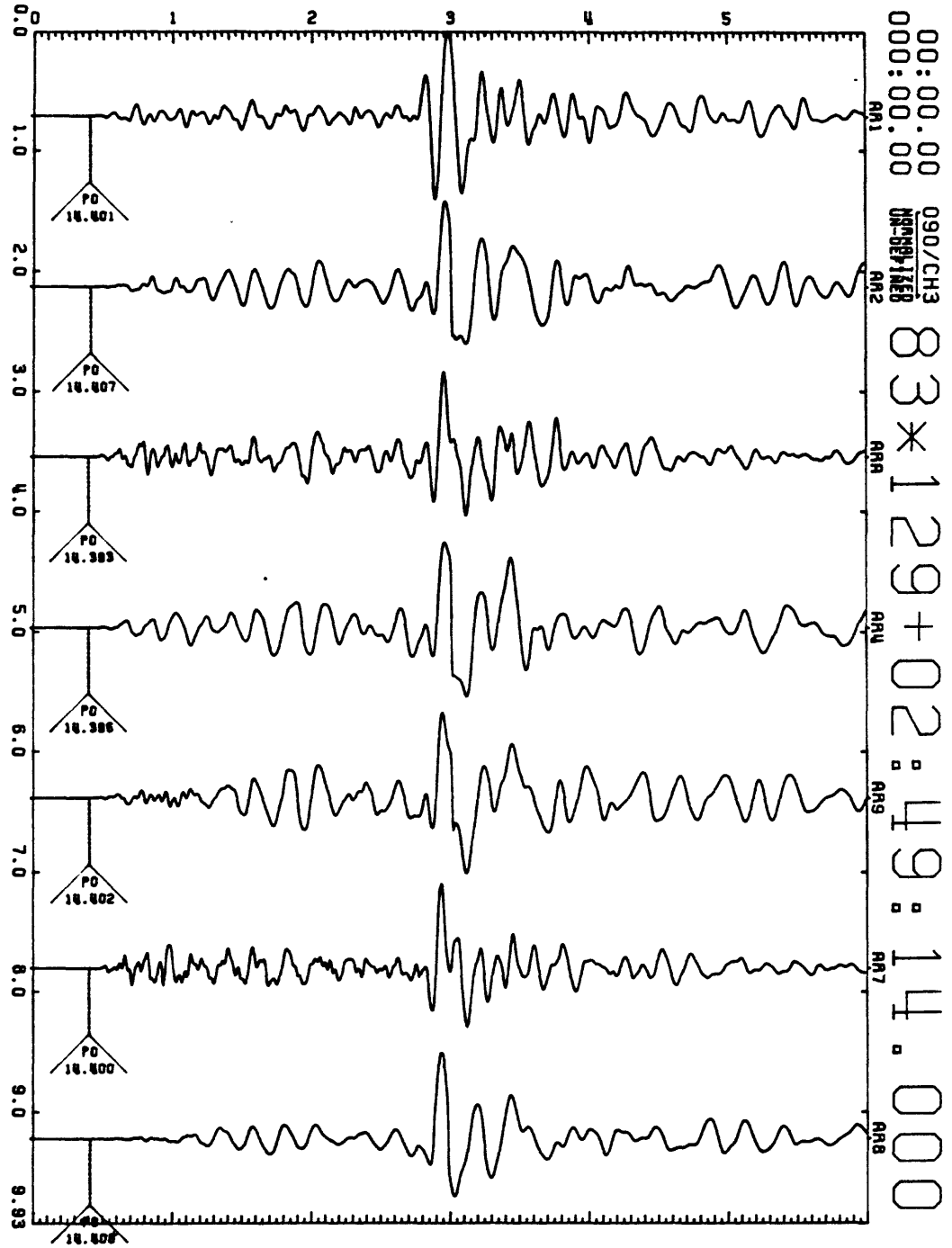

Figure 6c: Six seconds of normalized acceleration and velocity time histories from the aftershock of May 9, 1983 (M 5.1) as recorded on the two-dimensional short-baseline array of DR-100 recorders. Velocity transducers were used at locations AR2, AR4, AR9, AR8, and force-balanced accelerometers were used at locations AR1, ARA, AR7. Three components of ground motion are shown (vertical, fig. 6a; east-west, fig. 6b; north-south, fig. 6c).

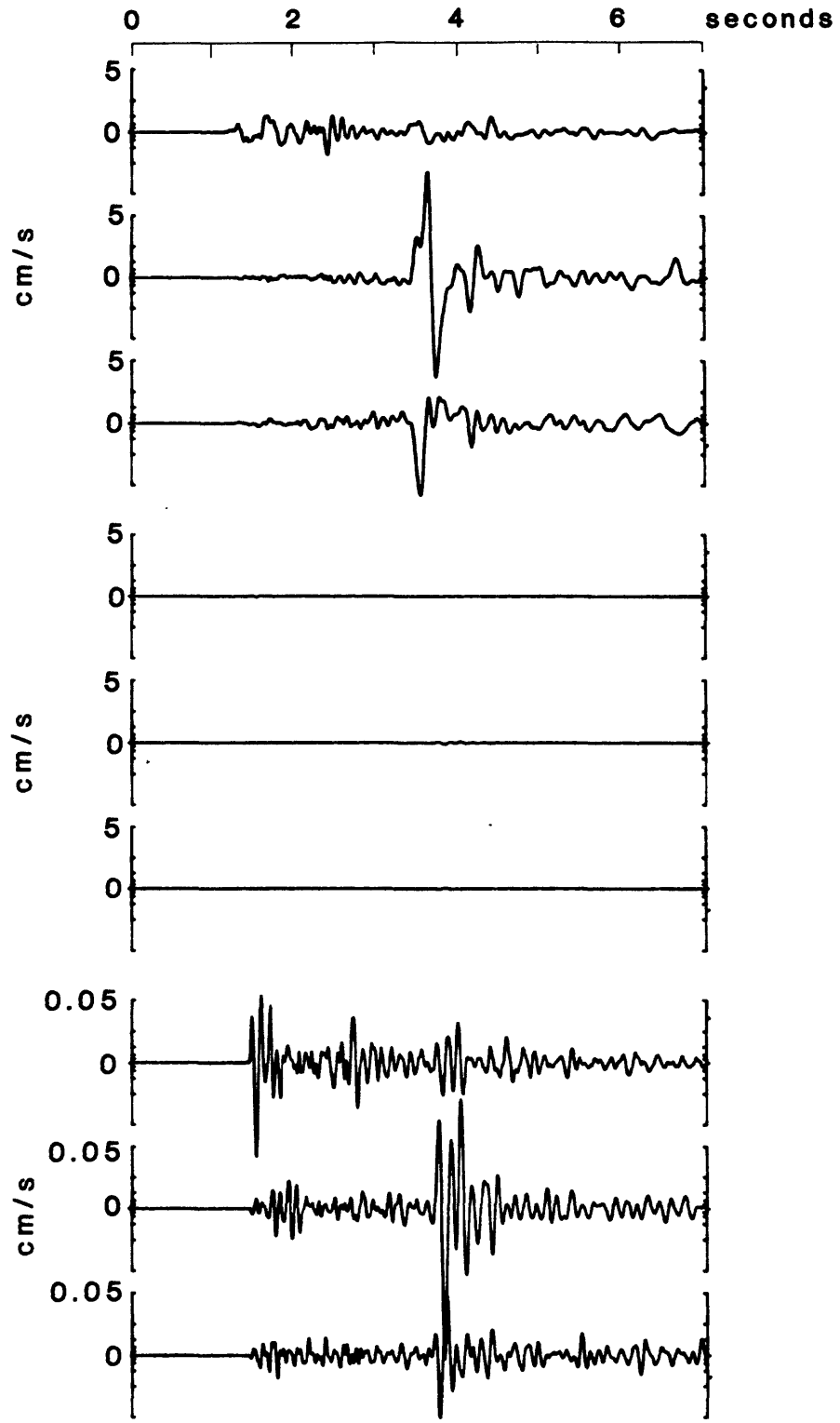

Figure 7: Three components of ground velocity recorded from an aftershock of magnitude 5 (upper 3 traces) and a magnitude 1 event (lower six traces) on a GEOS system at station SUB. Event locations are approximately the same. The recordings of the M 1 event are plotted at two scales (intermediate three traces are at same scale as those for M 5 event; lower three traces are at a scale expanded by a factor of 100). Comparison of seismic noise level on lower three traces with maximum amplitude of upper three traces provides a partial indication of resolution and dynamic range for recorded data.

Parkfield area by Lindh (oral commun.). This long-period component is especially apparent when the high resolution digital data is plotted at an expanded amplitude scale.

Important aspects of the digital data set collected for the Coalinga aftershock sequence are the completeness of the data set for events larger than magnitude about 1 and quality of the recordings. The GEOS recordings were made with high signal resolution (16 bit, 96 db) and with two sets of sensors (velocity transducers and forced-balanced accelerometers). Signal strengths ranging from that of the seismic background noise to that of the largest event were recorded on scale without change in gain settings (maximum dynamic range for system is 192 db with appropriate gain settings).

To provide some indication of data quality, two aftershocks as recorded on one GEOS at the Pleasant Valley pump plant (station SUB) are plotted in figure 7. The top three traces correspond to the integrated acceleration (or velocity) traces recorded from the May 9 (M 5.1) event. The next three traces correspond to a magnitude 1 event at about the same location about 1 hr later. The lower set of three traces are the same velocity recordings of the magnitude 1 event but plotted at an amplitude scale expanded by a factor of 100. Comparison of the seismic background noise level as indicated on the lower three traces with the maximum amplitude of the magnitude 5.1 event (upper three traces) provides a partial indication of signal resolution and effective dynamic range, over which events have been recorded in the epicentral region of the aftershock zone. As an additional indication of signal resolution, the east-west components of ground velocity as shown in figure 7 for the two events are plotted at an expanded amplitude scale in figure 8. The two traces recorded on the same system for the magnitude 1 and magnitude 5 events are plotted at amplitude scales differing by a factor of 100.

REFERENCE CITED

Borcherdt, R. D., Fletcher, J. B., Eckels, C. W., Brodine, R. C., Van Schaack, J. R., and Warrick, R. E., 1979, A General Earthquake Observation System (GEOS-I), EOS, American Geophysical Union Transactions, v. 60, p. 889.

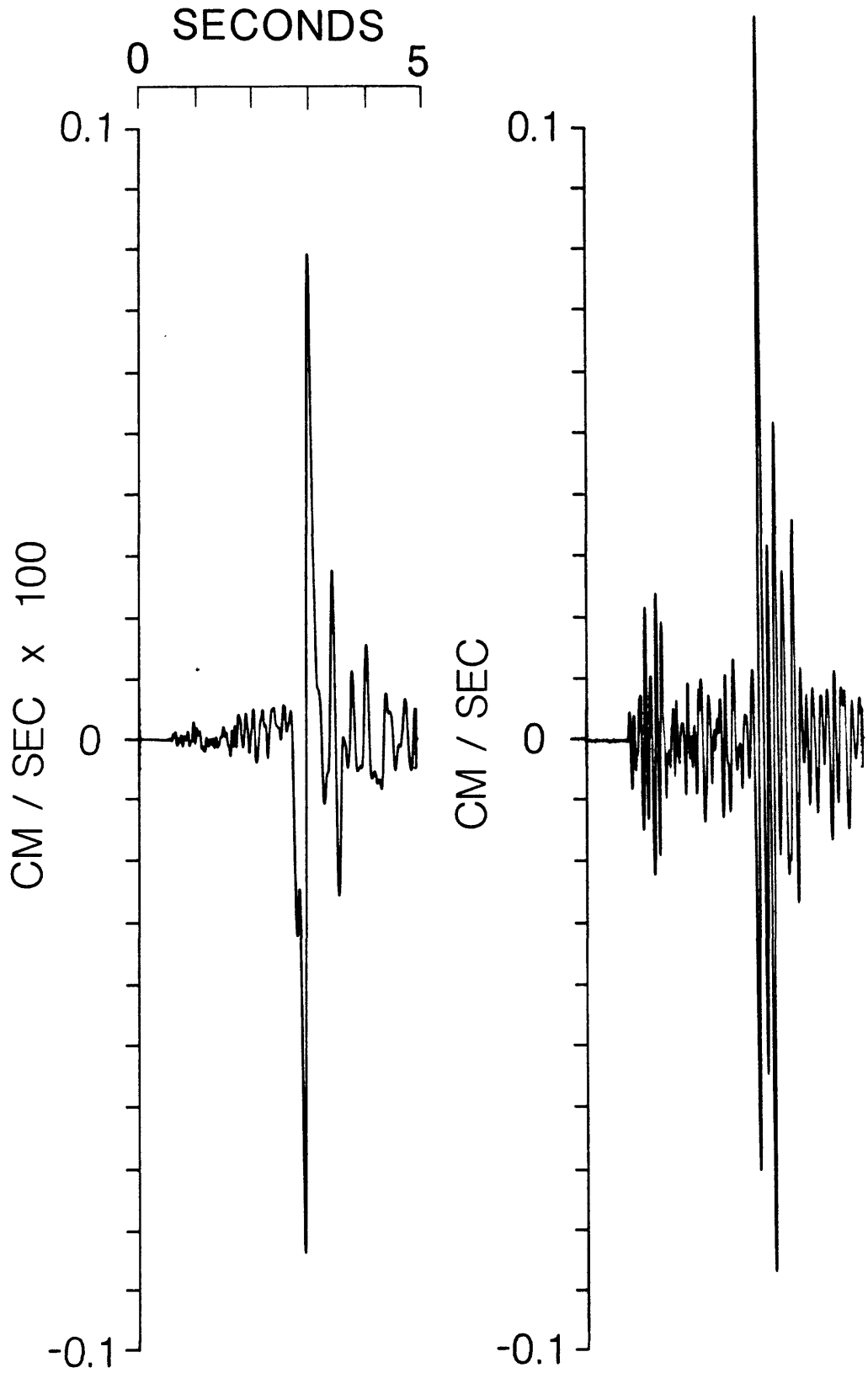

Figure 8: East-west components of ground velocity shown in figure 7 plotted at an expanded amplitude scale to illustrate data resolution (Pleasant Valley pump plant, SUB). Left trace corresponds to magnitude 5 event, right trace corresponds to magnitude 1 event. Amplitude scales differ by a factor of 100.

PRECISE RELEVELING OF THE COALINGA EPICENTRAL REGION AND ADJACENT PORTIONS OF THE SAN ANDREAS FAULT

Ross S. Stein, Allan G. Lindh, Wayne R. Thatcher, and Michael J. Rymer

U.S. Geological Survey
345 Middlefield Road
Menlo Park, CA 94025

Leveling routes in three localities that were surveyed using first-order double-run standards between 1966 and 1982 will be resurveyed to detect elevation changes associated with the May 2, 1983 Coalinga earthquake.

The network of leveling routes in the epicentral region of the Coalinga earthquake (fig. 1) were last surveyed in 1966. Resurvey of these routes will enable measurement of the coseismic elevation changes. However, subsidence caused by groundwater withdrawal will limit our ability to segregate the earthquake displacements from those caused by groundwater- and oil-withdrawal in the region. Bull (1975) reports that the crest of Anticline Ridge subsided at a rate of 3 mm/yr and the northeastern and southwestern flanks of the ridge subsided at 7 mm/yr with respect to the southern end of the line during 1933-1966. These changes are probably caused by fluid withdrawal.

The Parkfield-Cholame segment of the San Andreas fault was first surveyed in 1980, and some portions of the net were resurveyed in 1982. This region was the site of the 1966 $M_L = 5.6$ ($M_0 = 1.4 \times 10^{25}$ dyne-cm) Parkfield earthquake. A complete resurvey was undertaken beginning 16 May 1983, and is almost completed.

A 15-km-long route that crosses the San Andreas fault at Mustang Ridge, west of Priest Valley, will be resurveyed during late June-early July 1983. It was last surveyed in 1975.

REFERENCE CITED

Bull, W. B., 1985, Land subsidence due to ground-water withdrawal in the Los Banos-Kettleman City Area, California, Part 2. Subsidence and compaction of deposits: U.S. Geological Survey Professional Paper 437-F, 90 p.

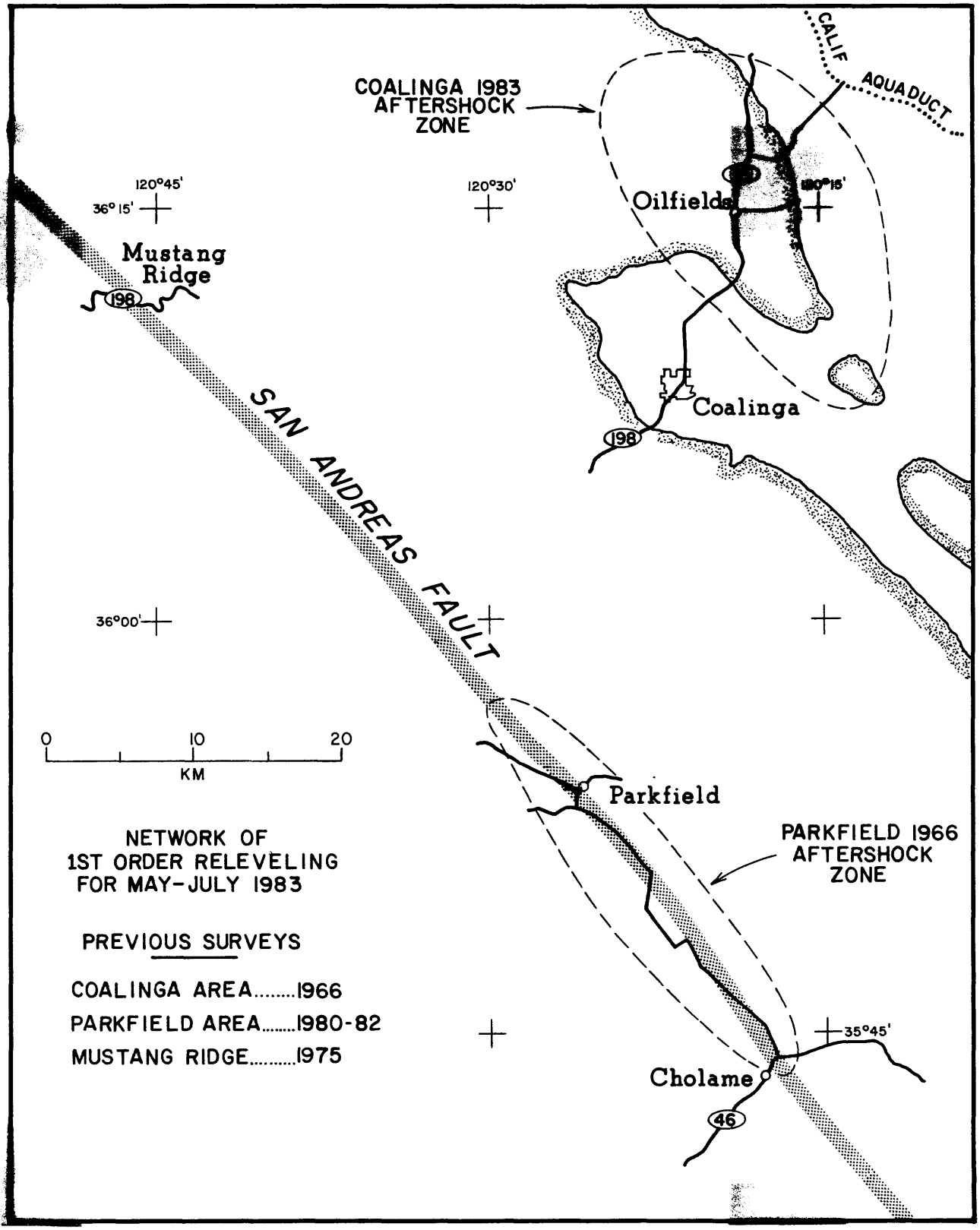

Figure 1. Map showing locations of first-order leveling routes resurveyed during May-July 1983.

ACKNOWLEDGEMENTS

Editorial review by Mike Rymer improved this report considerably. The outstanding efforts of Barbara Gessner, in transcribing handwritten materials from many different sources, and those of Ray Eis and Richard Buszka, in turning illegible drawings into presentable figures, were instrumental in completing this document in a timely fashion.